UNIVERSITY OF CALIFORNIA SAN DIEGO

Synthesis of Alpha-Synuclein Proteolytic Targeting Chimeras and Selective Tau Tubulin Kinase I Inhibitors

A Thesis submitted in partial satisfaction of the requirements
for the degree Master of Science

in

Chemistry

by

Stanley Buczynski

Committee in charge:

Professor Fleur Ferguson, Chair
Professor Galia Debelouchina
Professor Dionicio Siegel
Professor Jerry Yang

2022

The Thesis of Stanley Buczynski is approved, and it is acceptable in quality and form for publication on microfilm and electronically.

University of California San Diego

2022

DEDICATION

I would like to dedicate this work to my family who have helped me achieve my dreams and encouraged me every step of the way. To the mentors and advisors who have guided me on this path I thank you for your contribution to my success and use this document as proof that your efforts matter not only to expanding diversity but the expansion of knowledge in the scientific community.

TABLE OF CONTENTS

LIST OF FIGURES

TABLE OF SPECTRUM

LIST OF ABBREVIATIONS

α-Syn	Alpha-Synuclein
SMI	Small Molecule Inhibitor
TTBK	Tau Tubulin Kinase
TTBK1	Tau Tubulin Kinase 1
TTBK2	Tau Tubulin Kinase 2
AD	Alzheimer's Disease
PD	Parkinson's Disease
TBDPS	Tert-butyl Diphenyl Silane
THP	Tetrahydropyran
DMAP	Dimethyl aminopyridine
DIPEA	Diisopropylethylamine
HATU	1-[Bis(dimethylamino)methylene]-1H-1,2,3-triazolo[4,5-b] pyridinium 3-oxide hexafluorophosphate
EDCi	1-(3-Dimethylaminopropyl)-3-ethylcarbodiimide hydrochloride
TEA	Triethyl amine
DCM	Dichloromethane
LCMS	Liquid Chromatography Mass Spec
TLC	Thin Layer Chromatography
DI water	Deionized Water

ACKNOWLEDGEMENTS

I want to thank Dr Fleur Ferguson for taking me in her lab and teaching me how to become a scientist. Through my struggles and her lessons, I have become a better researcher and mentor to others. Special thanks to Dr. Jiewei Jiang and my undergraduate Shane Douty for helping me with my chemistry as well as Gigi Gadbois for collaboration work with the biology. I would also like to thank Georges Leconte, Andrew Tao, Nate Tran, and Bridget Boyle for continuous support.

Thank you to the Bridge Program at UCSD and bridge faculty Dr. Joerg Schlatterer, Dr. Brian Leigh, Dr. Elizabeth Komives, and Dr. Haim Weizman. I would like to acknowledge the rest of the bridge students at UCSD for comradery and for always being great colleagues.

Thank you to Dr. Anthony Mrse and Dr. Brendan Duggan for NMR use and expert advice on NMR analysis.

Thank you to Dr. Yitzhak Tor, Dr. Eric Romero, and Dr. Philip Low, Dr. Spencer Lindeman, and Dr. Adam Myers for being people I could reach out to during this period.

Lastly thank you to my good friends Javier Sanlley-hernandez, Marc Morizono, Connor Brandenburg, Julianna Follmar, and Ilker Deveci who all gave me tremendous support in tough times, with special thanks to Brianne Mundt.

VITA

Education

M.S. Chemical Biology June 2022
University of California San Diego, La Jolla, CA
- Master's Thesis: *Development of PROTACs for Alpha-synuclein in Parkinson's Disease and Synthesis of Selective Small Molecule Inhibitors for Tau Tubulin Kinase 1*

B.S. Honors Chemistry May 2020
Purdue University, West Lafayette, IN

Experience

Graduate Research Assistant October 2020-May 2022
Dr. Fleur Ferguson Laboratory, UC San Diego, La Jolla, CA
- Developed mechanism and synthesize a library of small molecule PROTACs, intended to induce ubiquitination and degrade aggregated alpha-synuclein targets.
- Purified and characterized compound by UPLC-MS, HPLC, flash chromatography, and NMR.
- Directly supervised undergraduate researchers, conducting training for organic synthesis

Undergraduate Research Assistant January 2018-July 2020
Dr. Philip Low Laboratory, Purdue University, West Lafayette, IN
- Synthesized various organic small molecule drug compounds toward the development of TLR7 agonist derivatives.
- Performed ELISA assays to investigate compound effectiveness.

Dr. Guangjun Zhang Laboratory, Purdue University, West Lafayette, IN
- Performed CRISPR-Cas9 injections and histology examination to establish PRMT5 mutated zebrafish lines for suspected oncogenes.
- Optimized PCR and visualized with gel electrophoresis.
- Maintained care for aquatic specimens and cell cultures.

Teaching Assistantships
Chemistry 40B, Organic Chemistry, UCSD Spring 2021, Winter 2022
Chemistry 7L, General Chemistry, UCSD Fall 2020-Winter 2021
Biology 150, Introductory Biology, Purdue University Spring 2019

Tutor: Anatomy and Physiology, Organic Chemistry August 2017-May 2020
Horizons Program, Purdue University, West Lafayette, IN
- Instructed and mentored students in weekly sessions for anatomy and organic chemistry.
- Customized lesson materials based on the requested needs of the students.

Publications

Tao, A; Gadbois, G; **Buczynski, S**; Ferguson, F. Targeted protein degradation: Emerging concepts and protein state-specific targeting principles. *Current Opinion in Chemical Biology.* April 2022

Presentations

Buczynski, S.; Victor-Napoleon, J; Low P. "Development of a Practical Synthesis of Toll-like Receptor Agonist PF-4171455:4-amino-1-benzyl-trifluoromethyl-1,3-dihydroimidazo[4,5-c] pyridine-2-one". Poster Presentation, Purdue LSAMP Poster Sessions, August 2019, October 2019, March 2020.

Buczynski, S. "Basics of Quality Improvement in Hospital ER and ICU". Lecture Presentation. NUR 100, March 2020

Buczynski, S. "Institute for Healthcare Improvement, Quality Improvement Certification" Weekly Certification Seminars. IHI Purdue, January-May 2020

Buczynski, S.; Zhang G; Kim, B. "Identification of CRISPR mutant for Polyarginine Methyl Transferase 5 genes in Zebrafish". Poster Presentation. Purdue LSAMP Poster Session, August 2018.

Honors and Awards

ACS Bridge Fellowship October 2020- May 2022

- Two-year guaranteed funding for an M.S. degree.

LSAMP Undergraduate Fellowship January 2018-May 2020

- Funded undergraduate research to prepare students for graduate study.

Semester Honors/Dean's List December 2017-May 2020

Learning Beyond the Classroom Certification May 2020

- Over 30 hours of career and professional development, service, citizenship, leadership, and experience with domestic and international diversity.

Recover Hope Campaign Leadership Academy Boston, MA July 2019

- Funded travel to learn and implement project ideas for treatment of substance use disorders.

Affiliations and Leadership

ChemPals Mentor September 2021- May 2022

- Mentor 3 incoming undergraduates in chemistry and provide opportunities for development.

American Chemical Society February 2019-Present

Institute for Healthcare Improvement (IHI), Purdue University August 2016- May 2020

- Purdue Chapter President, supporting club activities and organizing leadership projects.
- Collaborated with IU Arnett Hospital to reduce patient fall rate by 5%, an issue shown within the healthcare system to improve community health.

Phi Kappa Tau May 2017-May 2020

- Executive Council Scholarship Officer, working to increase cumulative Chapter GPA.

Student Hiring Committee, Purdue College of Health and Human Sciences June 2019

- Served in the hiring process for the Student Program Coordinator and Academic Advisor

ABSTRACT OF THE THESIS

Development of PROTACs for Alpha-synuclein in Parkinson's Disease and Selective Small Molecule Inhibitors for Tau Tubulin Kinase 1

by

Stanley Buczynski

Master of Science in Chemistry

University of California San Diego, 2022

Professor Fleur Ferguson, Chair

Misfolded alpha-synuclein has been identified as a potential target to developing disease modifying or preventative therapies for Parkinson's Disease. Proteolytic Targeting Chimeras (PROTACs) have been demonstrated as chemical tools and selective degraders for protein targets in neurodegenerative diseases. PROTACs have already been demonstrated as chemical tools and selective degraders for other neurodegenerative diseases such as targeting tau protein for Frontal Temporal Dementia. Taking previously known binders of alpha-synuclein and proteasomal ligand recruiters a library of PROTACs was synthesized in addition to small molecule degraders with a guanosine-derived autophagy tag, or Autophagy Targeting Chimera (AUTAC), as an alternative form of degradation. Successful development of a selective and potent degrader would allow a better understanding of alpha-synuclein and its role in Parkinson's Disease.

Hyperphosphorylation of Tau is a hallmark of many neurodegenerative diseases. Tau Tubulin Kinase 1 (TTBK1) participates in tau phosphorylation and has been indicated to phosphorylate tau at pathologically relevant sites making it a promising drug target. Small molecule inhibitors exist that can inhibit TTBK1 with off target effects on TTBK2 which has essential functions throughout the nervous system. Utilizing known crystal structures of TTBK1 and TTBK2, selective small molecules were synthesized taking advantage of a peripheral lysine residue which can covalently react with a flour sulfonyl moiety. Using this strategy, separation of TTBK1 and 2 would allow for detailed understanding of their separate and overlapping substrates and biological functions.

CHAPTER 1: Targeted Protein Degradation

1. Intro to Targeted Protein Degradation

Of all drugs currently in the market today about 47% function by inhibiting protein targets to achieve therapeutic effects.[1] This effect is achieved when the drug binds to the protein's active site or in a way that impacts activity at this active site, resulting in inhibition of that protein's activity. This mechanism of inhibition is called occupancy driven pharmacology and through the use of small molecules, new treatment options for disorders have been developed resulting in large quantities of Small Molecule Inhibitors (SMIs) as therapeutic options.[2,3] Unfortunately, these occupancy approaches only can access about 20% of the proteome.[4] Despite continuous medicinal chemistry development for potent and selective SMIs,

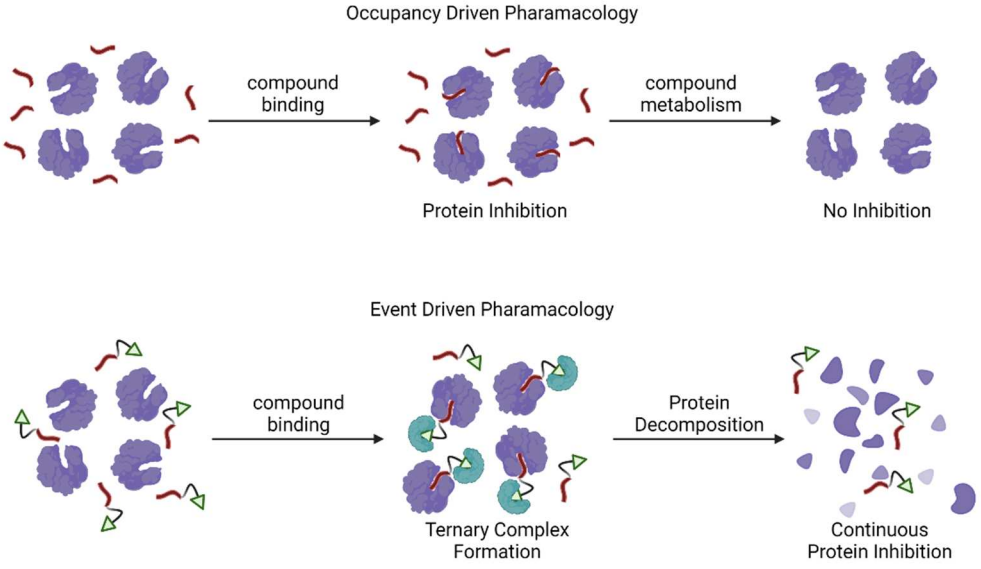

Figure 1 Occupancy Vs Event Driven Pharmacology

there remains a number of "unreachable" protein targets with high biomedical relevance. Biologic modalities such as monoclonal antibodies and oligonucleotide therapies can provide opportunities to address such targets, but these have limitations such as selectivity, intracellular

targeting, tissue penetration, and systemic delivery.[5,6] In the past two decades, emerging therapeutic modalities utilizing small-molecule ligands have been used to redirect cellular protein homeostasis machinery as an alternative development. This novel technique called Targeted Protein Degradation (TPD) has introduced event-driven pharmacology which has proved a powerful tool to overcome these limitations. This method exemplifies superiority over SMIs and other modalities, by eliminating the entire target to delete its scaffolding functions and having the potential to impact non-enzymatic targets. TPD compounds also present a new chemical tool for rapid targeted protein knock-down. (Figure 1) Previously this was possible using gene modification techniques such as CRISPR, RNA interference, or transcription activator-like effector nucleases; however, these approaches have limitations such as not being able to affect rapid protein removal, extending for long durations to achieve desired effect, and also have the potential for complications such as introduction of undesired mutations and cell mortality.[7] For these reasons TPD small molecules has much promise to advance medicine and chemical biology, demanding further research on expansion potential targets for therapeutics and protein knockdown studies.

An important characteristic of these TPD small molecule degraders is the recruitment of endogenous cellular enzymes to degrade protein targets. Protein degradation in cells is a well-regulated process for the turnover of proteins, functioning as a mechanism of quality control during protein folding and ability to degrade proteins based on changes in cellular signals[6]. The Ubiquitin Proteasome System (UPS) is responsible for degrading 80-90% of proteins[8] in cells through two successive steps: covalent attachment of multiple ubiquitin molecules to target protein and degradation of the tagged protein largely by the 26S proteasome. In the first step a ubiquitin is activated by the ubiquitin activating enzyme (E1), a ubiquitin-carrier protein (E2-

ligase) then transfers it to a member of the ubiquitin-protein ligase family (E3-ligase) to which the substrate protein is bound, whereby the ubiquitin then becomes attached to the protein of interest on a lysine or N terminal residue of the substrate.[9] This process is repeated to form a polyubiquitinated chain, this which is then recognized and degraded by nearby proteasomes.

Normally in cells protein degradation takes place based on cell signaling to employ these individual enzymes. However, TPD small molecules can directly recruit the E3-ligases to target proteins. This substrate binding is not required to be an active site of a protein but rather can take place on any site of the protein, significantly increasing the number of possible protein targets. Once binding to both substrates has occurred, a ternary complex is formed, and proximity-based interactions ensue which results in the target protein being ubiquitinated. The ternary complex dissociates and the TPD small molecule can then recruit another target protein.

Currently these TPD small molecules are divided as either bifunctional molecules or molecular glues, however they both functionally bring the protein and E3-ligase within proximity of one another. The main difference is that bifunctional molecules are chimeras consisting of two recruiting moieties connected with a linker where molecular glues bind to an E3-ligase substrate adaptor protein, altering its surface and thereby promoting new interactions with non-endogenous substrates. (Figure 2). Bifunctional molecules are further categorized by mechanism of degradation such as Proteolytic Targeting Chimeras (PROTACs) which utilize the UPS system for degradation, and Autophagy Targeting Chimera (AUTACs)[10] which utilizes the lysosomal dependent mechanism for degradation.[11,12,13]

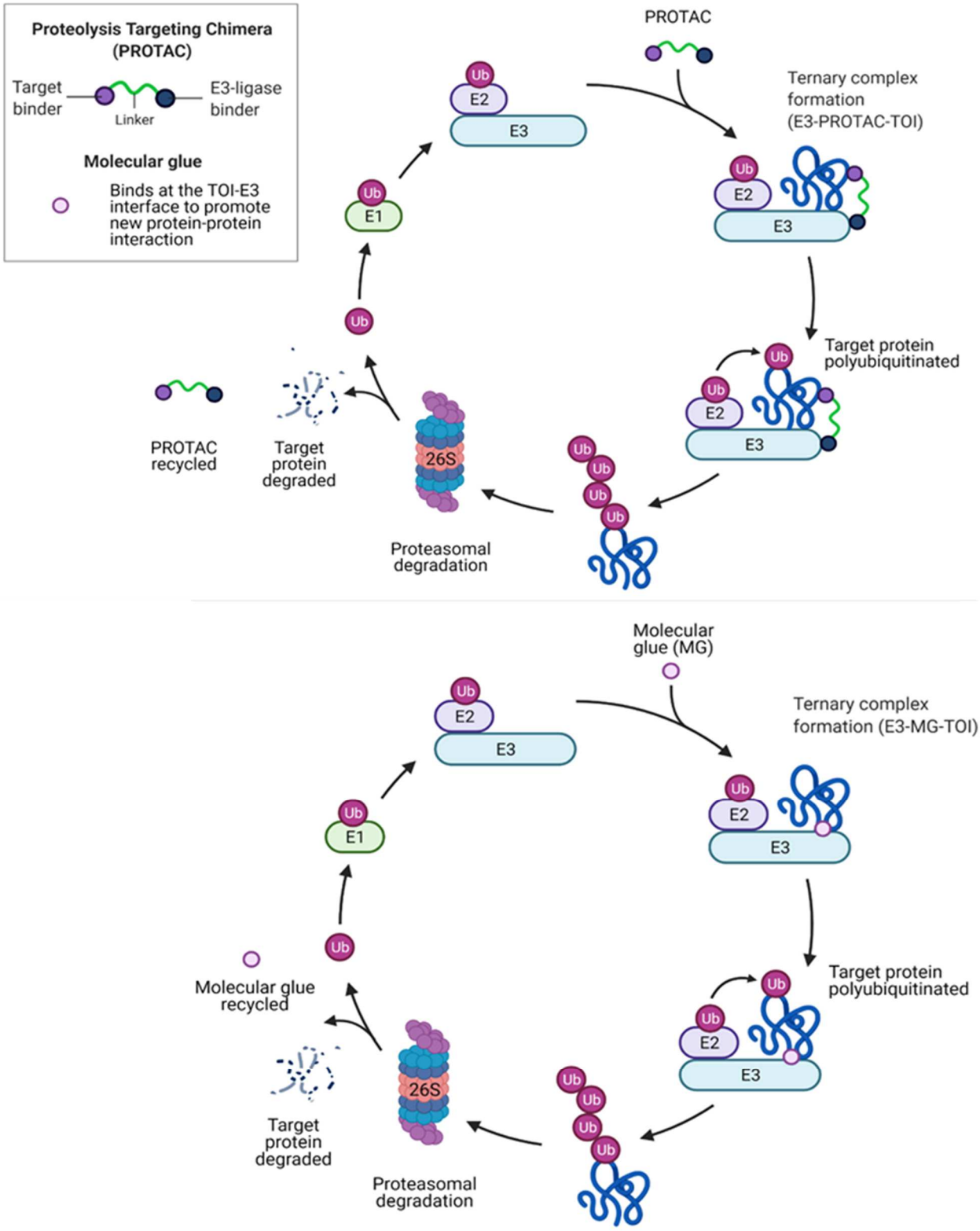

Figure 2 Event Driven Mechanism of Molecular Glues and PROTACs.
TPD small molecules function catalytically on the target of interest (TOI) and are recycled propagating protein degradation.

2. Development of Targeted Protein Degradation

In the late 1900's, potent immunosuppressant natural products rapamycin, and FK506 were shown to modulate T cell activation[14] but there was no obvious connection between their structure and function. This was especially of interest since Cyclosporin A, a substrate of the immunosuppressant cyclophilin[15] was significantly less potent than FK506 despite not showing potent binding to the cyclophilins. Extensive studies by Jun Liu et al. elucidated that unlike Cyclosporin A, FK506 formed a complex with FKBP12, yet both bound to the protein phosphatase calcineurin to express immunosuppressant activity. While they both had different substrates upon which they dimerized it was fascinating to find that these compounds were able to bring two proteins together. It was this discovery in 1991 that prompted the term molecular glue and gave inspiration for what is now the drug space of Targeted Protein degradation.[16]

In 2001, Deshaies lab developed bifunctional peptides that recruited the SCFβ-TRCP E3-ligase to induce the degradation of methionine aminopeptidase-2, exhibiting the first use of a PROTAC in literature to degrade a target of interest.[17] This first report was then followed by development of a hormone linked to a phospho-peptide PROTAC that when microinjected into a cell could induced degradation of androgen and estrogen receptors expanding the target scope.[18] This was further developed by Sakamoto et al in 2004, by using a 9 amino acid peptide fragment as the target bait, they developed molecules that could penetrate the cell membrane, and degrade the androgen targets.[19] Kim, et al built on this in 2007 by using a 5 amino acid length peptide.[20] While these results are groundbreaking for chemical biology and medicine, many issues

persisted still such as the micromolar potency and the use of peptide E3-ligase recruiters which lead to poor cell permeability and compound stability.

This issue was remedied by the significant advancement of small molecule based VHL recruiting ligands which lead to the first all small molecule PROTAC developed by Craig Crews in 2008 [21] showing that developing cell permeable PROTACS are feasible. Efforts to develop more potent degraders were further developed with the identification of the E3-ligase substrate adaptor protein cereblon as the molecular target of small molecule IMiDs such as thalidomide, lenolidomide, and pomalidomide.[22,23] The access to all small molecule based PROTACs with more drug like traits made it possible to then generate highly potent, cell permeable PROTACs leading to the development of these chemical tools being able to induce degradation with a sub-nano molar DC_{50} (concentration at which the target is degraded by 50%).[24]

Today more potent molecular glues and bifunctional molecules are being developed with a focus on finding new degrader ligands and expanding the range of protein targets. One target class that has been challenging to address with traditional methods are the misfolded proteins that occur in neurodegenerative disease. These disorders are characterized by toxic larger order structure composed of misfolded, mis localized, and oligomerized monomers that lack a well-defined active site or fold making them difficult to bind selectively over healthy monomers. In 2019 joint efforts to target these arduous proteins developed one of the first small molecule PROTACs for hyper phosphorylated tau protein in Frontal Temporal Dementia. Their PROTAC, QC-01-175, effectively cleared out tau in patient derived neuronal cell models with minimal impact on tau from healthy neurons indicating specificity for disease relevant forms. This work demonstrated that PROTACs have the potential to be used for other neurodegenerative diseases classified by similar toxic misfolded proteins. Taking inspiration from this study, this work

described seeks to extend the PROTAC space, and develop potent, selective targeted protein degraders of misfolded alpha-synuclein, α-Syn, protein in Parkinsons disease.

CHAPTER 2: Alpha-Synuclein in Parkinson's Disease

1. Introduction

Parkinson's disease is projected as one of the world's fastest growing neurodegenerative disorders in 2017 having a total economic burden of $51.9 billion with estimates of this increasing to $79 billion by 2037.[25] Today there exist treatments only for mild to moderate Parkinson progression with most options only controlling cognitive and behavioral symptoms or reducing impact with dopamine analog drugs. In addition, the exact source and mechanism of PD remains unknown.[26] As a result, there is a critical need for further research into the disease with the hopes of developing disease modifying and potentially preventative therapeutics. The protein alpha-synuclein, α-Syn, has been a major area of study to understand the pathology of PD. A characteristic phenotype seen in patient's brain tissues with this disorder is the accumulation of α-Syn found in a variety of forms as soluble oligomers and as insoluble fibrils found in Lewy Bodies.[27] (Figure 3)

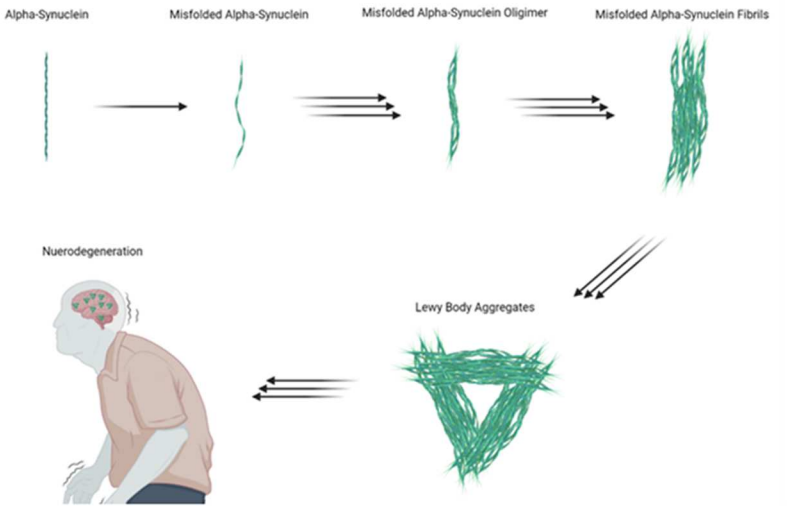

Figure 3 Characteristic formation of Lewy Bodies in Parkinson's Disease

In addition, neuropathological evidence has suggested the presence of aberrant protein as a potential genesis and/or factor which facilitates the propagation of late-stage Parkinson's disease.[28] Healthy α-Syn has been shown to be essential in synaptic neurotransmission and neurotransmitter synthesis as well as in the regulation of genes, calcium levels, and mitochondrial function.[29] Given these findings, it becomes crucial to understand the role of misfolded α-Syn as it accumulates and spreads within the nervous system. Key efforts in understanding its role in PD focus on knocking out mutated SNCA genes, while keeping wild type forms intact. In 2015 research conducted by Burton, et al.[30] showed that shRNA mediated reduction of α-Syn by up to 85% in nigral dopaminergic neurons and dendrites attenuated PD phenotypes, however this treatment also showed various depletions of cell function viability in addition to a 20% decrease in dopamine levels. This result was consistent with previous studies as well.[31,32] The mechanisms underlying these changes are unclear, but potentially reflect an impact on dopamine synthesis, reuptake, or storage occurring in the absence of α-Syn, as part of a wider picture of alterations in neurotransmitter handling at dopaminergic terminals. Other small biologics such as exosome bearing a Lamp2b-RVG (rabies virus glycoprotein) have been explored all with varying degrees of success as well but encounter issues with uses as chemical knockdown tools such as clearance of all healthy alpha-synuclein protein. Utilizing event driven pharmacology in PROTACs have the potential to ameliorate these shortcomings.

PROTACs have been developed for other neurodegenerative disease targets such as misfolded tau protein in Frontotemporal Dementia.[33,34] Using this as motivation, the following study focuses on extending this previous work, to develop PROTACs that target aberrant α-Syn for PD. We hypothesize that using small molecule bifunctional degraders will provide a robust

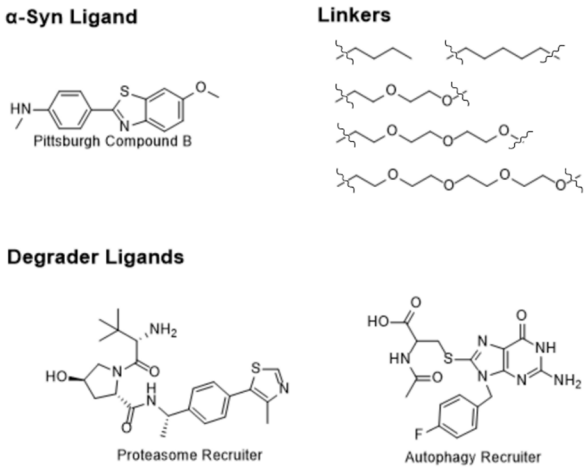

Figure 4 Scaffolds and linker combinations
Proteasome recruiters: Thalidomide variant (left) and Von Hippel Lindau Ligand (right)

and selective method for misfolded α-Syn clearance in cells. To achieve this, a library of bifunctional α-Syn degrader compounds will be produced utilizing known E3-ligase ligands and the established PET tracer Pittsburgh Compound B as the α-Syn recruiter. The linker length and composition will be varied. (Figure 4) In the case that proteasomal degradation does not optimally degrade α-Syn, an alternative library will be synthesized to redirect α-Syn to the autophagy-lysosome pathway (Autophagy Targeting Chimera, AUTAC)[10], which is reported to be the endogenous clearance pathway for intracellular aggregates.[35] Cellular assays will be performed to test E3-ligase cellular target engagement, cell viability, and degradation activity of these small molecules. Afterward if these compounds show promising results, dose response experiments and phenotypic assays will be completed in Parkinson's patient iPSC-derived dopaminergic neurons. (Figure 5) Through the completion of these experiments, we will attempt to identify potent α-Syn small molecule degraders that can be used to investigate its function in disease and perform target validation.

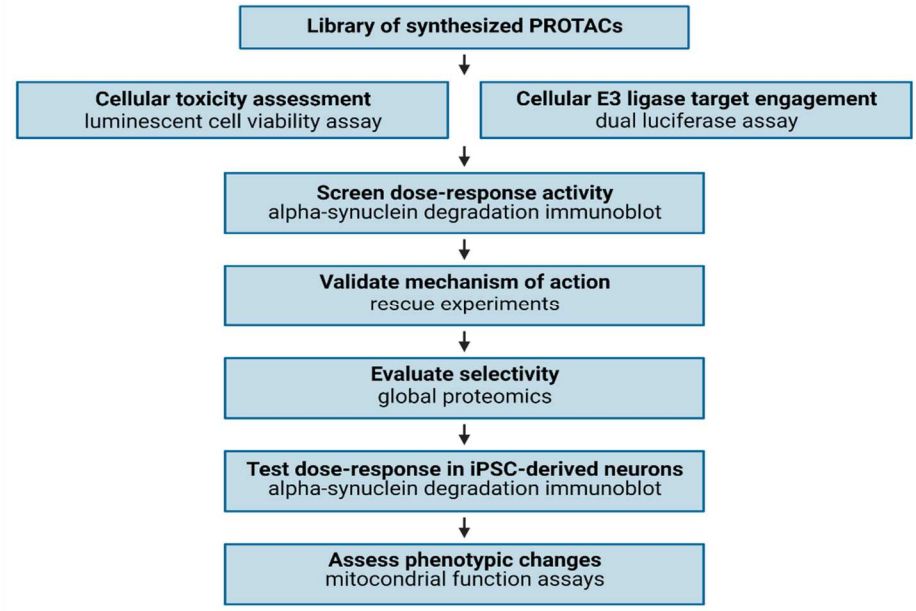

Figure 5 Compound testing workflow.

2. Synthesis

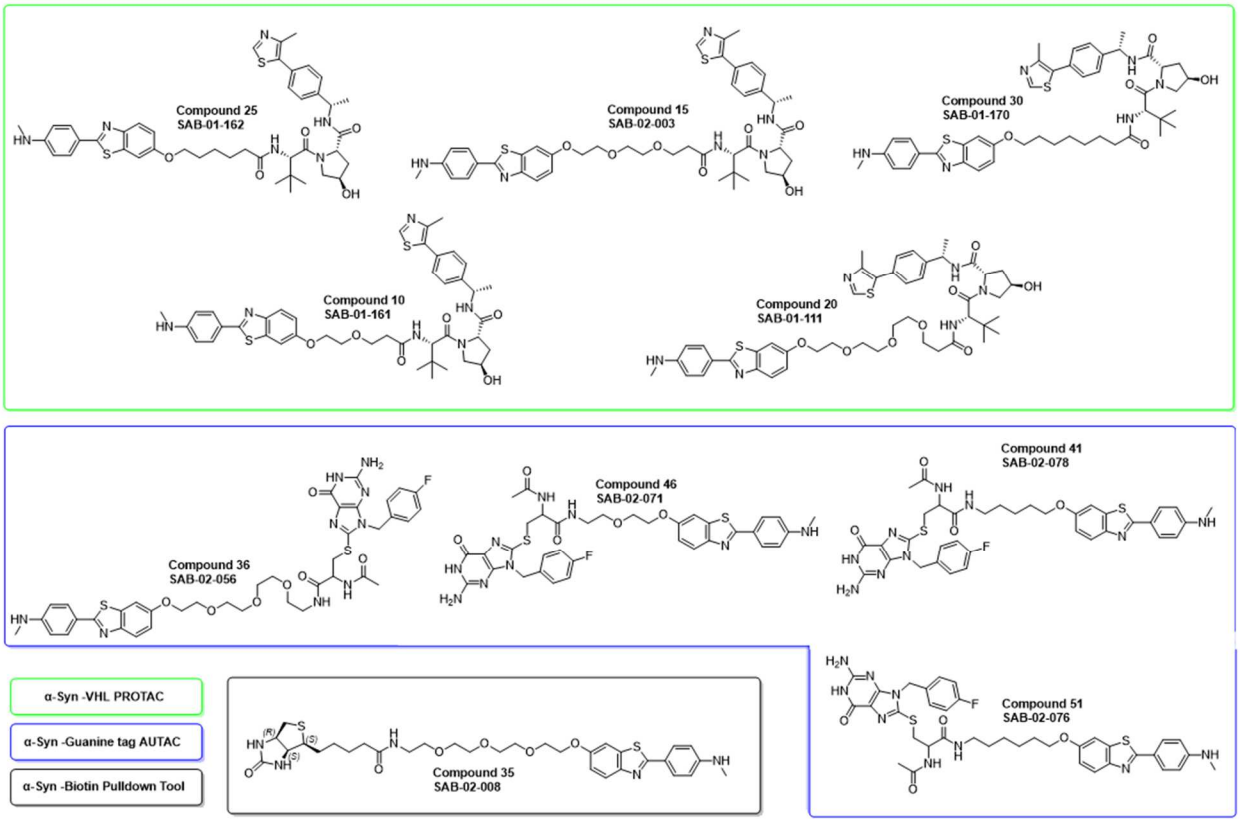

Figure 6 PROTAC, AUTAC, and biotin pulldown compounds synthesized.

A family of small molecules PROTACs was synthesized inspired by the earlier PROTACs in the literature. (Figure 6) This family of compounds consists of structural changes solely with the linker as this would affect ternary complex formation. Linker starting materials were tosylated at the free alcohols. Linker attachment point to the α-Syn ligand was done using a substitution of a tosylate with a phenol. The adjacent side of the linker was a tert-butyl protected acid which was cleaved using Trifluoroacetic acid and subsequently reacted with the free amine of the VH032, VHL ligand, in a HATU coupling to give the final compounds. Various linker lengths were used based on availability and cost. The synthesis of a three-carbon linker PROTAC was attempted but could not be completed due to the rapid reversion of tosylated linker to the free alcohol form. All final compounds were purified on the HPLC without .1%

Trifluoroacetic acid due to observation of α-Syn ligand decomposing with long exposure in acid even when stored in the salt form. Unclear why cleavage of tert-butyl protecting groups did not show decomposition of the α-Syn ligand, however it was verified that decomposition requires several hours before detectable percentages of compound loss occurs. As the deprotection steps took a couple minutes to reach completion and immediately taken to final step after removing solvent in vacuum, the decomposition was not observed until storing in freezer and removed. Future deprotections were changed to hydrochloric acid in dioxane and then in methanol due to better solubility. No decomposition was observed with α-Syn ligand under any amount of time under these conditions.

A second generation of TPD small molecules AUTACs were synthesized focusing on using a guanine tag to recruit the autophagy system of degradation as an alternative to proteasomal degradation. (Figure 7) The synthetic method mirrors that of the PROTAC library, rather utilizing linkers with boc-protected amines. This family of compounds consists of structural changes solely with the linker as this would impact ternary complex formation. Various linker lengths were used based on availability and cost. Upon addition of α-Syn ligand and sequential cleavage of protecting group, the free carboxylic acid of the guanine tag was attached using EDCi coupling conditions. The conversion of product in the EDCi coupling with LCMS and TLC analysis showed good conversion of starting materials however purification was difficult via HPLC due to compound sticking to C18 column. Due to limited starting materials

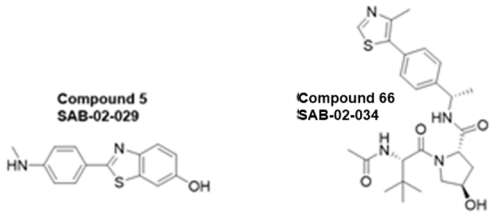

Figure 7 Left PIB, α-Syn binding ligand. Right VHL, VH032 ligand control.

different methods of purification were not attempted since product was being isolated and future work should focus on this when more generations of AUTAC compound are generated. Lastly a biotin variant was synthesized using the same synthetic scheme as the AUTAC series for measuring predicted physical interactions between α-Syn ligand and fibrils.

Compound 5 was produced in an efficient three step scheme using Suzuki coupling conditions followed by reductive amination, and then demethylation using boron tribromide. Compound 66 was produced from a HATU coupling reaction of VH032 with acetic acid. All final PROTACs, AUTACs, ligands, and control compounds were dissolved in deuterated DMSO as a 10mM stock solution and stored in a -20C^{o} freezer.

3. Cell Viability

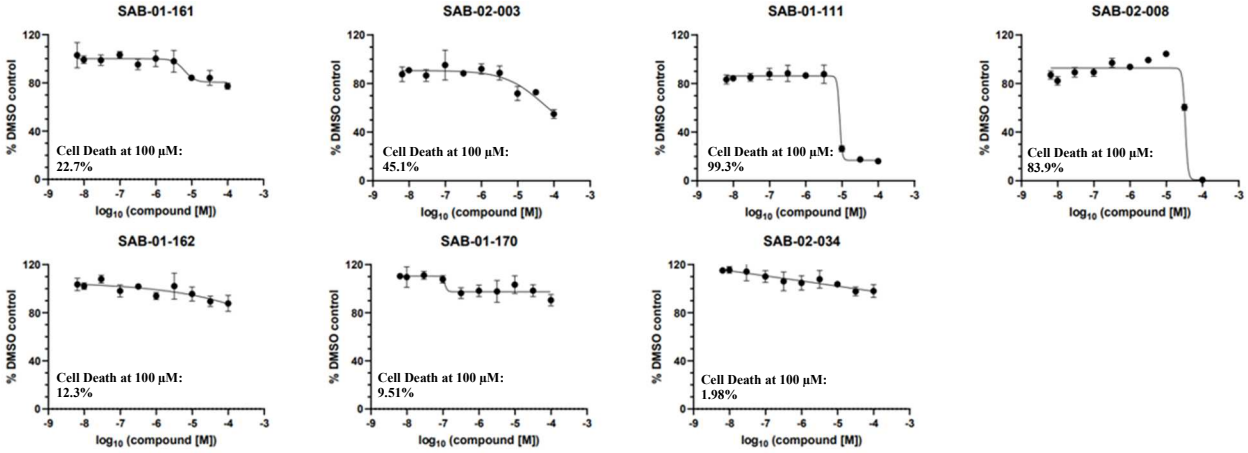

Figure 8 Cell Titer Glow Viability Assay collected in triplicate. %DMSO defines percentage of cell viability compared to DMSO control as a function of concentration.

Cell viability experiment performed to determine toxicity of compounds. This was achieved using a cell titer glow kit. Cells were plated and exposed to varying concentrations of compound. Oxyluciferin was then mixed with plated cells and allowed to react with ATP produced by mitochondria in living cells which produced a luminescence. This was measured

and compared with a control to determine cell viability. This result will be used to help optimize conditions for degradation assays. Compounds SAB-01-111 had an IC50= 33.9 μM and 99.3% cell death at 100 μM. Compounds SAB-02-008 had an IC50= 8.7 μM and 83.9% cell death at 100 μM. These two compounds both had significant increases in potency while the remainder showed minimal cytotoxicity. (Figure 8) It's unclear why both compounds show increased mortality in cells, but both compounds are comprised of PEG-4 linkers suggesting that increased linker length may adversely affect cell viability. Typical dosing of PROTACs range from micro molar, 10^{-6}, to nano molar, 10^{-9} and these values indicate that at these standard values there should not be cell death observed.

4. E3 Ligase Target Engagement

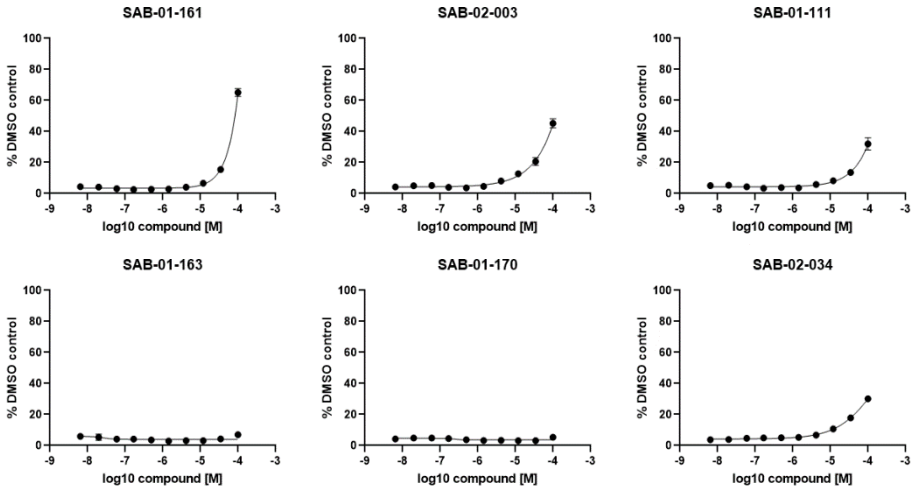

Figure 9 Dual luciferase dTAG competition assay collected in triplicate. %DMSO defines percentage of fluorescence compared to DMSO control as a function of concentration.

This experiment measures cellular target engagement of targeted protein degraders using a dual luciferase competition assay. Higher NLuc:Fluc ratios or % DMSO indicates more Target Engagement. The control compound SAB-02-034 shows lower target engagement than desired compared to tested variable compounds. Compounds from SAB-01-161, SAB-02-003, and SAB-

01-111 seem to penetrate and engage VHL at the highest concentration. (Figure 9) These engaged compounds all have polyethylene glycol linkers suggesting that this may help with permeation of cell membrane unlike SAB-01-162 and SAB-01-170 which have aliphatic linkers. However, no, or little target engagement has been seen for compounds that are able to penetrate the cells and engage E3 Ligase.

5. Western Blots

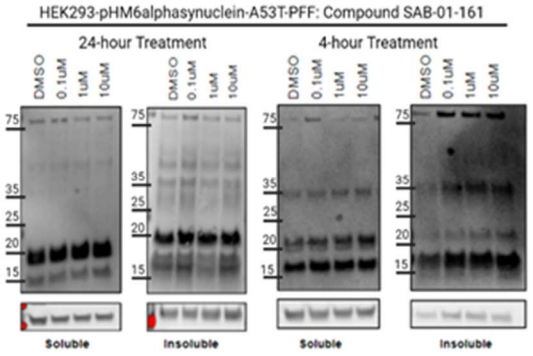

Figure 10 Alpha Synuclein degradation visualized with western blots of HEK 293 cells. Cells treated with preformed alpha-synuclein fibrils. Ladder values measured in kDa.

The results of this experiment test a range of optimum protein degradation conditions. Plated cells are exposed to compound for varying amount of time and differing concentrations. The cells are then lysed, and protein concentrations quantified with western blots. This data shows an example of what the results will look like for all compound synthesized. The blots shown above for SAB-01-161 does not show significant degradation of alpha-synuclein protein. (Figure 10) This is evidence that this compound is likely not going to be promising for studies in differentiated neurons.

6. Conclusion

Preliminary batches of compounds have been synthesized with ongoing analysis continuing. From results obtained, exclusively PEG4 containing compounds SAB-01-111 and

SAB-02-008 are toxic to cells at higher concentrations. This is important for determining dose concentrations to be used for degradation experiments. In the case that these compounds do exhibit activity this observation must be further investigated to understand this toxicity or the PROTAC's optimized to reduce toxicity while keeping potency. The E3 ligase target engagement experiments show that PROTAC's with PEG linkers are the most cell permeable regardless of length. While promising data for positive target engagement it must be noted that compounds that perform poorly in this experiment can be potent degraders. This could be a result of the catalytic, event driven pharmacology activity of PROTACs where even small amounts of target engagement can be enough for potent target degradation. The relationship between linker length and composition is not clear given these results. Data from the dose response experiments are ongoing. Future directions of this study from a synthesis perspective would be to focus on making other small molecules using other known α-synuclein ligands with different combination of linkers and degraders. Current options of alternative degraders are not as expansive, but much research is being done to elucidate these other mechanisms. Collaborations with computational labs can also be useful to model the ternary complex formation with variations of the linker, binder, or degrader. This could be used to predict compounds that would have favorable ternary complex functions for better target protein degradation. It is very likely that these compounds produced will not end up being potent compounds which is why it is important to follow up on these alternative options.

CHAPTER 3: Tau Tubulin Kinase

1. Introduction

Hyperphosphorylation of Tau protein is hallmark of many neurodegenerative diseases. Tau Tubulin Kinases (TTBKs) are kinases involved in tau phosphorylation and have been indicated to phosphorylate tau at pathologically relevant sites making them promising drug targets. TTBK's are a serine/threonine and tyrosine kinase closely related to the large family of casein kinase 1 proteins. There are two isoforms of TTBK: Tau Tubulin Kinase 1 (TTBK1) first described in 2006 as a protein playing a role in tau phosphorylation at Alzheimer's Disease related sites in addition with tau aggregation[36], and Tau Tubulin Kinase 2 (TTBK2) presented in 1995 as a novel tau-tubulin kinase purified from bovine brain[37]. TTBK1 is a central nervous system kinase while TTBK2 is ubiquitously expressed that in addition to phosphorylating tau has cellular processes such as mitosis[38], ciliogenesis[39], microtubule dynamics[40], and neurotransmitter trafficking.[41]

Mutation in both isoforms have been shown to result in different pathological outcomes. TTBK2 variants cause a rare neurological disorder called spinocerebellar ataxia type 11 (SCA11), characterized by cerebellar atrophy, loss of Purkinje cells and abnormal tau deposition in the brain stem and cerebral cortex. Furthermore Bouskila et al has shown that in TTBK2 homozygous modified mice, very serious brain developmental deficiencies and indistinct brain subdivision occur showing the importance of TTBK2 and its deleterious effect when inhibited.[42] Both TTBK1 and TTBK2 have been implicated in amyotrophic lateral sclerosis and frontal temporal dementia, where they phosphorylate Ser409 and Ser410 known to be key characteristics of toxic TAR DNA binding aggregation.[43] Phosphorylation of Ser208, Ser210, Ser198, Ser199, Ser202, and Ser422 by TTBKs are linked to phenotypes observed in

Alzheimer's Disease with TTBK1 found to be upregulated in the frontal cortex of patients with the devastating disease.[44]

2. Tau Tubulin Kinase Selectivity

The two isoforms of TTBK are encoded from different genes, have different tissue localizations, yet have 87% of a homology, and their active sites have a 96% similarity with the same lysine and aspartic acid catalytic residues in their kinase domain.[36] The similarity between TTBK1 and TTBK2 makes it difficult to create a selective inhibitor. Previous work has identified inhibitors that are able to bind to both TTBKs which prevents the isolated study of each protein in the brain. This is especially important for TTBK1 which has a more critical role in phosphorylation for Alzheimer's Disease. As such there is need to investigate alternative ways of targeting TTBK1 selectively over TTBK2 to understand its physiological role in pathology.

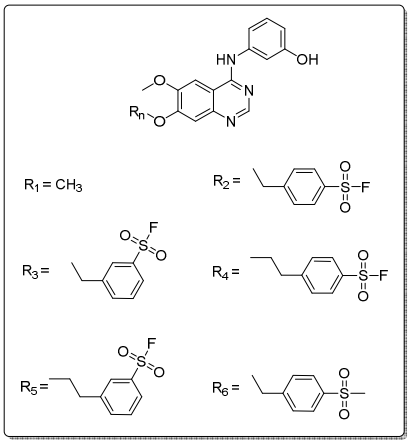

Figure 11 DTQ (R_1) and variations (R_2, R_3, R_4, R_5,) for targeted TTBK1 inhibition. Para methyl sulfonyl moiety (R6) acts as a reversible control in kinase activity experiments.

Molecular docking simulations from collaborators at the University of Chicago have shown that the previous small molecule inhibitor, 3-((6,7-dimethoxyquinazolin-4-yl)amino)phenol (DTQ), has the potential to be modified with a fluoro-sulfonyl moiety. (Figure 11) Attaching this functional group on the "down" methoxy with variations of its position can take advantage of a free lysine residue next to the ATP binding site in TTBK1 that does not exist in TTBK2. The nucleophilic amine on the lysine would covalently interact with the fluoro-sulfonyl group whereas the arginine in TTBK2 would not. (Figure 12) This covalent binding strategy would selectively cause the small molecule to bind in this ATP pocket and remain bound due to fluorine substitution cause by the inherent structure of TTBK1. We hypothesize that the small molecule inhibitors would show a preference for TTBK1 over TTBK2 allowing it to be studied in isolation of TTBK2 inhibition. To achieve this a set of compounds based on DTQ will be synthesized: DTQ fluoro-sulfonyl modified compounds with the fluoro-sulfonyl in the para and meta position, a methyl substituted sulfonyl group located on the para position to act as a control, and the original DTQ control compound. The structure activity relationships from this study will not only prove beneficial for future drug development, but it will also allow us to learn more about the cellular consequences of inhibiting TTBK1 kinase activity.

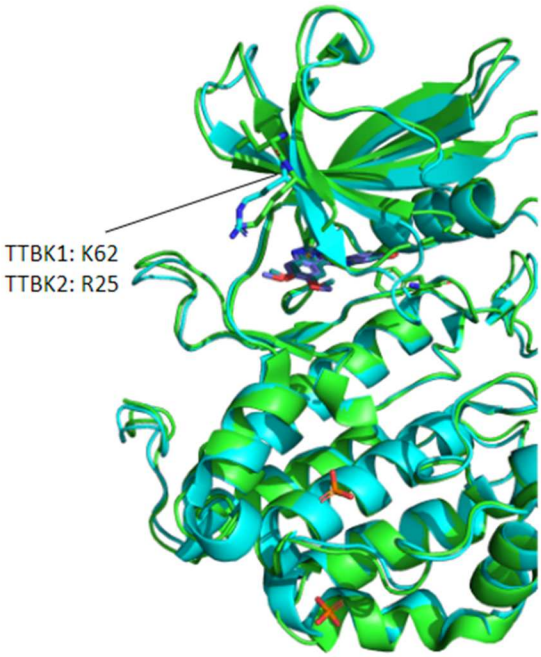

Figure 12 PDB structure 4BTK of TTBK1 with free lysine residue.

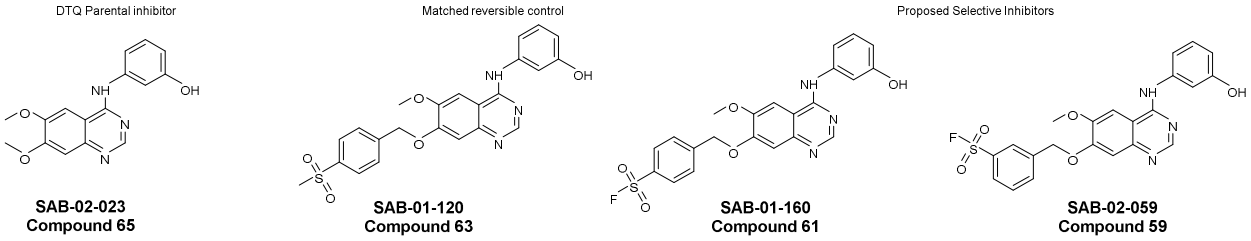

Figure 13 Compounds synthesized for TTBK1 selectivity.

Small molecules were synthesized based on the Parental Inhibitor DTQ. (Figure 13) This family of compounds consists of structural changes at the bottom methoxy group with additions of sulfonyl-benzenes at different positions with either a fluorine or methyl at the sulfonyl group. 3-nitrophenol starting material was protected at the alcohol with a tetrahydropyran ether with catalytic 4-methylbenzene sulfonic acid. The nitro group subsequently reduced with palladium on carbon to give an aniline. This aniline was suitable for an electrophilic aromatic substation by refluxing isopropanol with dimethoxy quinazoline to yield compound 65, DTQ parental inhibitor, after TFA deprotection of tetrahydropyran.

For the remainder of the compounds a similar approach was taken and the aniline starting material was then reacted with 7-(benzyloxy)-4-chloro-6-methoxyquinazoline and the benzyl ether cleaved with a palladium on carbon reduction to give the free phenol. The following reaction required the use of a benzo-haloalkane to be reacted with the phenol. However, upon completion the reaction it was found that the benzo-haloalkane had preferred electrophilicity for the secondary amine over the alcohol. (Figure 14a) As such it was determined that the amine

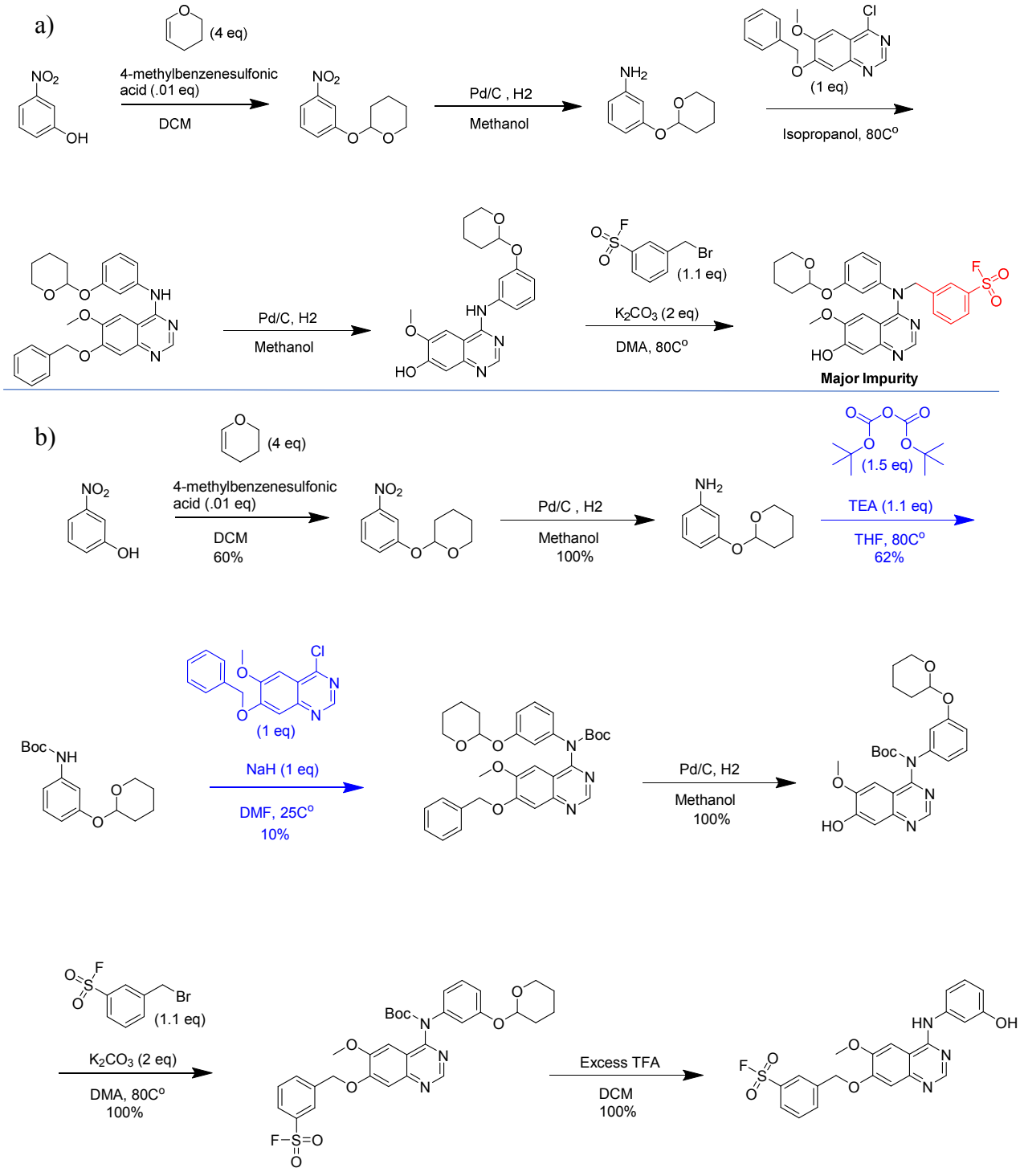

Figure 14 Adjustment to TTBK1 compound scheme.

must be protected. However, developing conditions was not successful to protect the amine while attached to the quinazoline ring. It was determined that the addition of a tert-butyl carbamate protecting group could be attached after generation of the free aniline from the nitro group but subsequent coupling to the quinazoline ring gave at most 10% yield. The most efficacious method was found to be a sodium hydride catalyzed coupling of the carbamide. Given the need to produce only milligrams of product, this was deemed sufficient for the scheme. The product of this sodium hydride coupling was then reduced at the benzyl ether with palladium on carbon to produce the free phenol. Benzo halo-alkane substitutions were effective without the competing amine and allowed easy TFA deprotection of tert-butyl carbamate and tetrahydropyran to final compounds 63, 61, and 59. (Figure 14b) All final compounds were purified on the HPLC and dissolved in deuterated DMSO as 10mM stock solutions. Final compounds subsequently stored in -20C for assay use.

4. Conclusion

The compounds synthesized were sent to be tested and results for their kinase specificity is ongoing. While these compounds were able to be synthesized, more work needs to be done to increase yield of the carbamide coupling. For the purposes of this study the results were sufficient but for producing more analogs, it is necessary to develop a better scheme. This coupling was repeated multiple times to achieve desired amounts of products which prolonged the results. It could be offered to upscale this step as the 10% yield was seen regardless of how much material was used, and all starting materials were able to be obtained in good yield. While requiring increased costs for more starting material is undesirable, the largest consideration is time spent needing to repeat the reaction. All other steps of the scheme were efficacious and as such it may not be necessary to amend this one step. More work can be done producing alternative analogs of the DTQ structure. For example, further changing the position of flour sulfonyl substitution, attaching the benzene moiety to the “up” methoxy, and including differing lengths from the parent quinazoline ring. There are other structures capable of binding to TTBKs and inhibiting their function as well which further provides more scaffolds to use if the compounds from this study prove ineffective.

EXPERIMENTAL

Experimental Procedures

Chapter 2

Chemical Compound Information

All chemicals, unless otherwise stated, were commercially available and used without further purification. 2-(4-(methylamino)phenyl)benzo[d]thiazol-6-ol[45], (2S,4R)-1-((S)-2-amino-3,3-dimethylbutanoyl)-4-hydroxy-N-((S)-1-(4-(4-methylthiazol-5-yl)phenyl)ethyl)pyrrolidine-2-carboxamide [46] were synthesized as previously described. All reactions were carried out in anhydrous conditions and commercially available anhydrous solvents were used. Analytical LCMS was performed using MilliQ water with .1% formic acid and acetonitrile using a packed column (Acquity UPLC BEH C18, 2.1mm x 50mm, 1.7 um). TLC was carried out on pre-coated silica plates 60F254 (Merck) with visualization via UV light (UV 254 nm). In 1H NMR data, chemical shifts are quoted in ppm and referenced to the residual solvent signals (DMSO-d6, d = 2.50; Methanol-d4, qu = 3.31; Chloroform-d, s = 7.26), and signal splitting patterns are described as singlet (s), doublet (d), triplet (t), quartet (q), quintet (qu), multiplet (m), and broad (br). Coupling constants (JH-H) are measured in Hz. Preparative HPLC was performed on a WATERS HPLC system using methanol and water with a Packed Column (XBridge Prep C18, 19 mm x 100 mm; 5 um OBD). Purities of assayed compounds were in all cases greater than 95%, as determined by reverse-phase HPLC analysis.

Synthesis of Compound 5 (SAB-01-100)

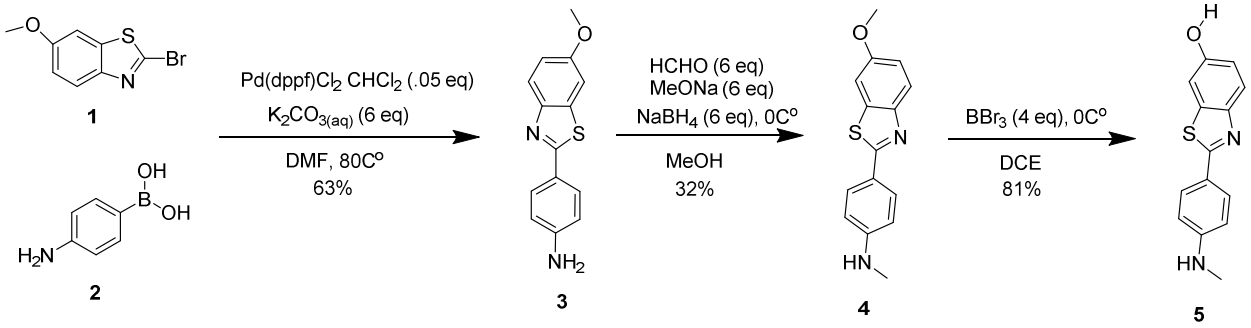

*(**1**)→ (**3**)*

4-(6-methoxybenzo[d]thiazol-2-yl)aniline

2-Bromo6-methoxybenzothiazole **1** (1 eq, 500 mg, 2.05 mmol) and 4-aminophenyl boronic acid, HCl **2** (1.1 eq, 391 mg, 2.25 mmol) were dissolved in 10 mL of DMF in the presence of 6.14 mL of 2 M K_2CO_3 (6.0 eq, 12.3 mmol). After 20 minutes under nitrogen bubbling, $Pd(dppf)Cl_2$, CH_2Cl_2 (.05 eq, 74.5 mg, 102 umol) was introduced, and the reaction was performed at 80 C for 3 h monitoring by LCMS and TLC. Once cooled down the reaction mixture was mixed with 100 mls of saturated sodium bicarbonate and extracted out with 3x 50ml washes of ethyl acetate. The organic layers were then combined and washed with 50mls of saturated sodium bicarbonate. This organic layer was then dried and prepped for flash column chromatography (20-60% ethyl acetate in hexane) to give **3** (331mgs, 2.05mmol, 63% yield) ^{1}H NMR (500 MHz, DMSO-D_6) δ 7.78 (dd, J = 8.8, 3.1 Hz, 1H), 7.73 – 7.66 (m, 2H), 7.60 (t, J = 2.4 Hz, 1H), 7.08 – 7.01 (m, 1H), 6.68 – 6.61 (m, 3H), 5.84 – 5.80 (m, 3H), 3.82 (d, J = 2.8 Hz, 3H). MS (ESI) m/z 255.32 [M+H]

*(**3**)→ (**4**)*

4-(6-methoxybenzo[d]thiazol-2-yl)-N-methylaniline

3 (1 eq, 200 mgs, 780 umol), sodium methoxide (6 eq, 253 mgs, 4.68 mmol), paraformaldehyde (6 eq, 380 mgs, 4.68 mmol), and sodium methoxide (6 eq, 253 mgs, 4.68 mmol) were dissolved in 5 ml anhydrous methanol and refluxed for 12 hours. Afterward the reaction was cooled down to room temperature and placed in an ice bath. Sodium borohydride (6 eq, 177 mgs, 4.68 mmol) was then added portion wise and the reaction stirred for 10 minutes before heating back to reflux for another 2 hours. Reaction was monitored with LCMS and TLC for consumption of starting material before methanol was removed in vacuo. The crude mixture was then mixed with 70mls of brine and extracted out with 3x 20mls washes of dichloromethane. This organic layer was dried down and purified with flash column chromatography (10-50% ethyl acetate in hexane) to give **4** as a yellow powder. (68 mgs, 249 umol, 32% yield) Starting material was able to be recovered for subsequent reactions. ^{1}H NMR (500 MHz, $CDCl_3$) δ 7.81 – 7.72 (m, 3H), 7.60 (t, J = 2.6 Hz, 1H), 7.05 (dd, J = 8.9, 2.6 Hz, 1H), 6.66 – 6.60 (m, 2H), 6.40 (q, J = 4.9 Hz, 1H), 3.82 (s, 3H), 2.74 (d, J = 4.9 Hz, 3H), 1.37 (s, 1H). MS (ESI) m/z 270.35 [M+H]

*(**4**)→ (**5**)*

2-(4-(methylamino)phenyl)benzo[d]thiazol-6-ol

4 (1 eq, 98 mgs, 360 mmol) was mixed with 4 mls dichloroethane and cooled down to 0C°. Bromine-tribromide (4 eq, 230 mgs, 91mmol) was then added and the reaction allowed to stir to room temperature. Then the mixture was heated to 80C° for 3 hours and monitored for product formation using LCMS and TLC. This reaction mixture was then cooled down and quenched using saturated sodium bicarbonate until pH was at 7. This aqueous mixture was then washed with 3x 30 ml of ethyl acetate or until aqueous layer began to lose its yellow color. The organic layer was then dried to give **5** (75 mgs, 290 mmol, 81% yield) as a yellow powder. ^{1}H NMR (500 MHz, DMSO-D6) δ 9.71 (s, 1H), 7.76 – 7.67 (m, 2H), 7.31 (d, J = 2.4 Hz, 1H), 6.90 (dd, J = 8.7, 2.4 Hz, 1H), 6.62 (dd, J = 9.2, 2.3 Hz, 2H), 6.36 (q, J = 4.8 Hz, 1H), 2.74 (d, J = 5.0 Hz, 3H). MS (ESI) m/z 256.32 [M+H]

Synthesis of Compound 10 (SAB-01-161)

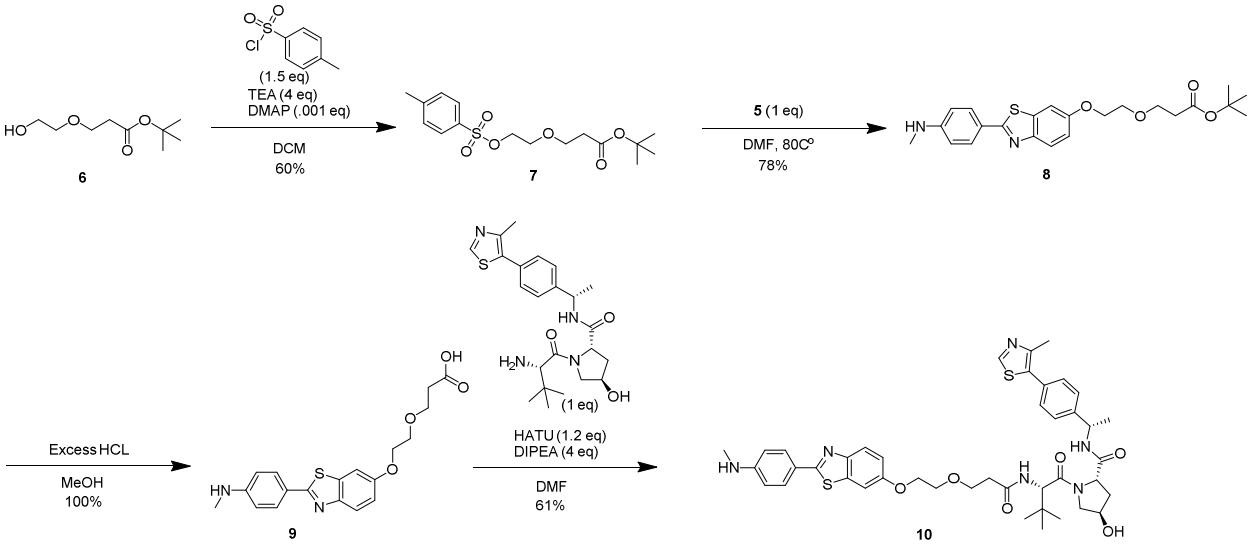

*(**6**)→ (**7**)*

tert-butyl 3-(2-(tosyloxy)ethoxy)propanoate

Tert-butyl 3-(2-hydroxyethoxy)propanoate **6** (1 eq, 50mgs, .26 mmol), triethylamine (4 eq, 0.15ml, 1.1 mmol), and catalytic DMAP (.001 eq, 32 ug, 0.26 umol) were mixed with 1 ml of dichloromethane under anhydrous conditions. The solution was cooled to 0°C in an ice bath and then 4-methylbenzenesulfonyl chloride (1.5 eq, 1.570 mgs, .37 mmol) was added dropwise. The reaction was removed from ice bath and left to mix overnight (12 hours). This was monitored by LCMS and TLC until reached completion. Crude reaction was mixed with 10mls of dichloromethane and washed with 3x 10mls of DI water. Organic layer was concentrated down and purified by flash column chromatography (0-30% ethyl acetate in hexane) to give **7** was a colorless oil. (54mgs, .16 mmol, 60% yield) ^{1}H NMR (500 MHz, $CDCl_3$) δ 7.78 (d, J = 8.0 Hz,

2H), 7.33 (d, J = 8.0 Hz, 2H), 4.12 (t, J = 4.9 Hz, 2H), 3.62 (q, J = 4.1 Hz, 4H), 2.43 (s, 3H), 2.40 (t, J = 6.4 Hz, 2H), 1.42 (s, 9H). MS (ESI) m/z 344.42 [M+Na]

*(**7**)→ (**8**)*

tert-butyl 3-(2-((2-(4-(methylamino)phenyl)benzo[d]thiazol-6-yl)oxy)ethoxy)propanoate

5 (1 eq, 20 mgs, 0.078mmol) was mixed with potassium carbonate (2 eq, 22mgs, 0.16 mmol) and 1 ml DMF 80C° for 10 minutes. Afterward **7** (1 eq, 20 mgs, 0.078 mmol) was added to this mixture and reaction monitored over 16 hours. Product was confirmed with LCMS and TLC. Reaction mixture was mixed with 30mls saturated sodium bicarbonate and extracted with 3x 10mls ethyl acetate. The organic layer was then washed with 10mls DI water and organic layer concentrated. This crude mixture was purified with flash column chromatography (0-50% ethyl acetate in hexane) to give **8** as a yellow wax. (26 mgs, .061 mmol, 78% yield). ^{1}H NMR (500 MHz, $CDCl_3$) δ 7.77 – 7.70 (m, 3H), 7.40 (d, J = 2.5 Hz, 1H), 7.05 (dd, J =8.9, 2.5 Hz, 1H), 6.65 – 6.59 (m, 2H), 4.16 (s, 2H), 3.81 (dd, J = 16.8, 10.4 Hz, 4H), 2.90 (s, 3H), 2.54 (t, J = 6.5 Hz, 2H), 1.44 (s, 9H). MS m/z 428.55 [M+H]

*(**8**)→ (**10**)*

(2S,4R)-1-((S)-3,3-dimethyl-2-(3-(2-((2-(4-(methylamino)phenyl)benzo[d]thiazol-6-yl)oxy)ethoxy)propanamido)butanoyl)-4-hydroxy-N-((S)-1-(4-(4-methylthiazol-5-yl)phenyl)ethyl)pyrrolidine-2-carboxamide

8 (26 mgs, 0.061 mmol) was mixed with 1 ml dichloromethane and 1 ml trifluoroacetic acid. After 5 minutes product conversion was observed on TLC and confirmed on the LCMS. Reaction mixture was concentrated down and dried further on the high vacuum to give **9** as a thick yellow oil. This dried mixture was then taken directly to the next step. MS (ESI) m/z 372.44 [M+H]
(2S,4R)-1-((S)-2-amino-3,3-dimethylbutanoyl)-4-hydroxy-N-((S)-1-(4-(4-methylthiazol-5-yl)phenyl)ethyl)pyrrolidine-2-carboxamide, Trifluoroacetic acid, (1 eq, 14 mgs, .025 mmol) was mixed with HATU (1.2 eq, 11 mgs, 0.030 mmol), DIPEA (4 eq, 17 ul, 0.099 mmol) in 1 ml of DMF for 15 minutes. Afterward **9** (1 eq, 12 mgs, 0.025 mmol) was added and reaction monitored by LCMS and TLC before full conversion was observed in 30 minutes. Reaction was then filtered with PTFE Syringe Filters, 0.22 um, 17mm and injected for purification with High Pressure Liquid Chromatography (0 to 80% H_2O/Methanol, duration of 45 min, flow rate of 20 mL/min, detection at 254 nm). Product fraction were concentrated down and lyophilized to give **10** as a white powder. (12.1 mgs, .0151 mmol, 61% yield) ^{1}H NMR (400 MHz, DMSO-D6) δ 8.98 (s, 1H), 8.39 (d, J = 7.8 Hz, 1H), 7.93 (d, J = 9.3 Hz, 1H), 7.81 – 7.71 (m, 3H), 7.60 (d, J = 2.6 Hz, 1H), 7.43 (d, J = 8.3 Hz, 2H), 7.39 – 7.29 (m, 2H), 7.05 (dd, J = 8.9, 2.6 Hz, 1H), 6.67 – 6.60 (m, 2H), 6.42 (d, J = 5.2 Hz, 1H), 5.13 (s, 1H), 4.91 (p, J = 7.1 Hz, 1H), 4.54 (d, J = 9.3 Hz, 1H), 4.42 (t, J = 8.1 Hz, 1H), 4.28 (s, 1H), 4.14 (t, J = 4.6 Hz, 2H), 3.82 – 3.54 (m, 6H), 2.74 (d, J = 3.9 Hz, 3H), 2.58 (dt, J = 14.5, 7.0 Hz, 1H), 2.47 – 2.34 (m, 4H), 2.01 (ddd, J = 10.6, 7.8, 2.5

Hz, 1H), 1.78 (ddd, J = 12.9, 8.6, 4.6 Hz, 1H), 1.36 (d, J = 7.0 Hz, 3H), 0.93 (s, 9H). MS (ESI) m/z 799.02 [M+H]+[M/2]

Synthesis of Compound 15 (SAB-02-003)

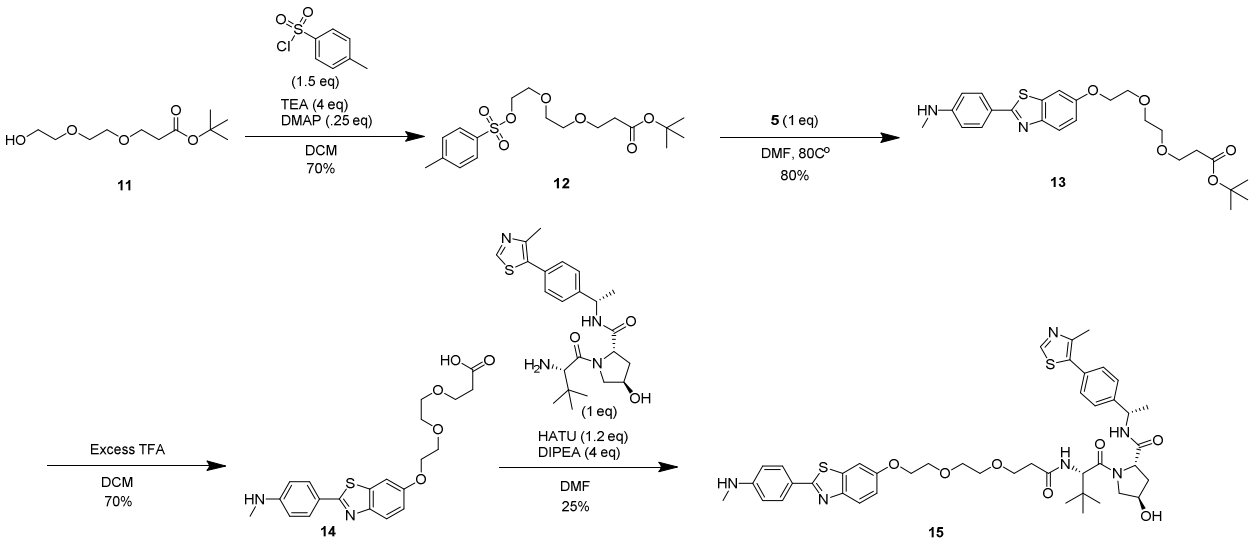

*(**11**)→ (**12**)*

tert -butyl 3-(2-(2-(tosyloxy)ethoxy)ethoxy)propanoate

tert-butyl 3-(2-(2-hydroxyethoxy)ethoxy)propanoate **11** (1 eq, 40mgs, 0.17 mmol), triethylamine (4 eq, 0.095ml, 0.68 mmol), and catalytic DMAP (0.25 eq, 5.2 mg, 0.043 mmol) were mixed with 1 ml of dichloromethane under anhydrous conditions. The solution was cooled to 0°C in an ice bath and then 4-methylbenzenesulfonyl chloride (1.5 eq, 49 mgs, 0.26 mmol) was added dropwise. The reaction was removed from ice bath and left to mix overnight (14 hours). This was monitored by LCMS and TLC until reached completion. Crude reaction was mixed with 10mls of dichloromethane and washed with 3x 10mls of DI water. Organic layer was concentrated down and purified by flash column chromatography (20-40% ethyl acetate in hexane) to give **12** as a colorless oil. (46.3mgs, 0.119 mmol, 70% yield) ^{1}H NMR (500 MHz, METHANOL-D4) δ 7.79 (d, J = 8.3 Hz, 2H), 7.44 (d, J = 8.0 Hz, 2H), 4.16 – 4.10 (m, 2H), 3.68 – 3.61 (m, 4H), 3.52 (s, 4H), 2.46 (s, 3H), 2.45 (t, J = 6.2 Hz, 2H), 1.44 (s, 9H). MS (ESI) m/z 388.16 [M+Na]

*(**12**)→ (**13**)*

tert-butyl 3-(2-(2-((2-(4-(methylamino)phenyl)benzo[d]thiazol-6-yl)oxy)ethoxy)ethoxy)propanoate

5 (1 eq, 15 mgs, 0.059mmol) was mixed with potassium carbonate (2 eq, 16mgs, 0.12 mmol) and 1 ml DMF 80C° for 10 minutes. Afterward **12** (1 eq, 23 mgs, 0.059 mmol) was added to this mixture and reaction monitored over 16 hours. Product was confirmed with LCMS and TLC. Reaction mixture was mixed with 30mls saturated sodium bicarbonate and extracted with 3x

10mls ethyl acetate. The organic layer was then washed with 10mls DI water and organic layer concentrated. This crude mixture was purified with flash column chromatography (20-50% ethyl acetate in hexane) to give **13** as a yellow wax. (22.4 mgs, 0.047 mmol, 80% yield). ^{1}H NMR (500 MHz, METHANOL-D4) δ 7.80 – 7.73 (m, 3H), 7.43 (d, J = 2.5 Hz, 1H), 7.08 (dd, J = 8.9, 2.5 Hz, 1H), 6.69 – 6.62 (m, 2H), 4.20 – 4.14 (m, 2H), 3.89 – 3.83 (m, 2H), 3.74 – 3.66 (m, 4H), 3.68 – 3.59 (m, 2H), 2.84 (s, 3H), 2.48 (t, J = 6.2 Hz, 2H), 1.44 (s, 9H). MS (ESI) m/z 472.60 [M+H]

(13)→ (15)

(2S,4R)-1-((S)-3,3-dimethyl-2-(3-(2-(2-((2-(4-(methylamino)phenyl)benzo[d]thiazol-6-yl)oxy)ethoxy)ethoxy)propanamido)butanoyl)-4-hydroxy-N-((S)-1-(4-(4-methylthiazol-5-yl)phenyl)ethyl)pyrrolidine-2-carboxamide

13 (22.4 mgs, 0.046 mmol) was mixed with 1 ml dichloromethane and 1 ml trifluoroacetic acid. After 5 minutes product conversion was observed on TLC and confirmed on the LCMS. Reaction mixture was concentrated down and dried further on the high vacuum to give **14** as a thick yellow oil. This dried mixture was then taken directly to the next step. MS (ESI) m/z 416.49 [M+H]

(2S,4R)-1-((S)-2-amino-3,3-dimethylbutanoyl)-4-hydroxy-N-((S)-1-(4-(4-methylthiazol-5-yl)phenyl)ethyl)pyrrolidine-2-carboxamide, Trifluoroacetic acid, (19.4 mgs, 0.046 mmol) was mixed with HATU (1.2 eq, 21.3 mgs, 0.055 mmol), DIPEA (4 eq, 32 ul, 0.186 mmol) in 1 ml of DMF for 15 minutes. Afterward **14** (1 eq, 19.4 mgs, 0.046 mmol) was added and reaction monitored by LCMS and TLC before full conversion was observed in 30 minutes. Reaction was then filtered with PTFE Syringe Filters, 0.22 um, 17mm and injected for purification with High Pressure Liquid Chromatography. (0 to 80% H_2O/Methanol, duration of 45 min, flow rate of 20 mL/min, detection at 254 nm) Product fraction were concentrated down and lyophilized to give **15** as a white powder. (10 mgs, 0.0120 mmol, 25% yield) ^{1}H NMR (500 MHz, DMSO-D6) δ 8.98 (s, 1H), 8.39 (d, J = 7.8 Hz, 1H), 7.89 (d, J = 9.3 Hz, 1H), 7.81 – 7.72 (m, 3H), 7.62 (d, J = 2.5 Hz, 1H), 7.45 – 7.40 (m, 2H), 7.39 – 7.31 (m, 2H), 7.06 (dd, J = 8.9, 2.5 Hz, 1H), 6.66 – 6.60 (m, 2H), 6.41 (q, J = 4.9 Hz, 1H), 5.12 (d, J = 3.5 Hz, 1H), 4.91 (p, J = 7.1 Hz, 1H), 4.53 (d, J = 9.3 Hz, 1H), 4.42 (t, J = 8.1 Hz, 1H), 4.27 (s, 1H), 4.15 (dd, J = 5.6, 3.7 Hz, 2H), 3.79 – 3.74 (m, 2H), 3.60 (dt, J = 13.1, 5.2 Hz, 6H), 3.58 – 3.51 (m, 1H), 3.51 (dd, J = 10.2, 4.9 Hz, 1H), 2.74 (d, J = 5.0 Hz, 3H), 2.55 (dd, J = 14.4, 7.0 Hz, 1H), 2.45 (s, 3H), 2.36 (dt, J = 14.6, 6.1 Hz, 1H), 2.01 (t, J = 10.3 Hz, 1H), 1.78 (ddd, J = 12.8, 8.6, 4.6 Hz, 1H), 1.36 (d, J = 7.0 Hz, 3H), 0.93 (s, 9H). MS (ESI) m/z 843.07 [M+H]+[M/2]

Synthesis of Compound 20 (SAB-01-111)

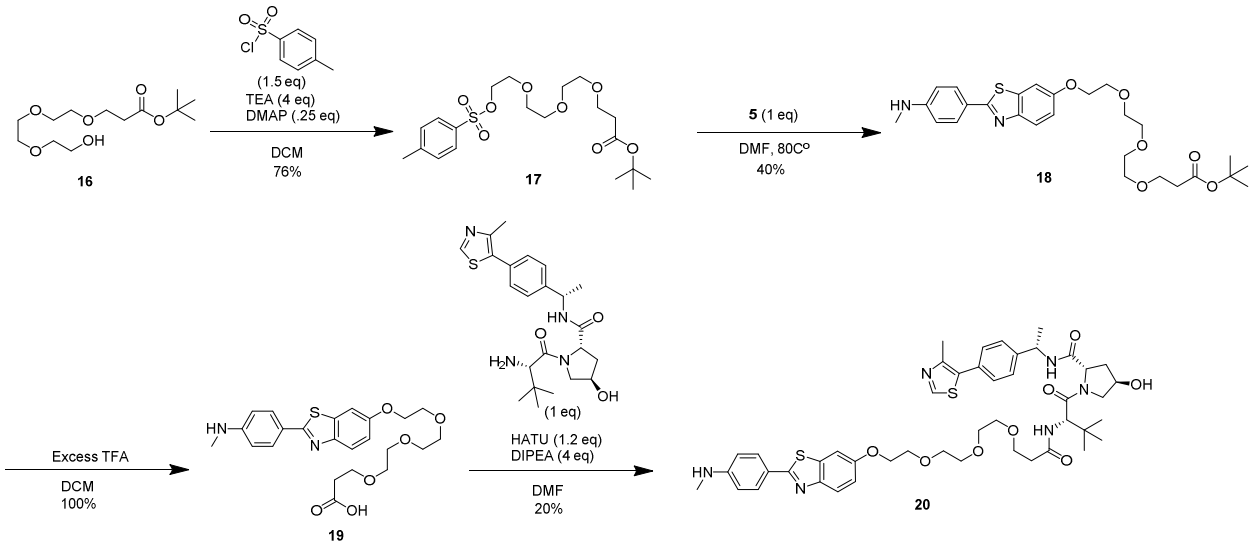

*(**16**)→ (**17**)*

tert-butyl 3-(2-(2-(2-(tosyloxy)ethoxy)ethoxy)ethoxy)propanoate tert-butyl 3-(2-(2-(2-hydroxyethoxy)ethoxy)ethoxy)propanoate

16 (1 eq, 50mgs, 0.18 mmol), triethylamine (4 eq, 0.10ml, 0.72 mmol), and catalytic DMAP (0.25 eq, 5.5 mg, 0.045 mmol) were mixed with 1 ml of dichloromethane under anhydrous conditions. The solution was cooled to 0C° in an ice bath and then 4-methylbenzenesulfonyl chloride (1.5 eq, 51 mgs, 0.27 mmol) was added dropwise. The reaction was removed from ice bath and left to mix overnight (12 hours). This was monitored by LCMS and TLC until reached completion. Crude reaction was mixed with 10mls of dichloromethane and washed with 3x 10mls of DI water. Organic layer was concentrated down and purified by flash column chromatography (20-100% ethyl acetate in hexane) to give **17** as a colorless oil. (59 mgs, .137 mmol, 76% yield) 1H NMR (500 MHz, DMSO-D6) δ 7.82 – 7.64 (m, 2H), 7.43 (dd, J = 20.0, 7.9 Hz, 2H), 4.09 – 4.00 (m, 2H), 3.57 – 3.47 (m, 5H), 3.41 (dd, J = 13.6, 7.0 Hz, 6H), 2.41 – 2.30 (m, 5H), 1.37 – 1.28 (m, 9H). MS (ESI) m/z 432.53 [M+Na]

*(**17**)→ (**18**)*

tert-butyl 3-(2-(2-(2-((2-(4-(methylamino)phenyl)benzo[d]thiazol-6-yl)oxy)ethoxy)ethoxy)ethoxy)propanoate

5 (1 eq, 10 mgs, 0.039 mmol) was mixed with potassium carbonate (2 eq, 11 mgs, 0.078 mmol) and 1 ml DMF 80C° for 10 minutes. Afterward **17** (1 eq, 17 mgs, 0.039 mmol) was added to this mixture and reaction monitored over 16 hours. Product was confirmed with LCMS and TLC.

Reaction mixture was mixed with 30mls saturated sodium bicarbonate and extracted with 3x 10mls ethyl acetate. The organic layer was then washed with 10mls DI water and organic layer concentrated. This crude mixture was purified with flash column chromatography (0-60% ethyl acetate in hexane) to give **18** as an off yellow wax. (9 mgs, .020 mmol, 40% yield). ^{1}H NMR (500 MHz, METHANOL-D4) δ 7.74 (dd, J = 10.3, 7.8 Hz, 3H), 7.46 – 7.40 (m, 1H), 7.06 (td, J = 9.1, 2.6 Hz, 1H), 6.66 – 6.59 (m, 2H), 4.16 (p, J = 4.5 Hz, 2H), 3.84 (p, J = 4.9 Hz, 2H), 3.72 – 3.51 (m, 10H), 3.31 – 3.25 (m, 4H), 2.81 (d, J = 9.0 Hz, 2H), 2.42 (qd, J = 6.2, 3.1 Hz, 2H), 1.41 (s, 9H). MS (ESI) m/z 516.16 [M+H]

(18)→ (20)

(2S,4R)-1-((S)-14-(tert-butyl)-1-((2-(4-(methylamino)phenyl)benzo[d]thiazol-6-yl)oxy)-12-oxo-3,6,9-trioxa-13-azapentadecan-15-oyl)-4-hydroxy-N-((S)-1-(4-(4-methylthiazol-5-yl)phenyl)ethyl)pyrrolidine-2-carboxamide, Trifluoroacetic acid

18 (72 mgs, 0.14 mmol) was mixed with 1 ml dichloromethane and 1 ml trifluoroacetic acid. After 5 minutes product conversion was observed on TLC and confirmed on the LCMS. Reaction mixture was concentrated down and dried further on the high vacuum to give **19** as a thick yellow oil. This dried mixture was then taken directly to the next step. MS (ESI) m/z 460 [M+H]

(2S,4R)-1-((S)-2-amino-3,3-dimethylbutanoyl)-4-hydroxy-N-((S)-1-(4-(4-methylthiazol-5-yl)phenyl)ethyl)pyrrolidine-2-carboxamide, Trifluoroacetic acid, (1 eq 17 mgs, 0.036 mmol) was mixed with HATU (1.2 eq, 16 mgs, 0.043 mmol), DIPEA (4 eq, 25 ul, 0.14 mmol) in 1 ml of DMF for 15 minutes. Afterward **19** (1 eq, 16 mgs, 0.036 mmol) was added and reaction monitored by LCMS and TLC before full conversion was observed in 30 minutes. Reaction was then filtered with PTFE Syringe Filters, 0.22 um, 17mm and injected for purification with High Pressure Liquid Chromatography (30 to 80% H_2O/Methanol, duration of 45 min, flow rate of 20 mL/min, detection at 254 nm). Product fraction were concentrated down and lyophilized to give **20** as a white powder. (7.1 mgs, 0.0071 mmol, 20% yield) 1H NMR (400 MHz, DMSO-D6) δ 8.98 (s, 1H), 8.39 (d, J = 7.8 Hz, 1H), 7.88 (d, J = 9.3 Hz, 1H), 7.81 – 7.72 (m, 3H), 7.62 (d, J = 2.6 Hz, 1H), 7.47 – 7.30 (m, 4H), 7.06 (dd, J = 8.9, 2.6 Hz, 1H), 6.67 – 6.59 (m, 2H), 6.41 (q, J = 5.0 Hz, 1H), 5.12 (d, J = 3.5 Hz, 1H), 4.92 (h, J = 7.1 Hz, 1H), 4.52 (d, J = 9.3 Hz, 1H), 4.42 (t, J = 8.1 Hz, 1H), 4.27 (s, 1H), 4.19 – 4.13 (m, 2H), 3.81 – 3.74 (m, 2H), 3.65 – 3.42 (m, 11H), 2.74 (d, J = 4.9 Hz, 3H), 2.54 (t, J = 3.8 Hz, 1H), 2.45 (s, 3H), 2.34 (dt, J = 14.5, 6.1 Hz, 1H), 2.01 (t, J = 10.2 Hz, 1H), 1.78 (ddd, J = 12.9, 8.6, 4.6 Hz, 1H), 1.36 (d, J = 7.0 Hz, 3H), 1.23 (s, 0H), 0.92 (s, 9H). MS (ESI) m/z 887.12 [M+H]+[M/2]

Synthesis of Compound 25 (SAB-01-162)

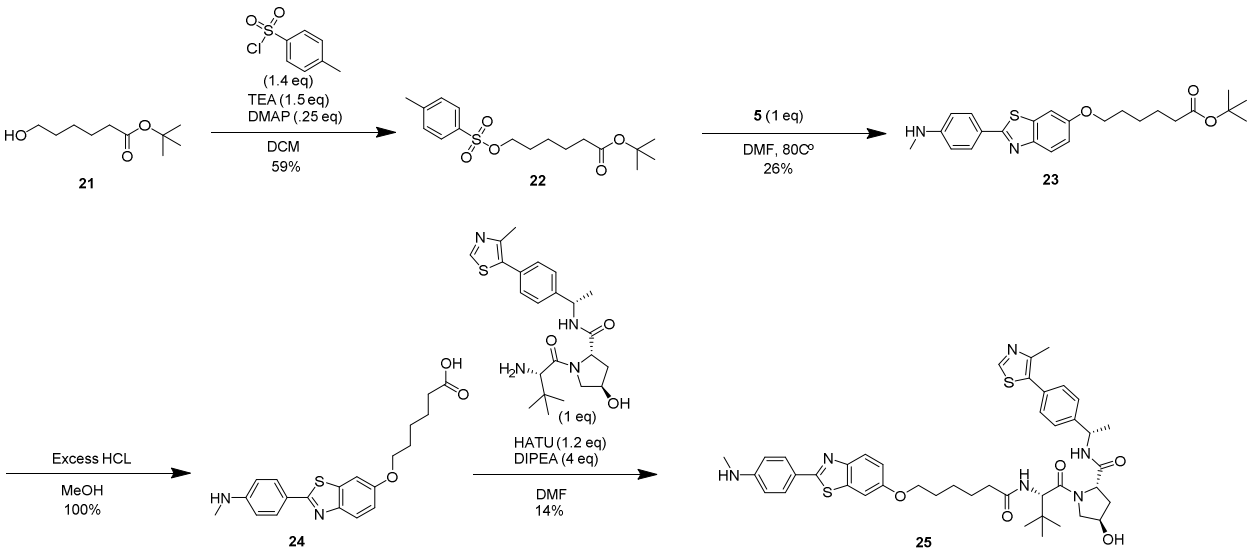

*(**21**)→ (**22**)*

tert-butyl 6-(tosyloxy)hexanoate

21 (1 eq, 40mgs, 0.21 mmol), triethylamine (1.5 eq, .44ul, 0.32 mmol), and catalytic DMAP (0.25 eq, 6.5 mg, 0.053 mmol) were mixed with 1 ml of dichloromethane under anhydrous conditions. The solution was cooled to 0C° in an ice bath and then 4-methylbenzenesulfonyl chloride (1.4 eq, 57 mgs, 0.30 mmol) was added dropwise. The reaction was removed from ice bath and left to mix overnight (10 hours). This was monitored by LCMS and TLC until reached completion. Crude reaction was mixed with 10mls of dichloromethane and washed with 3x 10mls of DI water. Organic layer was concentrated down and purified by flash column chromatography (0-20% ethyl acetate in hexane) to give **22** as a colorless oil. (43.1 mgs, 0.126 mmol, 59% yield) ^{1}H NMR (500 MHz, $CDCl_3$) δ 7.78 (d, J = 8.4 Hz, 2H), 7.34 (d, J = 8.3 Hz, 2H), 4.01 (t, J = 6.5 Hz, 2H), 2.44 (s, 3H), 2.17 (t, J = 3.1 Hz, 2H), 2.15 (d, J = 7.5 Hz, 1H), 1.69 – 1.60 (m, 3H), 1.52 (p, J = 7.5 Hz, 2H), 1.42 (s, 9H), 1.37 – 1.27 (m, 2H). MS (ESI) m/z 342.45 [M+Na]

*(**22**)→ (**23**)*

tert-butyl 6-((2-(4-(methylamino)phenyl)benzo[d]thiazol-6-yl)oxy)hexanoate

5 (1 eq, 15 mgs, 0.059 mmol) was mixed with potassium carbonate (2 eq, 16 mgs, 0.12 mmol) and 1 ml DMF 80C° for 10 minutes. Afterward **22** (1.7 eq, 35 mgs, 0.10 mmol) was added to this mixture and reaction monitored over 16 hours. Product was confirmed with LCMS and TLC. Reaction mixture was mixed with 30mls saturated sodium bicarbonate and extracted with 2x 20mls ethyl acetate. The organic layer was then washed with 10mls DI water and organic layer

concentrated. This crude mixture was purified with flash column chromatography (0-60% ethyl acetate in hexane) to give **23** as an off yellow wax. (6.6 mgs, 0.015 mmol, 26% yield). 1H NMR (400 MHz, DMSO-D6) δ 7.78 – 7.67 (m, 3H), 7.59 – 7.52 (m, 1H), 6.98 (dd, J = 8.9, 2.5 Hz, 1H), 6.59 (d, J = 8.7 Hz, 2H), 6.37 (q, J = 4.9 Hz, 1H), 3.98 (t, J = 6.4 Hz, 2H), 2.70 (d, J = 4.9 Hz, 3H), 2.18 (t, J = 7.2 Hz, 2H), 1.70 (p, J = 6.6 Hz, 2H), 1.52 (p, J = 7.4 Hz, 2H), 1.39 (qd, J = 7.5, 4.1 Hz, 2H), 1.35 (s, 9H). MS (ESI) m/z 426.58 [M+H]

(23)→ (25)

(2S,4R)-1-((S)-3,3-dimethyl-2-(6-((2-(4-(methylamino)phenyl)benzo[d]thiazol-6-yl)oxy)hexanamido)butanoyl)-4-hydroxy-N-((S)-1-(4-(4-methylthiazol-5-yl)phenyl)ethyl)pyrrolidine-2-carboxamide

23 (14.4 mgs, 0.034 mmol) was mixed with 1 ml dichloromethane and 1 ml trifluoroacetic acid. After 5 minutes product conversion was observed on TLC and confirmed on the LCMS. Reaction mixture was concentrated down and dried further on the high vacuum to give **24** as a thick yellow oil. This dried mixture was then taken directly to the next step. MS (ESI) m/z 404.92 [M+H]

(2S,4R)-1-((S)-2-amino-3,3-dimethylbutanoyl)-4-hydroxy-N-((S)-1-(4-(4-methylthiazol-5-yl)phenyl)ethyl)pyrrolidine-2-carboxamide, Trifluoroacetic acid, (1 eq, 14 mgs, 0.032 mmol) was mixed with HATU (1.2 eq, 15 mgs, 0.039 mmol), DIPEA (4 eq, 23 ul, 0.13 mmol) in 1 ml of DMF for 15 minutes. Afterward **24** (1 eq, 14 mgs, 0.032 mmol) was added and reaction monitored by LCMS and TLC before full conversion was observed in 30 minutes. Reaction was then filtered with PTFE Syringe Filters, 0.22 um, 17 mm and injected for purification with High Pressure Liquid Chromatography. (30 to 80% H_2O/Methanol, duration of 45 min, flow rate of 20 mL/min, detection at 254 nm) Product fraction was concentrated down and lyophilized to give **25** as a white powder. (3.7 mgs, 0.0046 mmol, 14% yield) ^{1}H NMR (599 MHz, DMSO-D6) δ 8.91 (s, 1H), 8.30 (d, J = 7.8 Hz, 1H), 7.76 (d, J = 9.3 Hz, 1H), 7.70 (dd, J = 10.2, 8.0 Hz, 3H), 7.52 (d, J = 2.5 Hz, 1H), 7.39 – 7.34 (m, 2H), 7.34 – 7.29 (m, 2H), 6.96 (dd, J = 8.8, 2.6 Hz, 1H), 6.59 – 6.54 (m, 2H), 6.33 (d, J = 5.1 Hz, 1H), 5.04 (d, J = 3.5 Hz, 1H), 4.90 – 4.80 (m, 1H), 4.46 (d, J = 9.3 Hz, 1H), 4.35 (t, J = 8.1 Hz, 1H), 4.21 (q, J = 3.6 Hz, 1H), 3.95 (t, J = 6.5 Hz, 2H), 3.58 – 3.50 (m, 2H), 2.68 (d, J = 4.9 Hz, 3H), 2.38 (s, 3H), 2.23 (dt, J = 14.7, 7.6 Hz, 1H), 2.14 – 2.03 (m, 1H), 1.94 (ddd, J = 11.7, 7.9, 2.7 Hz, 1H), 1.76 – 1.64 (m, 3H), 1.51 (dtt, J = 20.8, 13.5, 7.0 Hz, 2H), 1.41 – 1.34 (m, 2H), 1.30 (d, J = 7.0 Hz, 3H), 0.87 (s, 9H). MS (ESI) m/z 797.05 [M+H]+[M/2]

Synthesis of Compound 30 (SAB-01-170)

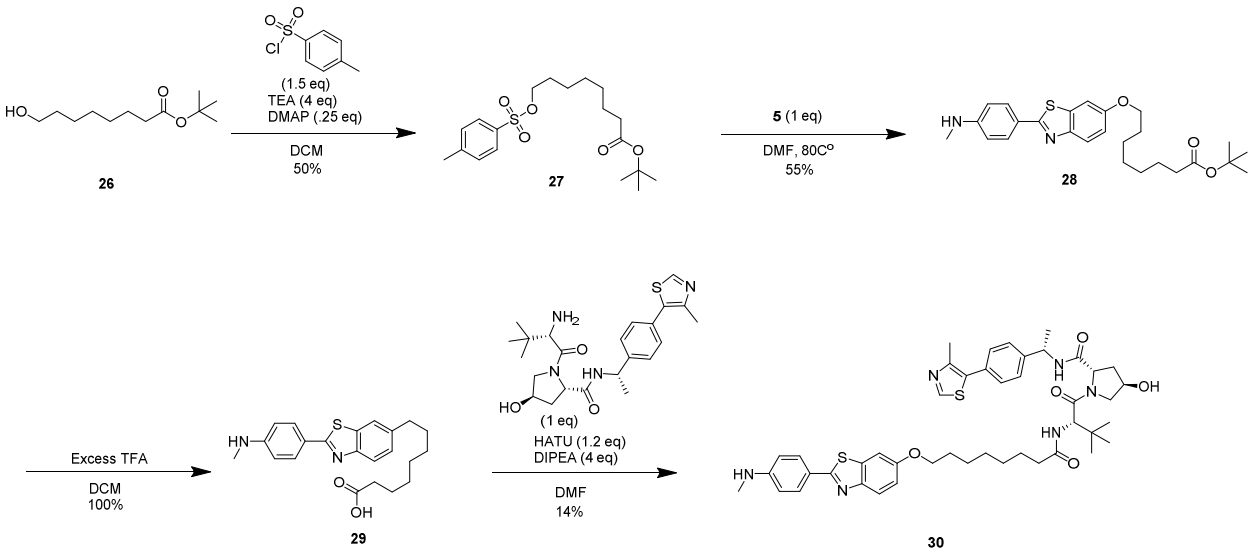

(26)→ (27)

tert-butyl 8-(tosyloxy)octanoate

26 (1 eq, 50mgs, 0.23 mmol), triethylamine (4 eq, 0.13ml, 0.92 mmol), and catalytic DMAP (0.25 eq, 7.1 mg, 0.058 mmol) were mixed with 1 ml of dichloromethane under anhydrous conditions. The solution was cooled to 0C° in an ice bath and then 4-methylbenzenesulfonyl chloride (1.5 eq, 66 mgs, 0.35 mmol) was added dropwise. The reaction was removed from the ice bath and left to mix overnight (16 hours). This was monitored by LCMS and TLC until reached completion. Crude reaction was mixed with 10mls of dichloromethane and washed with 3x 10mls of DI water. Organic layer was concentrated down and purified by flash column chromatography (0-20% ethyl acetate in hexane) to give **27** as a colorless oil. (43.1 mgs, 0.12 mmol, 50% yield) ^{1}H NMR (500 MHz, $CDCl_3$) δ 7.77 (d, J = 7.9 Hz, 2H), 7.33 (d, J = 7.9 Hz, 2H), 3.99 (t, J = 6.5 Hz, 2H), 2.43 (s, 3H), 2.16 (t, J = 7.5 Hz, 2H), 1.61 (p, J = 6.7 Hz, 2H), 1.51 (p, J = 8.3 Hz, 2H), 1.42 (s, 9H), 1.33 – 1.19 (m, 6H). MS (ESI) m/z 370.50 [M+Na]

(27)→ (28)

tert-butyl 8-((2-(4-(methylamino)phenyl)benzo[d]thiazol-6-yl)oxy)octanoate

5 (1 eq, 15 mgs, 0.059 mmol) was mixed with potassium carbonate (2 eq, 18 mgs, 0.13 mmol) and 1 ml DMF 80C° for 10 minutes. Afterward **27** (1.1 eq, 28 mgs, 0.076 mmol) was added to this mixture and reaction monitored over 16 hours. Product was confirmed with LCMS and TLC. Reaction mixture was mixed with 30mls saturated sodium bicarbonate and extracted with 2x 20mls ethyl acetate. The organic layer was then washed with 10mls DI water and organic layer concentrated. This crude mixture was purified with flash column chromatography (20-60% ethyl

acetate in hexane) to give **28** as an off yellow wax. (15.2 mgs, .033 mmol, 55% yield). ^{1}H NMR (400 MHz, DMSO-D6) δ 7.76 (dd, J = 8.7, 4.9 Hz, 3H), 7.59 (d, J = 2.5 Hz, 1H), 7.03 (dd, J = 8.9, 2.5 Hz, 1H), 6.66 – 6.60 (m, 2H), 6.41 (q, J = 4.9 Hz, 1H), 5.76 (s, 1H), 4.07 – 3.98 (m, 2H), 2.74 (d, J = 4.9 Hz, 3H), 2.18 (t, J = 7.3 Hz, 2H), 1.73 (p, J = 6.7 Hz, 2H), 1.47 (tt, J = 15.0, 7.6 Hz, 4H), 1.38 (s, 9H), 1.36 – 1.21 (m, 4H). MS (ESI) m/z 453.63 [M+H]

(28)→ (30)

(2S,4R)-1-((S)-3,3-dimethyl-2-(6-((2-(4-(methylamino)phenyl)benzo[d]thiazol-6-yl)oxy)hexanamido)butanoyl)-4-hydroxy-N-((S)-1-(4-(4-methylthiazol-5-yl)phenyl)ethyl)pyrrolidine-2-carboxamide

28 (27 mgs, 0.059 mmol) was mixed with 1 ml dichloromethane and 1 ml trifluoroacetic acid. After 5 minutes product conversion was observed on TLC and confirmed on the LCMS. Reaction mixture was concentrated down and dried further on the high vacuum to give **29** as a thick yellow oil. This dried mixture was then taken directly to the next step. MS (ESI) m/z 398.02 [M+H]

(2S,4R)-1-((S)-2-amino-3,3-dimethylbutanoyl)-4-hydroxy-N-((S)-1-(4-(4-methylthiazol-5-yl)phenyl)ethyl)pyrrolidine-2-carboxamide, Trifluoroacetic acid, (1 eq, 27 mgs, 0.060 mmol) was mixed with HATU (1.2 eq, 27 mgs, 0.072 mmol), DIPEA (4 eq, 34 ul, 0.24 mmol) in 1 ml of DMF for 15 minutes. Afterward **29** (1 eq, 24 mgs, 0.060 mmol) was added and reaction monitored by LCMS and TLC before full conversion was observed in 30 minutes. Reaction was then filtered with PTFE Syringe Filters, 0.22 um, 17mm and injected for purification with High Pressure Liquid Chromatography. (50 to 85% H_2O/Methanol, duration of 45 min, flow rate of 20 mL/min, detection at 254 nm) Product fraction were concentrated down and lyophilized to give **30** as a white powder. (3.7 mgs, 0.0046 mmol, 14% yield) ^{1}H NMR (500 MHz, DMSO-D6) δ 8.98 (s, 1H), 8.38 (d, J = 7.8 Hz, 1H), 7.84 – 7.72 (m, 4H), 7.61 – 7.54 (m, 1H), 7.47 – 7.39 (m, 2H), 7.39 – 7.30 (m, 2H), 7.03 (dd, J = 8.9, 2.5 Hz, 1H), 6.66 – 6.60 (m, 2H), 6.40 (q, J = 4.9 Hz, 1H), 5.11 (d, J = 3.5 Hz, 1H), 4.98 – 4.86 (m, 1H), 4.52 (d, J = 9.3 Hz, 1H), 4.42 (t, J = 8.1 Hz, 1H), 4.27 (s, 1H), 4.02 (t, J = 6.6 Hz, 2H), 3.60 (d, J = 3.9 Hz, 2H), 2.74 (d, J = 4.9 Hz, 3H), 2.45 (s, 3H), 2.26 (dt, J = 14.6, 7.6 Hz, 1H), 2.16 – 2.07 (m, 1H), 2.01 (ddd, J = 11.0, 7.6, 2.8 Hz, 1H), 1.83 – 1.68 (m, 2H), 1.73 (s, 1H), 1.52 (ddd, J = 18.2, 12.6, 7.1 Hz, 1H), 1.49 – 1.40 (m, 1H), 1.37 (d, J = 7.0 Hz, 3H), 1.29 (ddd, J = 33.2, 15.7, 9.6 Hz, 2H), 0.93 (s, 9H). MS (ESI) m/z 825.10 [M+H]+[M/2]

Synthesis of Compound 35 (SAB-02-008)

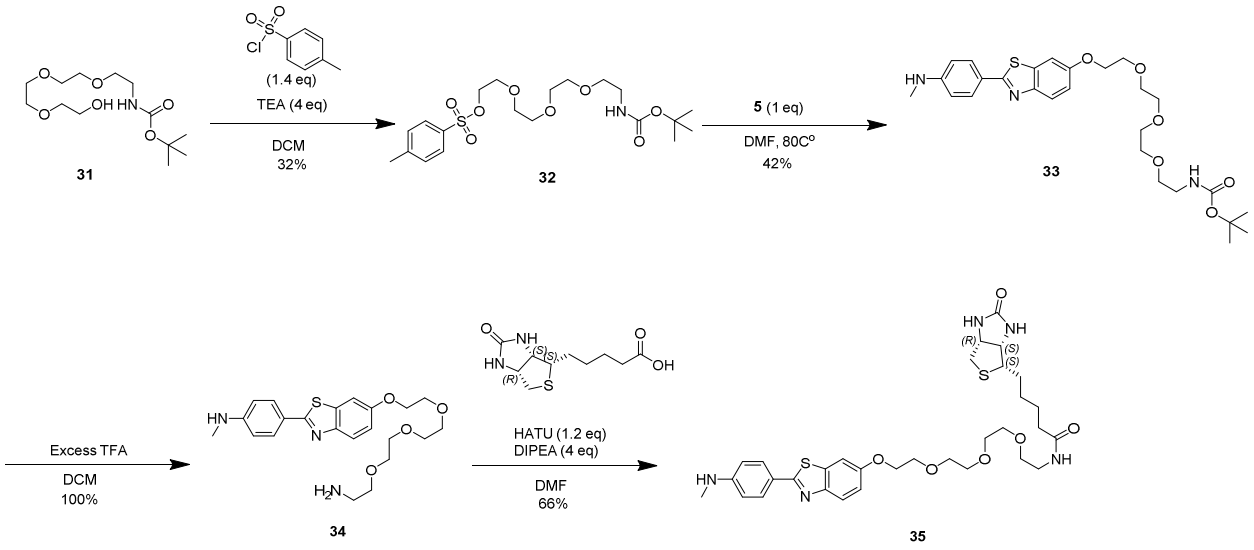

*(**31**)→ (**32**)*

2,2-dimethyl-4-oxo-3,8,11,14-tetraoxa-5-azahexadecan-16-yl 4-methylbenzenesulfonate

31 (1 eq, 80mgs, .27 mmol) and triethylamine (4 eq, .15ml, 1.1 mmol) and catalytic DMAP (0.25 eq, 7.1 mg, 0.067 mmol) were mixed with 1 ml of dichloromethane under anhydrous conditions. The solution was cooled to 0C° in an ice bath and then 4-methylbenzenesulfonyl chloride (1.4 eq, 73 mgs, 0.38 mmol) was added dropwise. The reaction was removed from the ice bath and left to mix overnight (16 hours). This was monitored by LCMS and TLC until reached completion. Crude reaction was mixed with 10mls of dichloromethane and washed with 3x 10mls of DI water. Organic layer was concentrated down and purified by flash column chromatography (0-70% ethyl acetate in hexane) to give **32** as a colorless oil. (39.1 mgs, 0.087 mmol, 32% yield) ^{1}H NMR (500 MHz, DMSO-D6) δ 7.78 (dt, J = 8.5, 1.8 Hz, 2H), 7.51 – 7.45 (m, 2H), 4.11 (ddd, J = 5.7, 3.2, 1.4 Hz, 2H), 3.60 – 3.54 (m, 2H), 3.47 (d, J = 1.3 Hz, 4H), 3.44 (d, J = 1.3 Hz, 4H), 3.36 (t, J = 6.1 Hz, 2H), 3.05 (q, J = 6.0 Hz, 2H), 2.42 (s, 3H), 1.36 (d, J = 1.3 Hz, 9H). MS (ESI) m/z 447.54 [M+Na]

*(**32**)→ (**33**)*

tert-butyl (2-(2-(2-(2-((2-(4-(methylamino)phenyl)benzo[d]thiazol-6-yl)oxy)ethoxy)ethoxy)ethoxy)ethyl)carbamate

5 (1 eq, 29 mgs, 0.11 mmol) was mixed with potassium carbonate (2 eq, 31 mgs, 0.22 mmol) and 1 ml DMF 80C° for 10 minutes. Afterward **32** (1 eq, 50 mgs, 0.11 mmol) was added to this mixture and reaction monitored over 16 hours. Product was confirmed with LCMS and TLC.

Reaction mixture was mixed with 30mls saturated sodium bicarbonate and extracted with 2x 20mls ethyl acetate. The organic layer was then washed with 10mls DI water and organic layer concentrated. This crude mixture was purified with flash column chromatography (30-70% ethyl acetate in hexane) to give **33** as an off yellow wax. (25 mgs, 0.047 mmol, 42% yield) ^{1}H NMR (500 MHz, METHANOL-D4) δ 7.80 – 7.71 (m, 3H), 7.42 (d, J = 2.5 Hz, 1H), 7.07 (dd, J = 8.9, 2.5 Hz, 1H), 6.68 – 6.61 (m, 2H), 4.19 – 4.13 (m, 2H), 3.88 – 3.83 (m, 2H), 3.74 – 3.69 (m, 2H), 3.69 – 3.58 (m, 4H), 3.61 – 3.53 (m, 2H), 3.48 (t, J = 5.6 Hz, 2H), 3.20 (q, J = 5.3 Hz, 2H), 2.83 (s, 3H), 1.41 (s, 9H). MS (ESI) m/z 531.67 [M+H]

(33)→ (35)

(2S,4R)-1-((S)-3,3-dimethyl-2-(6-((2-(4-(methylamino)phenyl)benzo[d]thiazol-6-yl)oxy)hexanamido)butanoyl)-4-hydroxy-N-((S)-1-(4-(4-methylthiazol-5-yl)phenyl)ethyl)pyrrolidine-2-carboxamide

33 (25 mgs, .059 mmol) was mixed with 1 ml dichloromethane and 1 ml trifluoroacetic acid. After 5 minutes product conversion was observed on TLC and confirmed on the LCMS. Reaction mixture was concentrated down and dried further on the high vacuum to give **34** as a thick yellow oil. This dried mixture was then taken directly to the next step. MS (ESI) m/z 431.55 [M+H]

5-((3aS,4S,6aR)-2-oxohexahydro-1H-thieno[3,4-d]imidazol-4-yl)pentanoic acid, (2 eq, 29 mgs, 0.12 mmol) was mixed with HATU (1.2 eq, 27 mgs, 0.072 mmol), DIPEA (4 eq, 31 ul, 0.24 mmol) in 1 ml of DMF for 15 minutes. Afterward **34** (1 eq, 26 mgs, 0.060 mmol) was added and reaction monitored by LCMS and TLC before full conversion was observed in 30 minutes. Reaction was then filtered with PTFE Syringe Filters, 0.22 um, 17mm and injected for purification with High Pressure Liquid Chromatography. (0 to 60% H_2O/Methanol, duration of 45 min, flow rate of 20 mL/min, detection at 254 nm) Product fraction were concentrated down and lyophilized to give **35** as a yellow powder. (26 mgs, 0.060 mmol, 66% yield) ^{1}H NMR (500 MHz, DMSO-D6) δ 7.83 (t, J = 5.7 Hz, 1H), 7.78 (d, J = 8.9 Hz, 1H), 7.77 – 7.74 (m, 2H), 7.62 (d, J = 2.6 Hz, 1H), 7.06 (dd, J = 8.9, 2.6 Hz, 1H), 6.67 – 6.60 (m, 2H), 6.41 (dd, J = 8.4, 3.4 Hz, 2H), 6.35 (s, 1H), 4.28 (dd, J = 7.7, 5.1 Hz, 1H), 4.19 – 4.13 (m, 2H), 4.13 – 4.07 (m, 1H), 3.80 – 3.75 (m, 2H), 3.60 (dd, J = 5.9, 3.3 Hz, 2H), 3.58 – 3.47 (m, 6H), 3.39 (t, J = 5.9 Hz, 2H), 3.17 (q, J = 5.9 Hz, 2H), 3.06 (ddd, J = 8.6, 6.2, 4.4 Hz, 1H), 2.80 (dd, J = 12.4, 5.1 Hz, 1H), 2.75 (d, J = 4.9 Hz, 3H), 2.59 – 2.52 (m, 1H), 2.05 (t, J = 7.4 Hz, 2H), 1.64 – 1.54 (m, 1H), 1.44 (ddd, J = 18.1, 12.4, 8.2 Hz, 3H), 1.28 (tt, J = 15.7, 7.9 Hz, 2H). MS (ESI) m/z 657.85 [M+H]+[M/2]

Synthesis of Compound 36 (SAB-02-056)

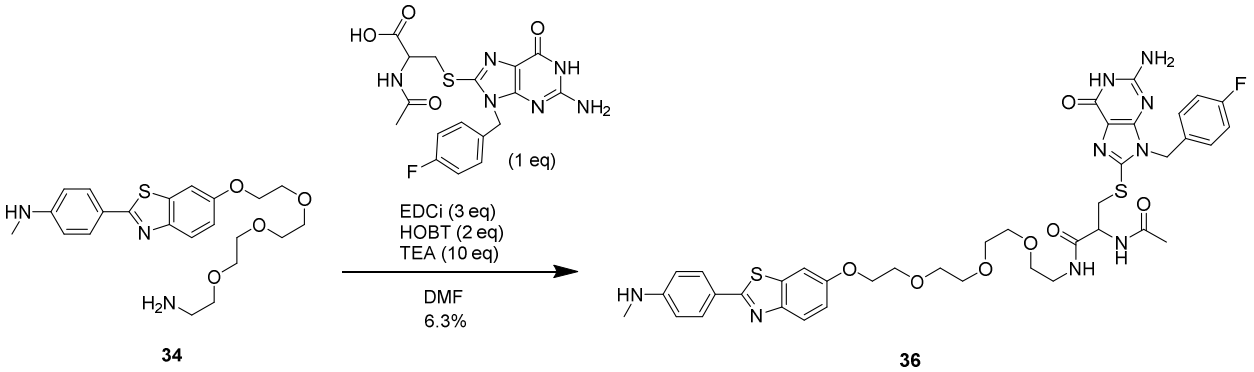

(34)→ (36)

2-acetamido-3-((2-amino-7-(4-fluorobenzyl)-6-oxo-6,7-dihydro-1H-purin-8-yl)thio)-N-(2-(2-(2-(2-((2-(4-(methylamino)phenyl)benzo[d]thiazol-6-yl)oxy)ethoxy)ethoxy)ethoxy)ethyl)propanamide

N-acetyl-S-(2-amino-7-(4-fluorobenzyl)-6-oxo-6,7-dihydro-1H-purin-8-yl)cysteine (1 eq, 19mgs, .029mmol) was mixed with 3-(((ethylimino)methylene)amino)-N,N-dimethylpropan-1-amine (3 eq, 13 mgs, 0.086 mmol), 1H-benzo[d][1,2,3]triazol-1-ol (2 eq, 7.7 mgs, 0.057 mmol), and Triethylamine (10 eq, 40ul, .29 mmol) in 1 ml of dry DMF. This was sonicated and then allowed to stir for 15 mins before **34** (1.5 eq, 19 mgs, 0.044 mmol) was added and the reaction mixture stirred overnight. In the morning, 16 hours later product was verified on the LCMS and then filtered with PTFE Syringe Filters, 0.22 um, 17mm before HPLC purification was completed (0 to 100% H_2O/Methanol, duration of 45 min, flow rate of 20 mL/min, detection at 254 nm). Product peaks were mixed with impurities, and this was recollected for another HPLC purification (50 to 70% H_2O/Methanol, duration of 45 min, flow rate of 20 mL/min, detection at 254 nm) to yield **36** as a yellow white powder. (1.5 mgs, 0.029 mmol, 6.3% yield) H NMR (599 MHz, DMSO-D6) δ 10.65 (s, 1H), 8.40 (d, J = 8.1 Hz, 1H), 8.08 (t, J = 5.6 Hz, 1H), 7.80 – 7.73 (m, 2H), 7.60 (d, J = 2.6 Hz, 1H), 7.20 (dd, J = 8.6, 5.5 Hz, 2H), 7.17 – 7.12 (m, 2H), 7.05 (dd, J = 8.8, 2.6 Hz, 1H), 6.67 – 6.61 (m, 2H), 6.54 (s, 1H), 6.53 (s, 2H), 6.40 (q, J = 5.1 Hz, 1H), 5.07 (s, 2H), 4.49 (td, J = 8.2, 5.2 Hz, 1H), 4.15 (t, J = 4.7 Hz, 2H), 3.76 (d, J = 4.7 Hz, 2H), 3.58 (dd, J = 5.8, 3.7 Hz, 2H), 3.55 – 3.36 (m, 9H), 3.26 (dd, J = 13.3, 8.3 Hz, 1H), 3.19 (hept, J = 7.0 Hz, 2H), 2.75 (d, J = 4.9 Hz, 3H), 1.84 (s, 3H). MS (ESI) m/z 843.96 [M+H]+[M/2]

Synthesis of Compound 41 (SAB-02-078)

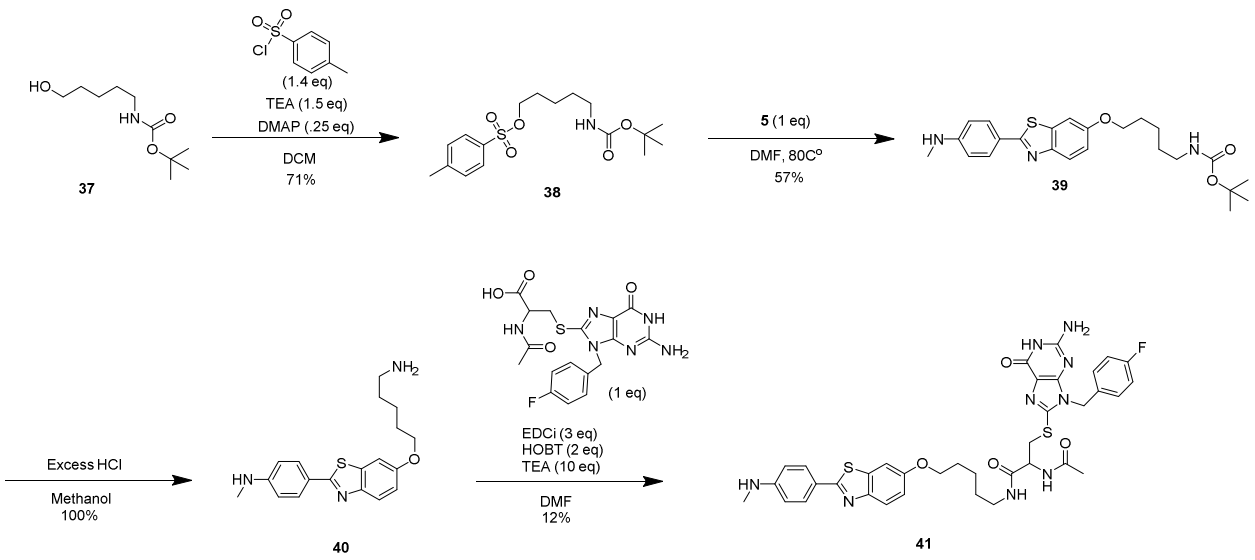

*(**37**)→ (**38**)*

5-((tert-butoxycarbonyl)amino)pentyl 4-methylbenzenesulfonate

37 (1 eq, 50 mgs, 0.25 mmol) and triethylamine (1.4 eq, 0.48 ul, 0.34 mmol) and catalytic DMAP (0.25 eq, 7.5 mg, 0.061 mmol) were mixed with 1 ml of dichloromethane under anhydrous conditions. The solution was cooled to 0C° in an ice bath and then 4-methylbenzenesulfonyl chloride (1.4 eq, 66 mgs, 0.34 mmol) was added dropwise. The reaction was removed from the ice bath and left to mix overnight (14 hours). This was monitored by LCMS and TLC until reached completion. Crude reaction was mixed with 10mls of dichloromethane and washed with 3x 10mls of DI water. Organic layer was concentrated down and purified by flash column chromatography (0-60% ethyl acetate in hexane) to give **38** as a colorless oil. (62 mgs, 0.17 mmol, 71% yield) ^{1}H NMR (500 MHz, METHANOL-D4) δ 7.76 (d, J = 8.1 Hz, 2H), 7.42 (d, J = 8.1 Hz, 2H), 4.00 (t, J = 6.3 Hz, 2H), 2.95 (t, J = 6.9 Hz, 2H), 2.43 (s, 3H), 1.60 (p, J = 6.6 Hz, 2H), 1.40 (s, 9H), 1.36 (q, J = 7.1 Hz, 2H), 1.33 – 1.22 (m, 2H). MS (ESI) m/z 357.47 [M+Na]

*(**38**)→ (**39**)*

tert-butyl (5-((2-(4-(methylamino)phenyl)benzo[d]thiazol-6-yl)oxy)pentyl)carbamate

5 (1 eq, 15 mgs, 0.059 mmol) was mixed with potassium carbonate (2 eq, 16 mgs, 0.12 mmol) and 1 ml DMF 80C° for 10 minutes. Afterward **38** (1.5 eq, 31 mgs, 0.088 mmol) was added to

this mixture and reaction monitored over 16 hours. Product was confirmed with LCMS and TLC. Reaction mixture was mixed with 30mls saturated sodium bicarbonate and extracted with 2x 20mls ethyl acetate. The organic layer was then washed with 10mls DI water and organic layer concentrated. This crude mixture was purified with flash column chromatography (20-60% ethyl acetate in hexane) to give **39** as an off yellow wax. (14.7 mgs, 0.033 mmol, 57% yield) 1H NMR (500 MHz, $CDCl_3$) δ 7.86 (t, J = 8.9 Hz, 3H), 7.29 (d, J = 2.5 Hz, 1H), 7.02 (dd, J = 8.7, 2.5 Hz, 1H), 6.67 – 6.61 (m, 2H), 4.55 (s, 1H), 4.01 (t, J = 6.3 Hz, 2H), 3.16 (d, J = 6.9 Hz, 2H), 2.91 (s, 3H), 1.84 (p, J = 6.7 Hz, 2H), 1.55 (tdd, J = 15.5, 8.3, 5.1 Hz, 3H), 1.44 (s, 9H).MS (ESI) m/z 441.59 [M+H]

(39)→ (41)

2-acetamido-3-((2-amino-7-(4-fluorobenzyl)-6-oxo-6,7-dihydro-1H-purin-8-yl)thio)-N-(5-((2-(4-(methylamino)phenyl)benzo[d]thiazol-6-yl)oxy)pentyl)propenamide

39 (14.7 mgs, 0.033 mmol) was mixed with 1 ml methanol and 1 ml hydrochloric acid. After 5 minutes product conversion was observed on TLC and confirmed on the LCMS. Reaction mixture was concentrated down and dried further on the high vacuum to give **40** as a yellow oil. This dried mixture was then taken directly to the next step. MS (ESI) m/z 341.47 [M+H]

N-acetyl-S-(2-amino-7-(4-fluorobenzyl)-6-oxo-6,7-dihydro-1H-purin-8-yl)cysteine, (1 eq, 10.7 mgs, 0.025 mmol), 1H-benzo[d][1,2,3]triazol-1-ol (2 eq, 6.7 mgs, 0.050 mmol), and Triethylamine (10 eq, 35.5ul, 0.025 mmol) in 1 ml of dry DMF. This was sonicated and then allowed to stir for 15 mins before **40** (1.3 eq, 11 mgs, 0.033 mmol) was added and the reaction mixture stirred overnight. In the morning, 16 hours later product was verified on the LCMS and then filtered with PTFE Syringe Filters, 0.22 um, 17mm before HPLC purification was completed (55 to 75% H_2O/Methanol, duration of 45 min, flow rate of 20 mL/min, detection at 254 nm) to yield **41** as a yellow white powder. (2.3 mgs, 0.003 mmol, 12% yield) ^{1}H NMR (599 MHz, DMSO) δ 10.65 (s, 1H), 8.40 (d, J = 8.1 Hz, 1H), 8.05 (t, J = 5.7 Hz, 1H), 7.75 (dd, J = 8.8, 2.5 Hz, 3H), 7.56 (d, J = 2.6 Hz, 1H), 7.20 (dd, J = 8.6, 5.5 Hz, 2H), 7.16 – 7.11 (m, 2H), 7.02 (dd, J = 8.8, 2.6 Hz, 1H), 6.63 (d, J = 8.5 Hz, 2H), 6.54 (s, 2H), 6.39 (d, J = 5.2 Hz, 1H), 5.07 (s, 2H), 4.47 (td, J = 8.0, 5.4 Hz, 1H), 3.99 (t, J = 6.5 Hz, 2H), 3.42 (dd, J = 13.3, 5.4 Hz, 1H), 3.28 (dd, J = 13.3, 8.1 Hz, 1H), 3.06 (dq, J = 13.5, 6.9 Hz, 2H), 2.75 (d, J = 5.0 Hz, 3H), 1.84 (s, 3H), 1.74 – 1.69 (m, 2H), 1.49 – 1.37 (m, 4H). MS (ESI) m/z 743.88 [M+H]+[M/2]

Synthesis of Compound 46 (SAB-02-071)

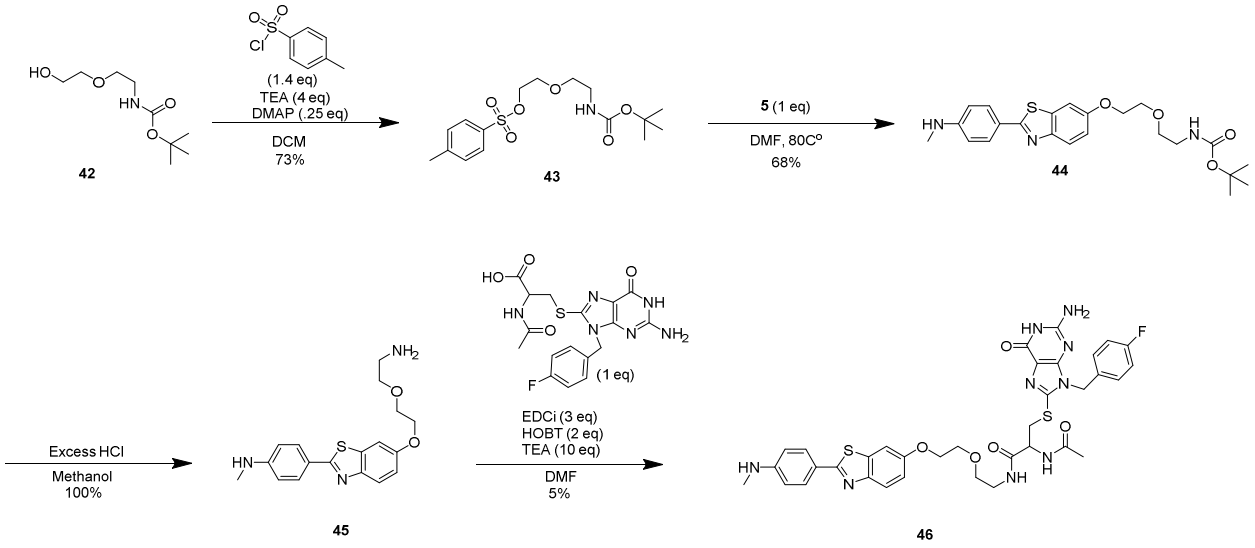

*(**42**)→ (**43**)*

2-(2-((tert-butoxycarbonyl)amino)ethoxy)ethyl 4-methylbenzenesulfonate

42 (1 eq, 96 mgs, 0.47 mmol) and triethylamine (1.4 eq, 0.91 ul, 0.66 mmol) and catalytic DMAP (0.25 eq, 14 mg, 0.12 mmol) were mixed with 1 ml of dichloromethane under anhydrous conditions. The solution was cooled to 0C° in an ice bath and then 4-methylbenzenesulfonyl chloride (1.4 eq, 125 mgs, 0.655 mmol) was added dropwise. The reaction was removed from the ice bath and left to mix overnight (16 hours). This was monitored by LCMS and TLC until reached completion. Crude reaction was mixed with 10mls of dichloromethane and washed with 3x 10mls of DI water. Organic layer was concentrated down and purified by flash column chromatography (0-50% ethyl acetate in hexane) to give **43** as a colorless oil. (122 mgs, 0.339 mmol, 73% yield) ^{1}H NMR (400 MHz, METHANOL-D_4) δ 7.78 (d, J = 8.3 Hz, 2H), 7.43 (d, J = 8.1 Hz, 2H), 4.16 – 4.12 (m, 2H), 3.66 – 3.57 (m, 2H), 3.41 (t, J = 5.7 Hz, 2H), 3.14 (t, J = 5.7 Hz, 2H), 2.44 (s, 3H), 1.42 (s, 11H). MS (ESI) m/z 359.44 [M+Na]

*(**43**)→ (**44**)*

tert-butyl (5-((2-(4-(methylamino)phenyl)benzo[d]thiazol-6-yl)oxy)pentyl)carbamate

5 (1 eq, 36 mgs, 0.14 mmol) was mixed with potassium carbonate (2 eq, 16 mgs, 0.12 mmol) and 1 ml DMF 80C° for 10 minutes. Afterward **43** (1 eq, 50 mgs, 0.14 mmol) was added to this mixture and reaction monitored over 16 hours. Product was confirmed with LCMS and TLC. Reaction mixture was mixed with 30mls saturated sodium bicarbonate and extracted with 2x

20mls ethyl acetate. The organic layer was then washed with 10mls DI water and organic layer concentrated. This crude mixture was purified with flash column chromatography (0-60% ethyl acetate in hexane) to give **44** as an off yellow wax. (42 mgs, 0.095 mmol, 68% yield) 1H NMR (500 MHz, $CDCl_3$) δ 7.86 (t, J = 8.9 Hz, 3H), 7.29 (d, J = 2.5 Hz, 1H), 7.02 (dd, J = 8.7, 2.5 Hz, 1H), 6.67 – 6.61 (m, 2H), 4.55 (s, 1H), 4.01 (t, J = 6.3 Hz, 2H), 3.16 (d, J = 6.9 Hz, 2H), 2.91 (s, 3H), 1.84 (p, J = 6.7 Hz, 2H), 1.55 (tdd, J = 15.5, 8.3, 5.1 Hz, 3H), 1.44 (s, 9H).MS (ESI) m/z 441.59 [M+H]

(44)→ (46)

2-acetamido-3-((2-amino-7-(4-fluorobenzyl)-6-oxo-6,7-dihydro-1H-purin-8-yl)thio)-N-(2-(2-((2-(4-(methylamino)phenyl)benzo[d]thiazol-6-yl)oxy)ethoxy)ethyl)propenamide

44 (14 mgs, 0.032 mmol) was mixed with 1 ml methanol and 1 ml hydrochloric acid. After 5 minutes product conversion was observed on TLC and confirmed on the LCMS. Reaction mixture was concentrated down and dried further on the high vacuum to give **45** as a yellow oil. This dried mixture was then taken directly to the next step. MS (ESI) m/z 342.47 [M+H]

N-acetyl-S-(2-amino-7-(4-fluorobenzyl)-6-oxo-6,7-dihydro-1H-purin-8-yl)cysteine, (1 eq, 10 mgs, 0.024 mmol), 1H-benzo[d][1,2,3]triazol-1-ol (2 eq, 6.4 mgs, 0.048 mmol), and Triethylamine (10 eq, 33ul, 0.024 mmol) in 1 ml of dry DMF. This was sonicated and then allowed to stir for 15 mins before **45** (1.4 eq, 11 mgs, 0.033 mmol) was added and the reaction mixture stirred overnight. In the morning, 16 hours later product was verified on the LCMS and then filtered with PTFE Syringe Filters, 0.22 um, 17mm before HPLC purification was completed (55-70% H_2O/Methanol, duration of 45 min, flow rate of 20 mL/min, detection at 254 nm) to yield **46** as an off yellow white powder. (0.8 mgs, 0.001 mmol, 5% yield) ^{1}H NMR (599 MHz, DMSO-D_6) δ 10.69 (s, 1H), 8.43 (d, J = 8.0 Hz, 1H), 8.14 (t, J = 5.8 Hz, 1H), 7.76 (dd, J = 8.7, 4.0 Hz, 3H), 7.59 (d, J = 2.5 Hz, 1H), 7.20 (dd, J = 8.6, 5.5 Hz, 2H), 7.14 (t, J = 8.8 Hz, 2H), 7.04 (dd, J = 8.8, 2.5 Hz, 1H), 6.64 (d, J = 8.7 Hz, 2H), 6.58 (s, 2H), 6.41 (q, J = 5.0 Hz, 1H), 5.08 (s, 2H), 4.50 (td, J = 8.1, 5.1 Hz, 1H), 4.14 (t, J = 4.7 Hz, 2H), 3.74 (t, J = 4.5 Hz, 2H), 3.51 – 3.38 (m, 4H), 3.31 – 3.18 (m, 2H), 2.75 (d, J = 4.9 Hz, 3H), 1.85 (s, 3H). MS (ESI) m/z 745.85 [M+H]+[M/2]

Synthesis of Compound 51 (SAB-02-076)

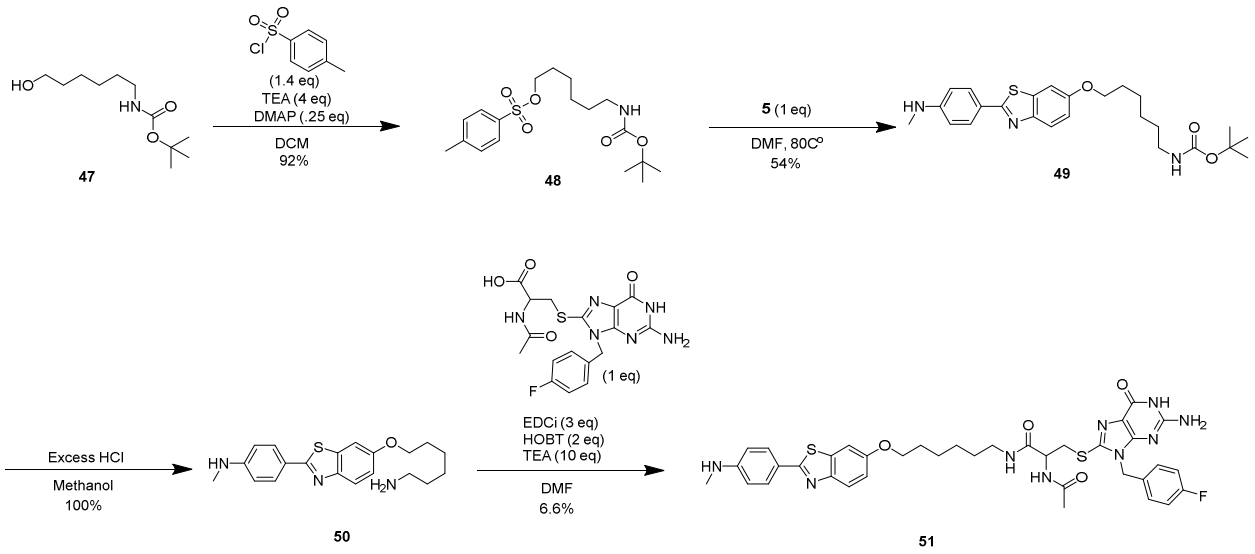

*(**47**)→ (**48**)*

6-((tert-butoxycarbonyl)amino)hexyl 4-methylbenzenesulfonate

47 (1 eq, 300 mgs, 1.38 mmol) and triethylamine (1.4 eq, .91 ul, 0.66 mmol) and catalytic DMAP (0.25 eq, 14 mg, 0.12 mmol) were mixed with 1 ml of dichloromethane under anhydrous conditions. The solution was cooled to 0C° in an ice bath and then 4-methylbenzenesulfonyl chloride (1.4 eq, 125 mgs, 0.655 mmol) was added dropwise. The reaction was removed from the ice bath and left to mix overnight (16 hours). This was monitored by LCMS and TLC until reached completion. Crude reaction was mixed with 10mls of dichloromethane and washed with 3x 10mls of DI water. Organic layer was concentrated down and purified by flash column chromatography (0-50% ethyl acetate in hexane) to give **43** as a colorless oil. (473 mgs, 1.27 mmol, 92% yield) ^{1}H NMR (500 MHz, METHANOL-D_4) δ 7.75 (d, J = 8.3 Hz, 2H), 7.41 (d, J = 8.1 Hz, 2H), 3.99 (t, J = 6.3 Hz, 2H), 2.95 (t, J = 7.0 Hz, 2H), 2.42 (s, 3H), 1.57 (dt, J = 8.0, 6.4 Hz, 2H), 1.40 (s, 9H), 1.36 (q, J = 7.2 Hz, 2H), 1.30 – 1.14 (m, 4H). MS (ESI) m/z 370.49 [M+Na]

*(**48**)→ (**49**)*

tert-butyl (6-((2-(4-(methylamino)phenyl)benzo[d]thiazol-6-yl)oxy)hexyl)carbamate

5 (1 eq, 45 mgs, 0.17 mmol) was mixed with potassium carbonate (2 eq, 48 mgs, 0.35 mmol) and 1 ml DMF 80C° for 10 minutes. Afterward **48** (1 eq, 65 mgs, 0.17 mmol) was added to this mixture and reaction monitored over 16 hours. Product was confirmed with LCMS and TLC.

Reaction mixture was mixed with 30 mls saturated sodium bicarbonate and extracted with 2x 20 mls ethyl acetate. The organic layer was then washed with 10mls DI water and organic layer concentrated. This crude mixture was purified with flash column chromatography (30-75% ethyl acetate in hexane) to give **49** as an off yellow wax. (43 mgs, 0.094 mmol, 54% yield) ^{1}H NMR (500 MHz, METHANOL-D_4) δ 7.76 (d, J = 8.5 Hz, 2H), 7.73 (d, J = 8.9 Hz, 1H), 7.41 (d, J = 2.5 Hz, 1H), 7.03 (dd, J = 8.9, 2.5 Hz, 1H), 6.64 (d, J = 8.5 Hz, 2H), 4.02 (t, J = 6.4 Hz, 2H), 3.52 (t, J = 6.6 Hz, 1H), 3.03 (t, J = 6.8 Hz, 3H), 2.82 (s, 3H), 1.80 (p, J = 6.7 Hz, 2H), 1.55 – 1.45 (m, 4H), 1.41 (s, 9H). MS (ESI) m/z 455.56 [M+H]

*(**49**)→ (**51**)*

2-acetamido-3-((2-amino-7-(4-fluorobenzyl)-6-oxo-6,7-dihydro-1H-purin-8-yl)thio)-N-(6-((2-(4-(methylamino)phenyl)benzo[d]thiazol-6-yl)oxy)hexyl)propenamide

49 (20.5 mgs, 0.045 mmol) was mixed with 1 ml methanol and 1 ml hydrochloric acid. After 5 minutes product conversion was observed on TLC and confirmed on the LCMS. Reaction mixture was concentrated down and dried further on the high vacuum to give **50** as a yellow oil. This dried mixture was then taken directly to the next step. MS (ESI) m/z 354.50 [M+H]

N-acetyl-S-(2-amino-7-(4-fluorobenzyl)-6-oxo-6,7-dihydro-1H-purin-8-yl)cysteine, (1 eq, 13 mgs, 0.031 mmol), 1H-benzo[d][1,2,3]triazol-1-ol (2 eq, 8.1 mgs, 0.060 mmol), and Triethylamine (10 eq, 42ul, 0.030 mmol) in 1 ml of dry DMF. This was sonicated and then allowed to stir for 15 mins before **50** (1.5 eq, 16 mgs, 0.045 mmol) was added and the reaction mixture stirred overnight. In the morning, 16 hours later product was verified on the LCMS and then filtered with PTFE Syringe Filters, 0.22 um, 17mm before HPLC purification was completed (15-75% H_2O/Methanol, duration of 45 min, flow rate of 20 mL/min, detection at 254 nm) to yield **51** as an off yellow white powder. (1.5 mgs, 0.002 mmol, 6.6% yield) ^{1}H NMR (599 MHz, DMSO-D_6) δ 8.42 (d, J = 8.1 Hz, 1H), 8.04 (t, J = 5.7 Hz, 1H), 7.75 (dd, J = 8.7, 5.2 Hz, 3H), 7.57 (d, J = 2.6 Hz, 1H), 7.20 (t, J = 6.8 Hz, 2H), 7.14 (t, J = 8.7 Hz, 2H), 7.02 (dd, J = 8.9, 2.5 Hz, 1H), 6.63 (d, J = 8.5 Hz, 3H), 6.39 (d, J = 5.2 Hz, 1H), 5.07 (s, 2H), 4.46 (q, J = 7.5 Hz, 1H), 4.00 (t, J = 6.5 Hz, 2H), 3.28 (dt, J = 13.4, 7.3 Hz, 1H), 3.17 (s, 1H), 3.07 – 3.01 (m, 2H), 2.74 (d, J = 4.9 Hz, 3H), 1.84 (s, 3H), 1.71 (t, J = 7.4 Hz, 2H), 1.40 (d, J = 7.3 Hz, 5H), 1.30 (d, J = 7.2 Hz, 1H), 1.23 (s, 3H). MS (ESI) m/z 757.90 [M+H]+[M/2]

Synthesis of Compound 66 (SAB-02-034)

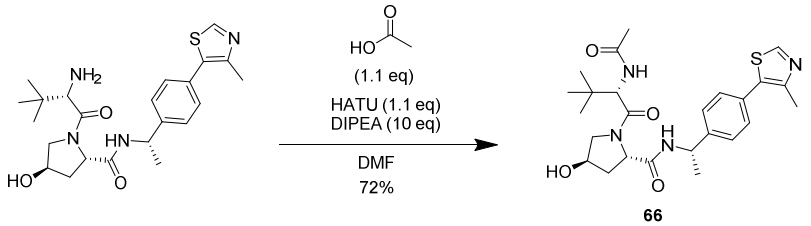

66

*(**66**)*

(2S,4R)-1-((S)-2-acetamido-3,3-dimethylbutanoyl)-4-hydroxy-N-((S)-1-(4-(4-methylthiazol-5-yl)phenyl)ethyl)pyrrolidine-2-carboxamide, Trifluoroacetic acid

(2S,4R)-1-((S)-2-amino-3,3-dimethylbutanoyl)-4-hydroxy-N-((S)-1-(4-(4-methylthiazol-5-yl)phenyl)ethyl)pyrrolidine-2-carboxamide (1 eq, 30 mgs, 0.067 mmol) was mixed with DIPEA (10 eq, .12 ml, .67 mmol), HATU (1.1 eq, 28 mgs, 0.074 mmol), and acetic acid (1.1 eq, 4.2 ul, 0.074 mmol) in 1 ml DMF. After 1 hour product was verified on the LCMS and then filtered with PTFE Syringe Filters, 0.22 um, 17mm before HPLC purification was completed (0-100% H_2O/Methanol, duration of 45 min, flow rate of 20 mL/min, detection at 254 nm) to yield **66** as a white powder. (29 mgs, 0.048 mmol, 72% yield) ^{1}H NMR (400 MHz, DMSO-D_6) δ 8.96 (s, 1H), 8.36 (d, J = 7.8 Hz, 1H), 7.87 (d, J = 9.3 Hz, 1H), 7.44 – 7.37 (m, 2H), 7.34 (d, J = 8.3 Hz, 2H), 4.87 (p, J = 7.2 Hz, 1H), 4.47 (d, J = 9.4 Hz, 1H), 4.37 (t, J = 8.1 Hz, 1H), 4.24 (q, J = 3.2 Hz, 1H), 3.55 (t, J = 3.1 Hz, 2H), 2.41 (s, 3H), 1.97 (ddd, J = 12.8, 7.8, 2.5 Hz, 1H), 1.83 – 1.69 (m, 1H), 1.33 (d, J = 7.0 Hz, 3H), 0.89 (s, 9H). MS (ESI) m/z 486.63 [M+H]

Chapter 3

Chemical Compound Information

All chemicals, unless otherwise stated, were commercially available and used without further purification. 2-(4-(methylamino)phenyl)benzo[d]thiazol-6-ol[45], (2S,4R)-1-((S)-2-amino-3,3-dimethylbutanoyl)-4-hydroxy-N-((S)-1-(4-(4-methylthiazol-5-yl)phenyl)ethyl)pyrrolidine-2-carboxamide [46] were synthesized as previously described. All reactions were carried out in anhydrous conditions and commercially available anhydrous solvents were used. Analytical LCMS was performed using MilliQ water with .1% formic acid and acetonitrile using a packed column (Acquity UPLC BEH C18, 2.1mm x 50mm, 1.7 um). TLC was carried out on pre-coated silica plates 60F254 (Merck) with visualization via UV light (UV 254 nm). In 1H NMR data, chemical shifts are quoted in ppm and referenced to the residual solvent signals (DMSO-d6, d = 2.50; Methanol-d4, qu = 3.31; Chloroform-d, s = 7.26), and signal splitting patterns are described as singlet (s), doublet (d), triplet (t), quartet (q), quintet (qu), multiplet (m), and broad (br). Coupling constants (JH-H) are measured in Hz. Preparative HPLC was performed on a WATERS HPLC system using methanol and water with a Packed Column (XBridge Prep C18,

19 mm x 100 mm; 5 um OBD). Purities of assayed compounds were in all cases greater than 95%, as determined by reverse-phase HPLC analysis.

Synthesis of Compound 59 (SAB-02-059)

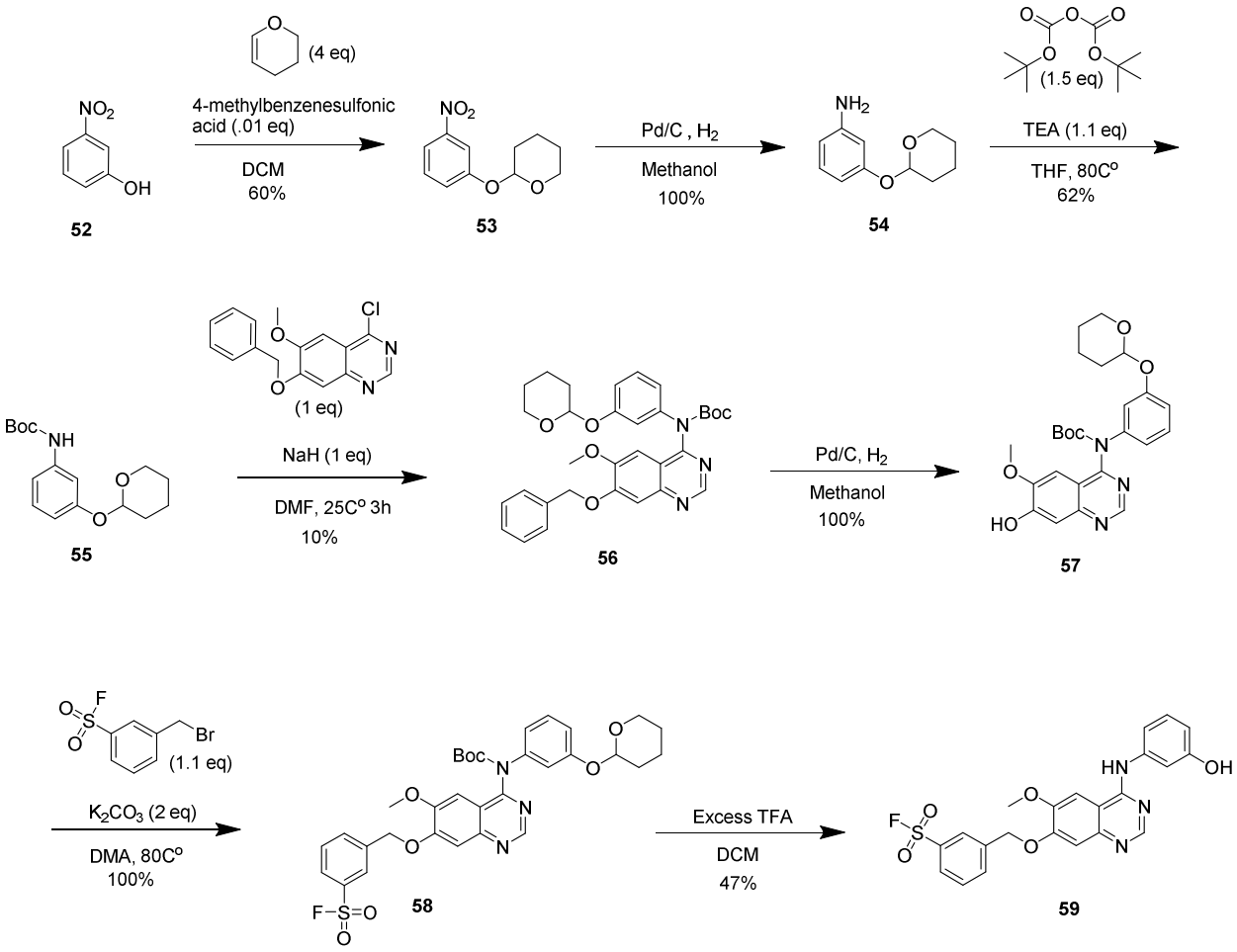

*(**52**)→ (**53**)*

2-(3-nitrophenoxy)tetrahydro-2H-pyran

3-nitrophenol, **52,** (1 eq, 100 mgs, 0.719 mmol) and 3,4-dihydro-2H-pyran (4 eq, 0.25 ml, 2.88 mmol) were mixed with 2 ml of dichloromethane under anhydrous conditions. To this solution catalytic 4-methylbenzenesulfonic acid (0.01 eq, 1.24 mg, 0.007 mmol) was added and the reaction mixture stirred overnight for 16 hour before product was confirmed by LCMS and TLC. Reaction mixture was mixed with 10 mls of DCM and extracted with 3x 20 ml washes of saturated sodium bicarbonate. The organic layer was dried down and purified with column chromatography (0-10% ethyl acetate in hexane) to give **53** as a colorless oil (96 mgs, 0.43 mmol, 60% yield) 1H NMR (500 MHz, $CDCl_3$) δ 7.90 (t, J = 2.3 Hz, 1H), 7.84 (ddt, J = 8.0, 2.2,

1.0 Hz, 1H), 7.42 (td, J = 8.2, 0.9 Hz, 1H), 7.35 (ddd, J = 8.3, 2.4, 1.1 Hz, 1H), 5.50 (t, J = 3.2 Hz, 1H), 3.84 (ddd, J = 11.1, 10.0, 3.1 Hz, 1H), 3.63 (dtd, J = 11.4, 4.1, 1.4 Hz, 1H), 2.06 – 1.94 (m, 1H), 1.89 (ddd, J = 7.8, 4.3, 3.1 Hz, 2H), 1.77 – 1.69 (m, 1H), 1.72 – 1.64 (m, 1H), 1.61 (ddq, J = 10.5, 6.5, 3.2 Hz, 1H). MS (ESI) m/z 138.01 [M-THP(84)]

(53)→ (55)

tert-butyl (3-((tetrahydro-2H-pyran-2-yl)oxy)phenyl)carbamate

53 (1 eq, 58 mgs, 0.26 mmol) was mixed with 2 mls of methanol and palladium on carbon (.2 eq, 5.8 mgs, 0.055 mmol). The reaction vessel was purged using a Schlenk line three times with nitrogen followed by bubbling hydrogen gas in the mixture. This was left to spin for 1 hour before LCMS and TLC confirmed conversion of starting material to product. The reaction mixture was then filtered through a frit packed with celite and washed with 20mls methanol. This organic layer was then dried down to give, *3-((tetrahydro-2H-pyran-2-yl)oxy)aniline,* **54** as a thick colorless oil which was then taken directly to the next step. MS (ESI) m/z 193.25 [M+H]

54 (1 eq, 50 mgs, .26 mmol) was mixed with TEA (1.1 eq, 40 ul, 0.28 mmol) and Boc_2O (1.5 eq, 85 mgs, 0.39 mmol) in 2mls THF. This reaction mixture was then heated to 80C° for 15 hours with product confirmed on LCMS and TLC. The reaction mixture was dried down and then extracted with 30 mls DCM with 3x 20 mls washes of brine. The organic layer was dried down and purified on column chromatography (0-40% ethyl acetate in hexane) to give **55** as a thick colorless oil. (47 mgs, 0.016 mmol, 62% yield) ^{1}H NMR (500 MHz, $CDCl_6$) δ 7.19 – 7.08 (m, 2H), 6.91 (d, J = 7.9 Hz, 1H), 6.72 (ddt, J = 8.3, 2.4, 1.4 Hz, 1H), 6.48 (s, 1H), 5.41 (q, J = 3.0 Hz, 1H), 3.89 (ddt, J = 11.1, 9.8, 2.8 Hz, 1H), 3.63 – 3.55 (m, 1H), 2.01 – 1.95 (m, 1H), 1.83 (ddt, J = 7.5, 4.6, 2.3 Hz, 2H), 1.71 – 1.61 (m, 4H), 1.50 (d, J = 2.3 Hz, 9H)
MS (ESI) m/z 293.25

(55)→ (56)

tert-butyl (7-(benzyloxy)-6-methoxyquinazolin-4-yl)(3-((tetrahydro-2H-pyran-2-yl)oxy)phenyl)carbamate

55 (1 eq, 205 mgs, 0.699 mmol) was mixed with sodium hydride (1 eq, 28 mgs, 0.699 mmol) in 3ml of DMF and purged with nitrogen gas three times. This was stirred for about 15 mins at 0C°. 7-(benzyloxy)-4-chloro-6-methoxyquinazoline (1 eq, 210 mgs, 0.699 mmol) was then mixed with 1 ml DMF and injected through a seal cap with **55** and sodium hydride. The reaction mixture was then heated to 50C for 3 hours and product conversion verified with LCMS and TLC. The reaction mixture was then cooled and quenched with saturated sodium bicarbonate until the pH of the reaction is at 7. Compound was extracted with 30ml of DI water in 3x 30 mls of DCM. The organic layer was then washed with 10 mls DI water and organic layer concentrated and purified on the column (10-50% ethyl acetate in hexane) to give **56** as a thick colorless oil. (39 mgs, 0.069 mmol, 10% yield) ^{1}H NMR (400 MHz, $CDCl_6$) δ 9.00 (s, 1H), 7.53 – 7.45 (m, 2H), 7.42 – 7.37 (m, 4H), 7.36 – 7.31 (m, 1H), 7.20 (t, J = 8.2 Hz, 1H), 7.15 (s, 1H),

6.98 (t, J = 2.2 Hz, 1H), 6.89 (ddd, J = 15.3, 8.0, 2.0 Hz, 2H), 5.34 (q, J = 3.1 Hz, 1H), 5.31 (s, 2H), 3.91 (s, 3H), 3.88 – 3.76 (m, 1H), 3.58 – 3.48 (m, 1H), 2.16 (d, J = 2.2 Hz, 1H), 1.87 – 1.75 (m, 2H), 1.71 – 1.50 (m, 11H), 1.39 (s, 9H), 1.24 (d, J = 1.8 Hz, 1H) MS (ESI) m/z 557.65 [M+H]

(56)→ (57)

tert-butyl (7-hydroxy-6-methoxyquinazolin-4-yl)(3-((tetrahydro-2H-pyran-2-yl)oxy)phenyl)carbamate

56 (1 eq, 44 mgs, 0.079 mmol) was mixed with 2 mls of methanol and palladium on carbon (0.5 eq, 4.4 mgs, 0.041 mmol). The reaction vessel was purged using a Schlenk line three times with nitrogen followed by bubbling hydrogen gas in the mixture. This was left to spin for 1 hour before LCMS and TLC confirmed conversion of starting material to product. The reaction mixture was then filtered through a frit packed with celite and washed with 20 mls methanol. This organic layer was then dried down to give **57** as a yellowish colorless oil. (38 mgs, 0.081 mmol, 101% yield) ^{1}H NMR (500 MHz, $CDCl_3$) δ 9.03 (s, 1H), 7.47 (d, *J* = 3.4 Hz, 1H), 7.19 (q, *J* = 9.4 Hz, 3H), 6.98 (d, *J* = 3.1 Hz, 1H), 6.89 (dd, *J* = 17.0, 8.0 Hz, 2H), 5.34 (s, 1H), 3.96 (s, 3H), 3.83 (t, *J* = 10.0 Hz, 1H), 3.56 (dd, *J* = 28.1, 11.0 Hz, 1H), 1.94 (s, 2H), 1.85 – 1.77 (m, 3H), 1.50 (s, 2H), 1.39 (s, 9H). MS (ESI) m/z 466.52 [M+H]

(57)→ (58)

tert-butyl (7-((3-(fluorosulfonyl)benzyl)oxy)-6-methoxyquinazolin-4-yl)(3-((tetrahydro-2H-pyran-2-yl)oxy)phenyl)carbamate

57 (1 eq, 17 mgs, .044 mmol) was mixed with potassium carbonate (2 eq, 12 mgs, 0.089 mmol) and 3-(bromomethyl)benzenesulfonyl fluoride (1.2 eq, 13 mgs, 0.053 mmol) in 1 ml of DMA. This was left to spin at 80C° for 1 hour before LCMS and TLC confirmed conversion of starting material to product. Compound was extracted with 30ml of DI water in 3x30mls of DCM. The organic layer was then washed with 10mls DI water and organic layer concentrated and purified on the column (10-50% ethyl acetate in hexane) to give **58** as a thick colorless oil. (28 mgs, 0.044 mmol, 100% yield) ^{1}H NMR (400 MHz, METHANOL-D_4) δ 8.94 (s, 1H), 8.24 (s, 1H), 8.03 (q, J = 6.6 Hz, 2H), 7.76 (td, J = 8.2, 3.8 Hz, 1H), 7.47 (s, 1H), 7.29 – 7.19 (m, 2H), 7.07 (t, J = 2.3 Hz, 1H), 6.99 – 6.83 (m, 2H), 5.45 (s, 2H), 5.41 – 5.32 (m, 1H), 3.91 (s, 3H), 3.80 (ddd, J = 12.2, 9.5, 3.4 Hz, 1H), 3.52 (dt, J = 11.4, 4.3 Hz, 1H), 2.17 (d, J = 9.5 Hz, 1H), 1.93 (dt, J = 14.5, 5.2 Hz, 1H), 1.80 (dddd, J = 17.9, 13.5, 11.1, 4.1 Hz, 2H), 1.64 (dt, J = 11.5, 4.1 Hz, 1H), 1.54 (ddd, J = 17.8, 9.2, 5.8 Hz, 1H), 1.43 (s, 9H), 1.31 – 1.25 (m, 1H). MS (ESI) m/z 639.70 [M+H]

(58)→ (59)

3-(((4-((3-hydroxyphenyl)amino)-6-methoxyquinazolin-7-yl)oxy)methyl)benzenesulfonyl fluoride, Trifluoroacetic acid

58 (1 eq, 12 mgs, 0.019 mmol) was mixed with 1ml DCM and 1ml TFA. Reaction mixture was monitored by LCMS and TLC with complete conversion is 5 minutes. Reaction mixture was filtered with PTFE Syringe Filters, 0.22 um, 17mm before HPLC purification was completed (0-100% H_2O/Methanol with 0.1% TFA, duration of 28 min, flow rate of 20 mL/min, detection at 254 nm) to yield **59** as a white powder. (3.1 mgs, 0.005 mmol, 29% yield) ^{1}H NMR (599 MHz, DMSO-D_6) δ 10.29 (s, 1H), 9.61 (s, 1H), 8.66 (s, 1H), 8.31 (s, 1H), 8.18 (d, J = 8.0 Hz, 1H), 8.10 (d, J = 7.8 Hz, 1H), 8.04 (s, 1H), 7.89 (t, J = 7.8 Hz, 1H), 7.37 (s, 1H), 7.23 (dd, J = 15.0, 6.9 Hz, 2H), 7.13 (d, J = 8.1 Hz, 1H), 6.65 (d, J = 8.2 Hz, 1H), 5.51 (s, 2H), 4.00 (s, 3H). Fluorine NMR (376 MHz, DMSO-D_6) δ -73.55 (s, 1F). MS (ESI) m/z 455.48 [M+H]

Synthesis of Compound 61 (SAB-01-160)

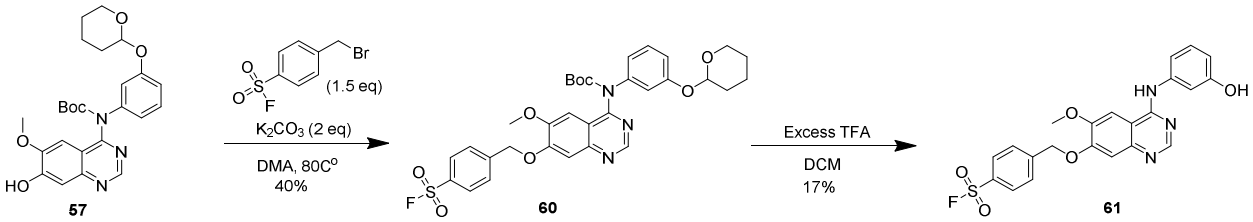

(57)→ (60)

tert-butyl (7-((4-(fluorosulfonyl)benzyl)oxy)-6-methoxyquinazolin-4-yl)(3-((tetrahydro-2H-pyran-2-yl)oxy)phenyl)carbamate

57 (1 eq, 45.3 mgs, 0.096 mmol) was mixed with potassium carbonate (2 eq, 26.8 mgs, 0.194 mmol) and 4-(bromomethyl)benzenesulfonyl fluoride (1.5 eq, 36.8 mgs, 0.145 mmol) in 1 ml of DMA. This was left to spin at 80C° for 1 hour before LCMS and TLC confirmed conversion of starting material to product. Compound was extracted with 30ml of DI water in 3x 30 mls of DCM. The organic layer was then washed with 10 mls DI water and organic layer concentrated and purified on the column (20-55% ethyl acetate in hexane) to give **60** as a thick colorless oil. (22.5 mgs, 0.035 mmol, 36% yield) ^{1}H NMR (400 MHz, $CDCl_6$) δ 9.01 (s, 1H), 8.05 (d, J = 8.3 Hz, 2H), 7.75 (d, J = 8.2 Hz, 2H), 7.34 (t, J = 2.0 Hz, 1H), 7.25 – 7.16 (m, 2H), 7.00 – 6.83 (m, 3H), 5.41 (s, 2H), 5.34 (t, J = 3.3 Hz, 1H), 3.93 (s, 3H), 3.82 (ddd, J = 11.3, 9.6, 3.1 Hz, 1H), 3.58 – 3.48 (m, 1H), 1.93 (ddt, J = 14.1, 11.1, 7.0 Hz, 1H), 1.79 (dt, J = 10.9, 4.4 Hz, 2H), 1.72 – 1.50 (m, 1H), 1.40 (s, 9H). MS (ESI) m/z 639.70 [M+H]

(60)→ (61)

4-(((4-((3-hydroxyphenyl)amino)-6-methoxyquinazolin-7-yl)oxy)methyl)benzenesulfonyl fluoride, Trifluoroacetic acid

60 (1 eq, 22.5 mgs, 0.035 mmol) was mixed with 1ml DCM and 1ml TFA. Reaction mixture was monitored by LCMS and TLC with complete conversion is 5 minutes. Reaction mixture was filtered with PTFE Syringe Filters, 0.22 um, 17mm before HPLC purification was completed (0-100% H_2O/Methanol with 0.1% TFA, duration of 28 min, flow rate of 20 mL/min, detection at 254 nm) to yield **61** as a white powder. (3.5 mgs, 0.006 mmol, 17% yield) ^{1}H NMR (400 MHz, DMSO-D_6) δ 10.46 (s, 1H), 9.62 (s, 1H), 8.73 (s, 1H), 8.20 (d, J = 8.3 Hz, 2H), 8.05 (s, 1H), 7.86 (d, J = 8.2 Hz, 2H), 7.31 (s, 1H), 7.20 (t, J = 8.1 Hz, 1H), 7.12 (t, J = 2.2 Hz, 1H), 7.06 (dd, J = 7.7, 1.9 Hz, 1H), 6.64 (dd, J = 8.2, 2.3 Hz, 1H), 6.54 (s, 1H), 5.53 (s, 2H), 3.98 (s, 3H). Fluorine NMR (376 MHz, DMSO-D_6) δ -73.64 (s, 1F). MS (ESI) m/z 455.48 [M+H]

Synthesis of Compound 63 (SAB-01-120)

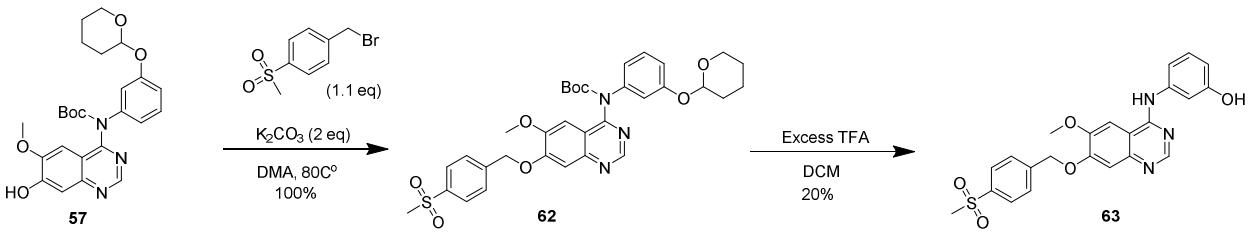

*(**57**)→ (**62**)*

tert-butyl (6-methoxy-7-((4-(methylsulfonyl)benzyl)oxy)quinazolin-4-yl)(3-((tetrahydro-2H-pyran-2-yl)oxy)phenyl)carbamate

57 (1 eq, 22 mgs, 0.047 mmol) was mixed with potassium carbonate (2 eq, 13 mgs, 0.094 mmol) and 4-(bromomethyl)benzenesulfonyl fluoride (1.1 eq, 13 mgs, 0.052 mmol) in 1 ml of DMA. This was left to spin at 80C° for 1 hour before LCMS and TLC confirmed conversion of starting material to product. Compound was extracted with 30 ml of DI water in 3x 30 mls of DCM. The organic layer was then washed with 10 mls DI water and organic layer concentrated and purified on the column (0-10% methanol in DCM) to give **62** as a thick colorless oil. (30 mgs, 0.047 mmol, 100% yield) ^{1}H NMR (400 MHz, DMSO-D_6) δ 10.33 (s, 1H), 9.58 (s, 1H), 8.63 (s, 1H), 8.02 – 7.91 (m, 3H), 7.77 –7.70 (m, 2H), 7.27 (s, 1H), 7.19 (t, J = 8.0 Hz, 1H), 7.14 (s, 1H), 7.10 – 7.04 (m, 1H), 6.62 (dd, J = 8.2, 2.3 Hz, 1H), 6.52 (s, 1H), 5.44 (s, 2H), 3.96 (s, 3H), 3.83 (t, J = 10.0 Hz, 1H), 3.56 (dd, J = 28.1, 11.0 Hz, 1H), 3.21 (s, 3H), 1.94 (s, 2H), 1.85 – 1.77 (m, 3H), 1.50 (s, 1H) 1.39 (s, 9H). MS (ESI) m/z 634.73 [M+H]

*(**62**)→ (**63**)*

3-((6-methoxy-7-((4-(methylsulfonyl)benzyl)oxy)quinazolin-4-yl)amino)phenol, Trifluoroacetic acid

62 (1 eq, 33.6 mgs, 0.061 mmol) was mixed with 1 ml DCM and 1 ml TFA. Reaction mixture was monitored by LCMS and TLC with complete conversion is 5 minutes. Reaction mixture was filtered with PTFE Syringe Filters, 0.22 um, 17 mm before HPLC purification was completed (0-100% H_2O/Methanol with .1% TFA, duration of 28 min, flow rate of 20 mL/min, detection at

254 nm) to yield **63** as a white powder. (8 mgs, 0.01 mmol, 20% yield) ^{1}H NMR (400 MHz, DMSO-D_6) δ 10.33 (s, 1H), 9.58 (s, 1H), 8.63 (s, 1H), 8.00 (s, 1H), 7.98 – 7.95 (m, 2H), 7.77 – 7.70 (m, 2H), 7.27 (s, 1H), 7.19 (t, J = 8.0 Hz, 1H), 7.14 (s, 1H), 7.10 – 7.04 (m, 1H), 6.62 (dd, J = 8.2, 2.3 Hz, 1H), 5.44 (s, 2H), 3.96 (s, 3H), 3.21 (s, 3H). MS (ESI) m/z 450.50 [M+H]

Synthesis of Compound 65 (SAB-02-023)

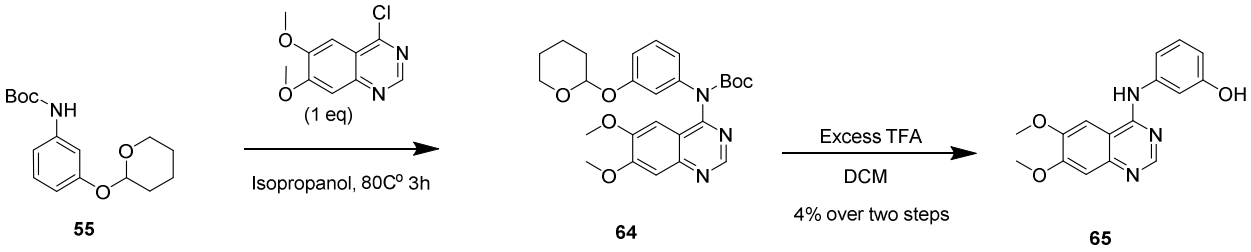

(55)→ (65)

3-((6,7-dimethoxyquinazolin-4-yl)amino)phenol, Trifluoroacetic acid

55 (1 eq, 45.3 mgs, 0.096 mmol) was mixed with 4-chloro-6,7-dimethoxyquinazoline (1 eq, 50 mgs, 0.145 mmol) in 1 ml of Isopropanol. This was left to spin at 80C° for 3 hours before LCMS and TLC confirmed complete conversion of starting material to product **64**. Compound was extracted with 30 ml of DI water in 3x30mls of DCM. The organic layer was then dried down and taken to next step. MS (ESI) m/z 379.46 [M+H]

6,7-dimethoxy-N-(3-((tetrahydro-2H-pyran-2-yl)oxy)phenyl)quinazolin-4-amine **64** (1 eq, 85 mgs, 0.22 mmol) was was mixed with 1 ml DCM and 1 ml TFA. Reaction mixture was monitored by LCMS and TLC with complete conversion is 5 minutes. Reaction mixture was filtered with PTFE Syringe Filters, 0.22 um, 17 mm before HPLC purification was completed (0-100% H_2O/Methanol with .1% TFA, duration of 28 min, flow rate of 20 mL/min, detection at 254 nm) to yield **63** as a white powder. (4 mgs, 0.01 mmol, 6% yield) 1H NMR (400 MHz, DMSO-D_6) δ 10.62 (s, 1H), 9.66 (s, 1H), 8.73 (s, 1H), 7.99 (s, 1H), 7.26 – 7.17 (m, 2H), 7.09 (d, J = 2.2 Hz, 1H), 7.07 – 7.01 (m, 1H), 6.66 (dd, J = 8.1, 2.3 Hz, 1H), 3.94 (d, J = 2.1 Hz, 6H). MS (ESI) m/z 297.31 [M+H]

NMR Spectra
Chapter 2

Spectrum 1 Compound 3 ^{1}H NMR

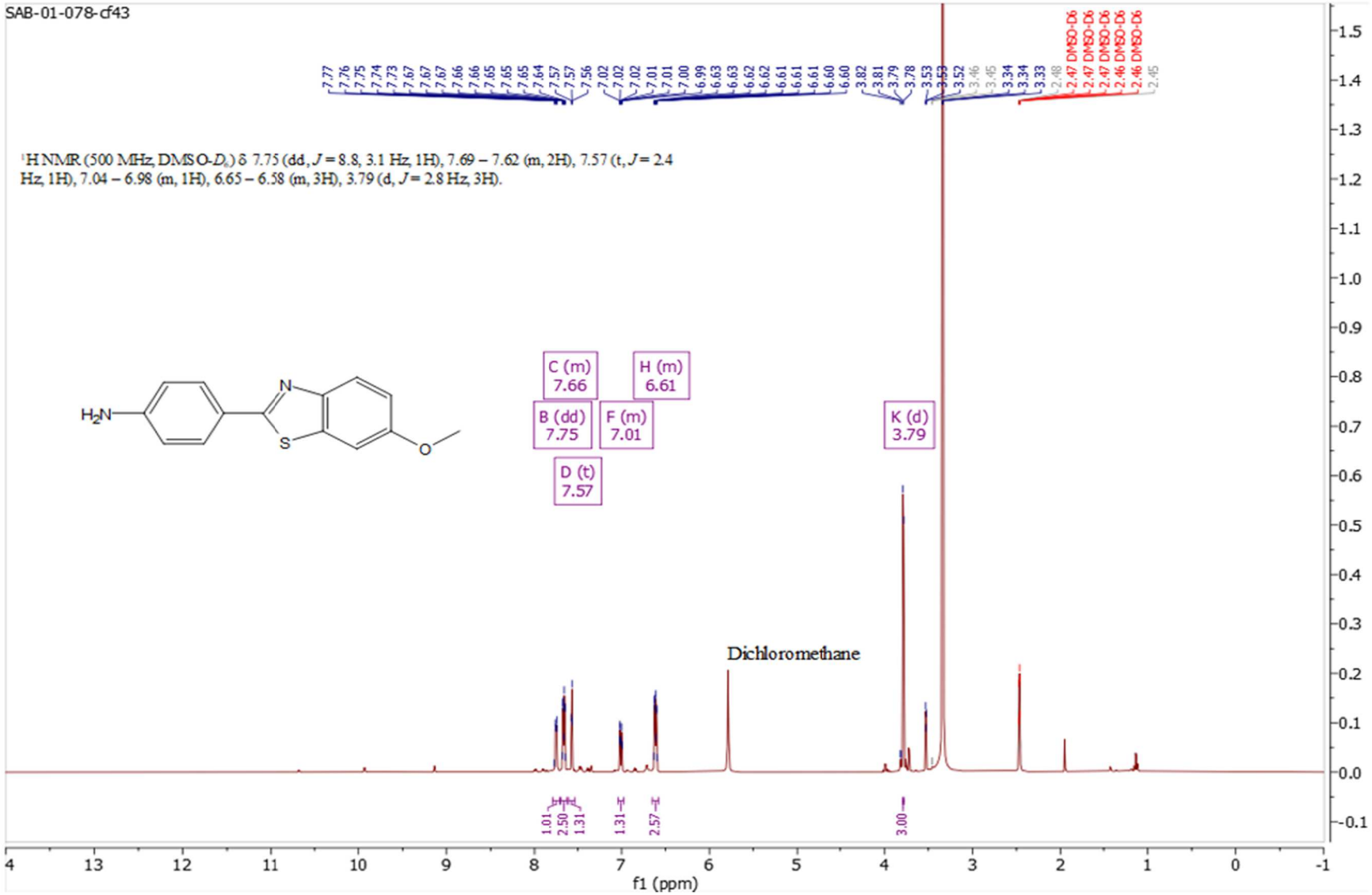

Spectrum 2 Compound 4 ^{1}H NMR

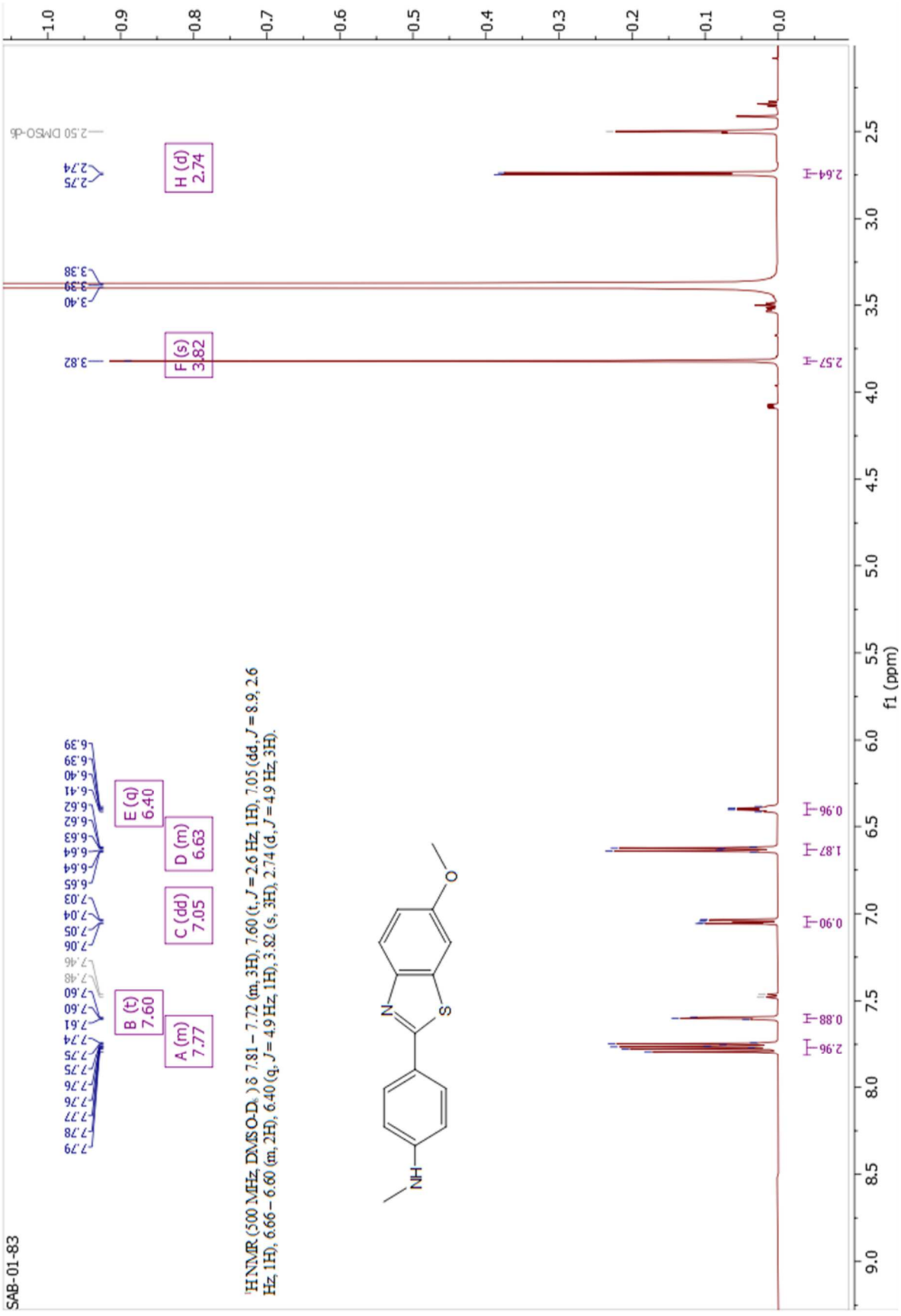

^{1}H NMR (500 MHz, DMSO-d_6) δ 7.81 – 7.72 (m, 3H), 7.60 (t, J = 2.6 Hz, 1H), 7.05 (dd, J = 8.9, 2.6 Hz, 1H), 6.66 – 6.60 (m, 2H), 6.40 (q, J = 4.9 Hz, 1H), 3.82 (s, 3H), 2.74 (d, J = 4.9 Hz, 3H).

Spectrum 3 Compound 5 ^{1}H NMR

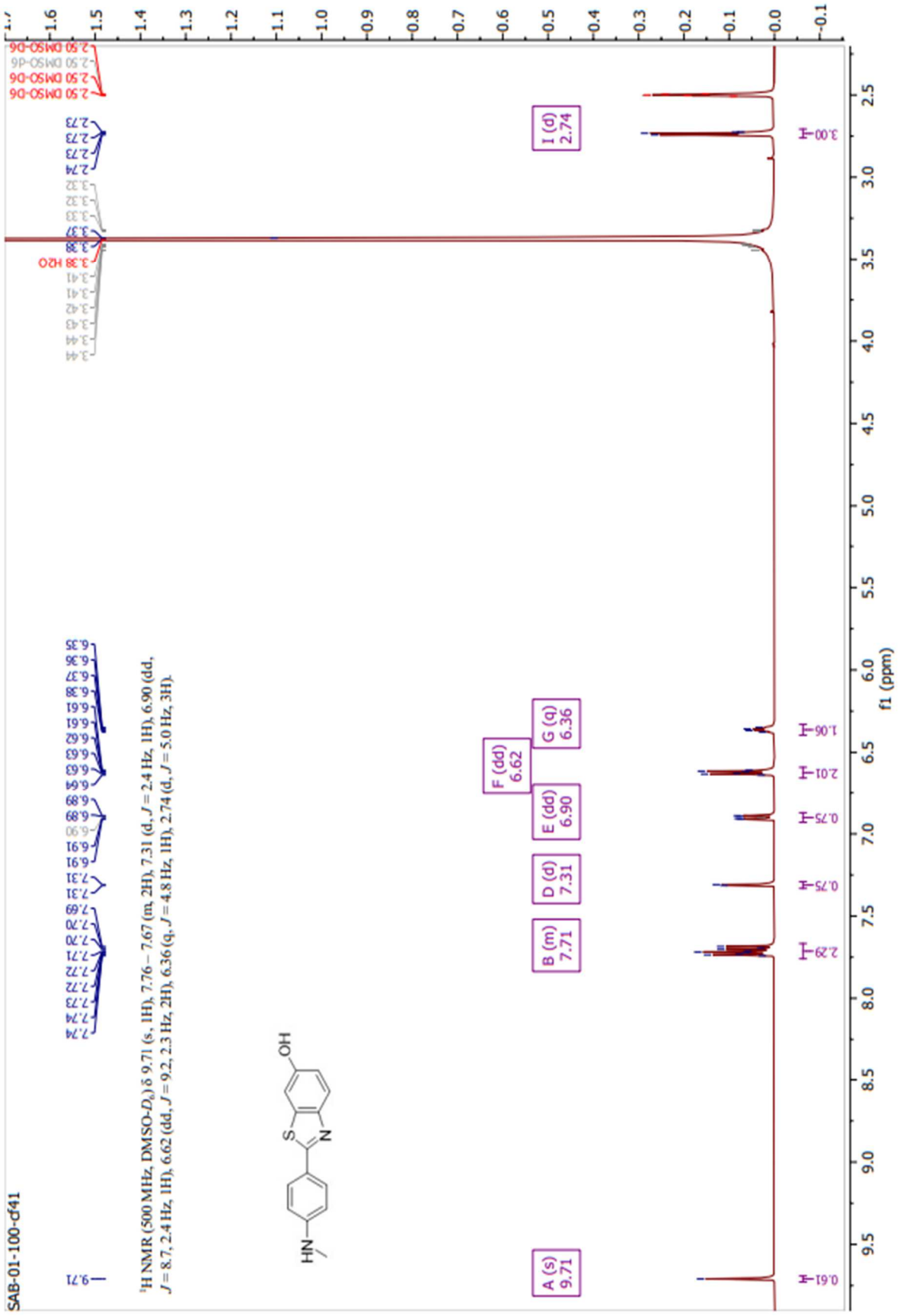

Spectrum 4 Compound 7 ^{1}H NMR

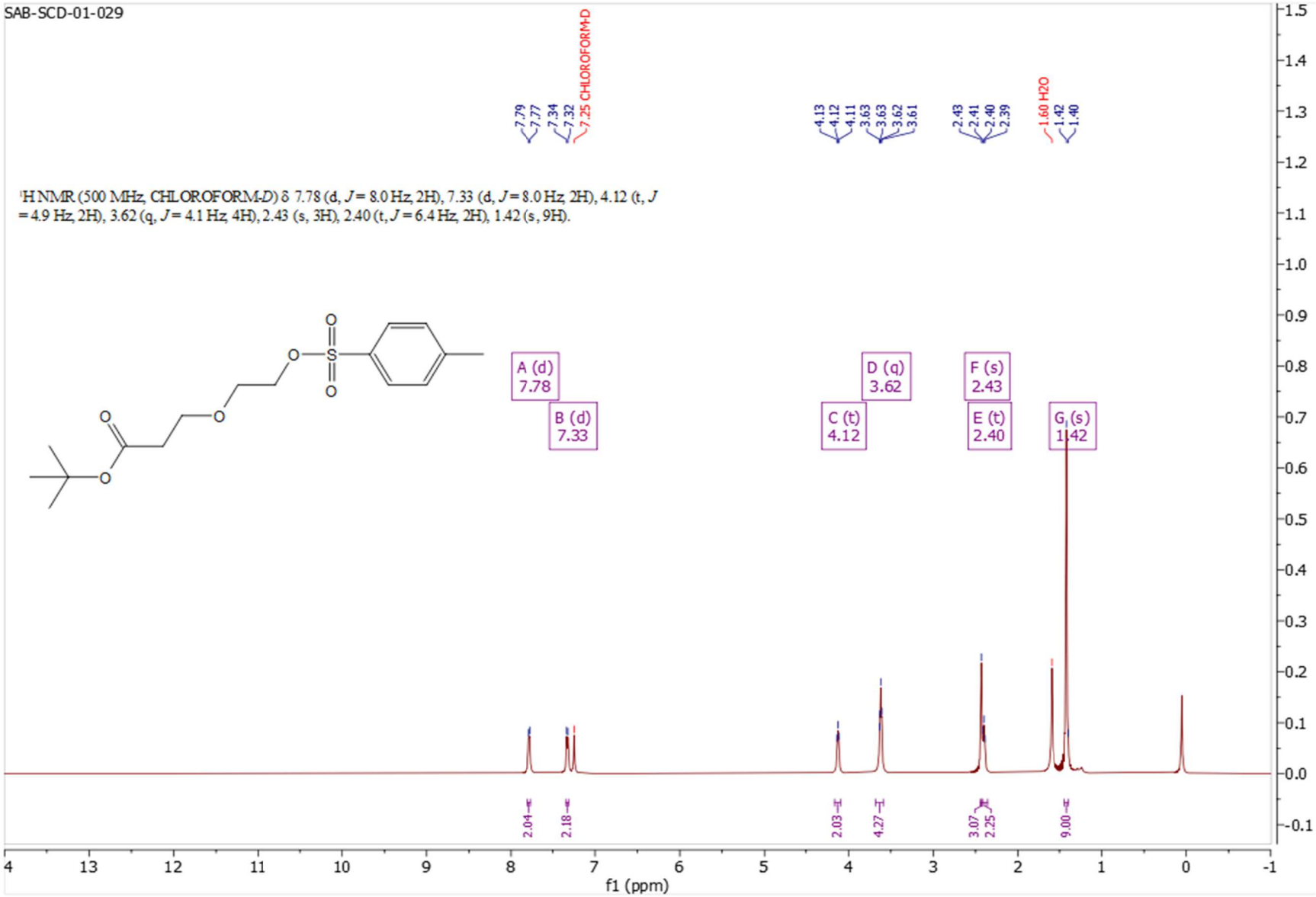

Spectrum 5 Compound 8 ^{1}H NMR

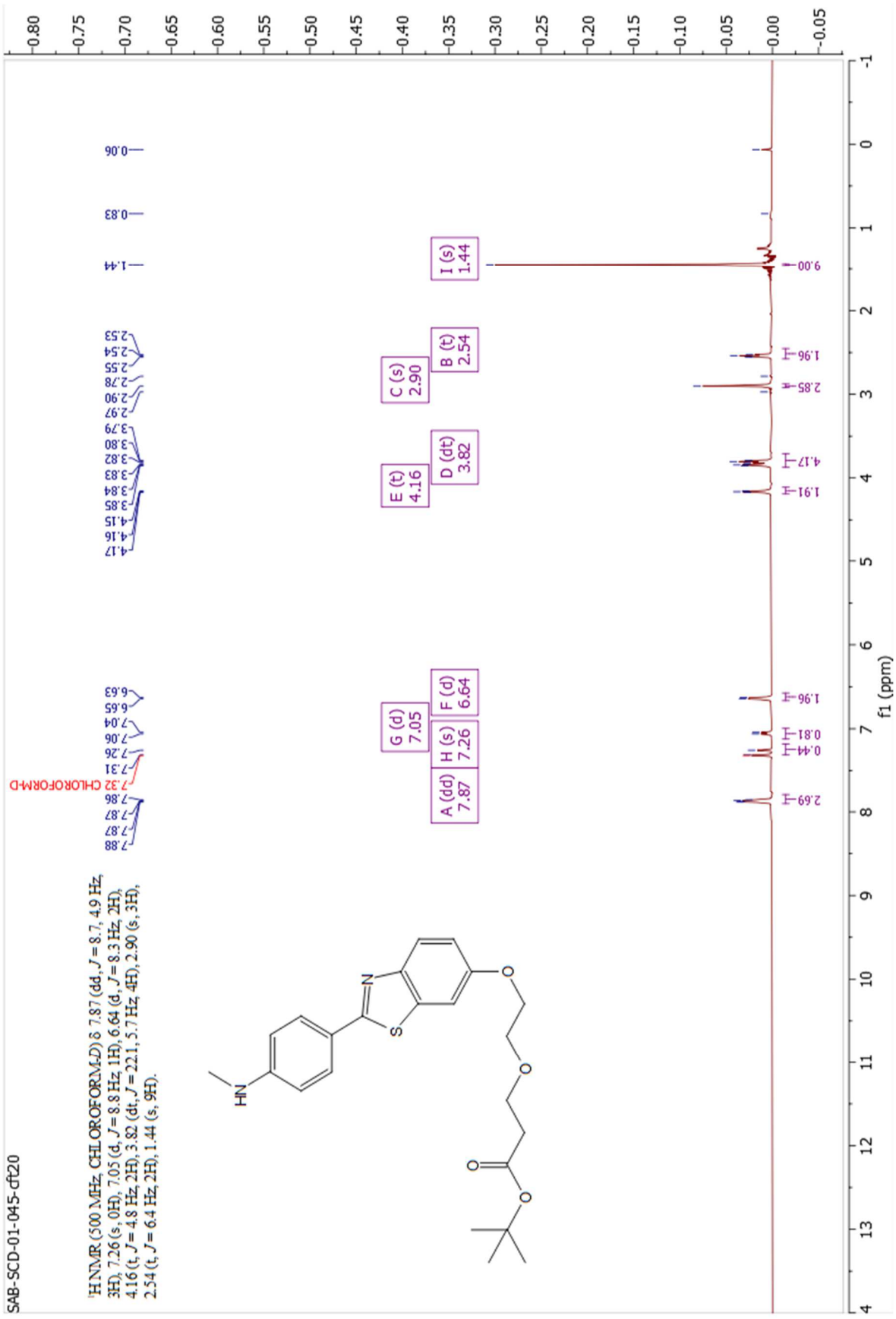

Spectrum 6 Compound 10 ^{1}H NMR

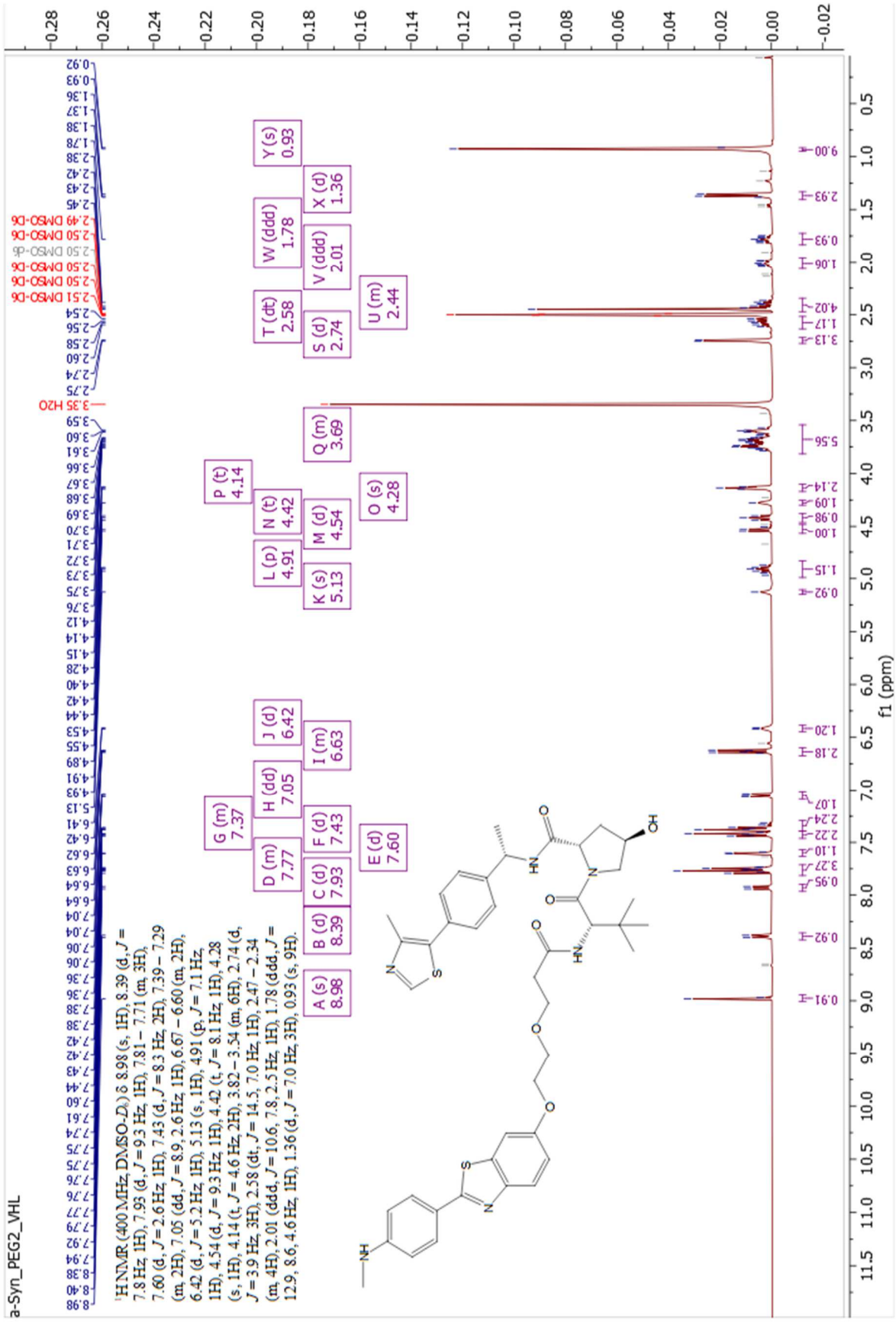

Spectrum 7 Compound 12 ^{1}H NMR

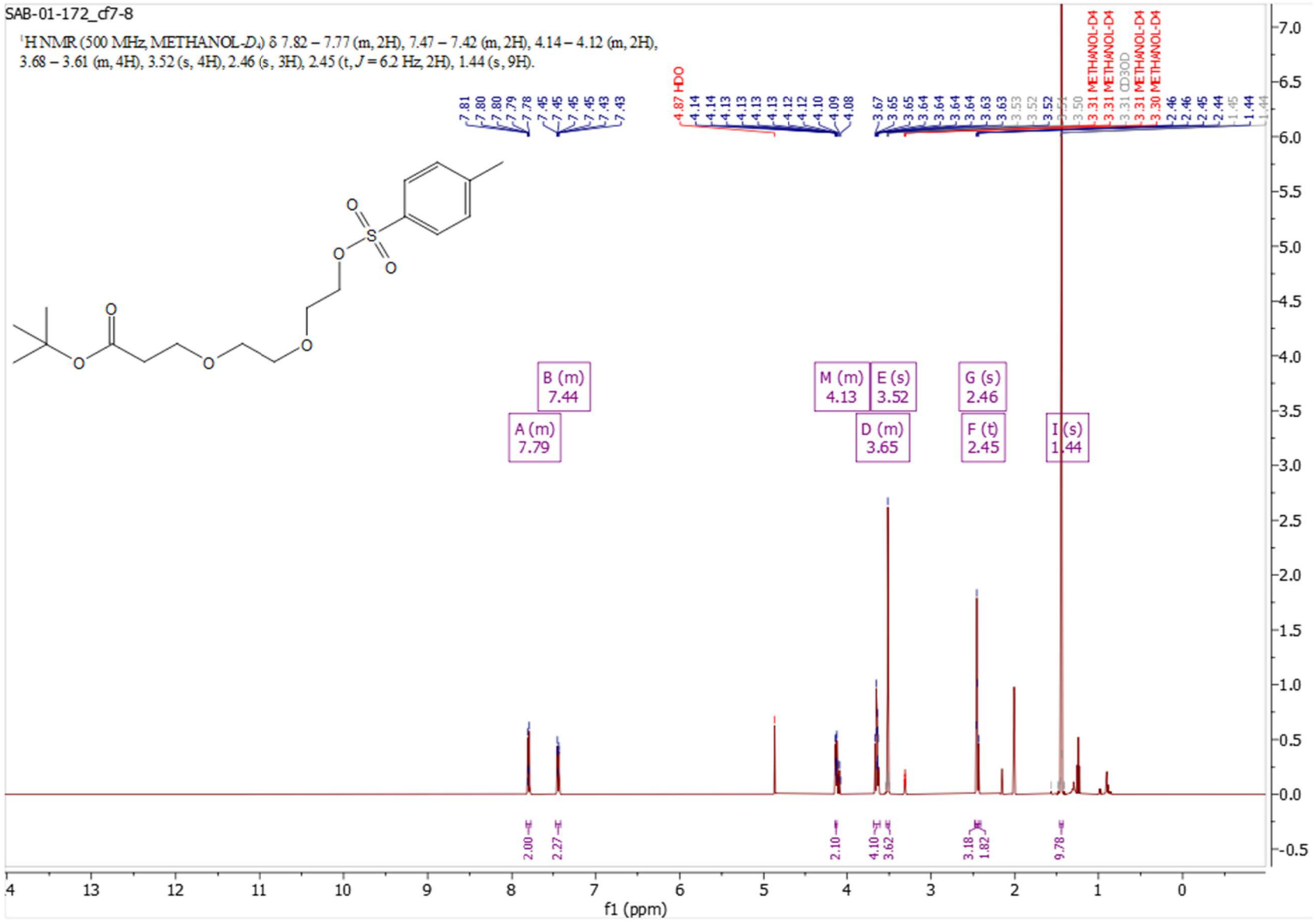

Spectrum 8 Compound 13 ^{1}H NMR

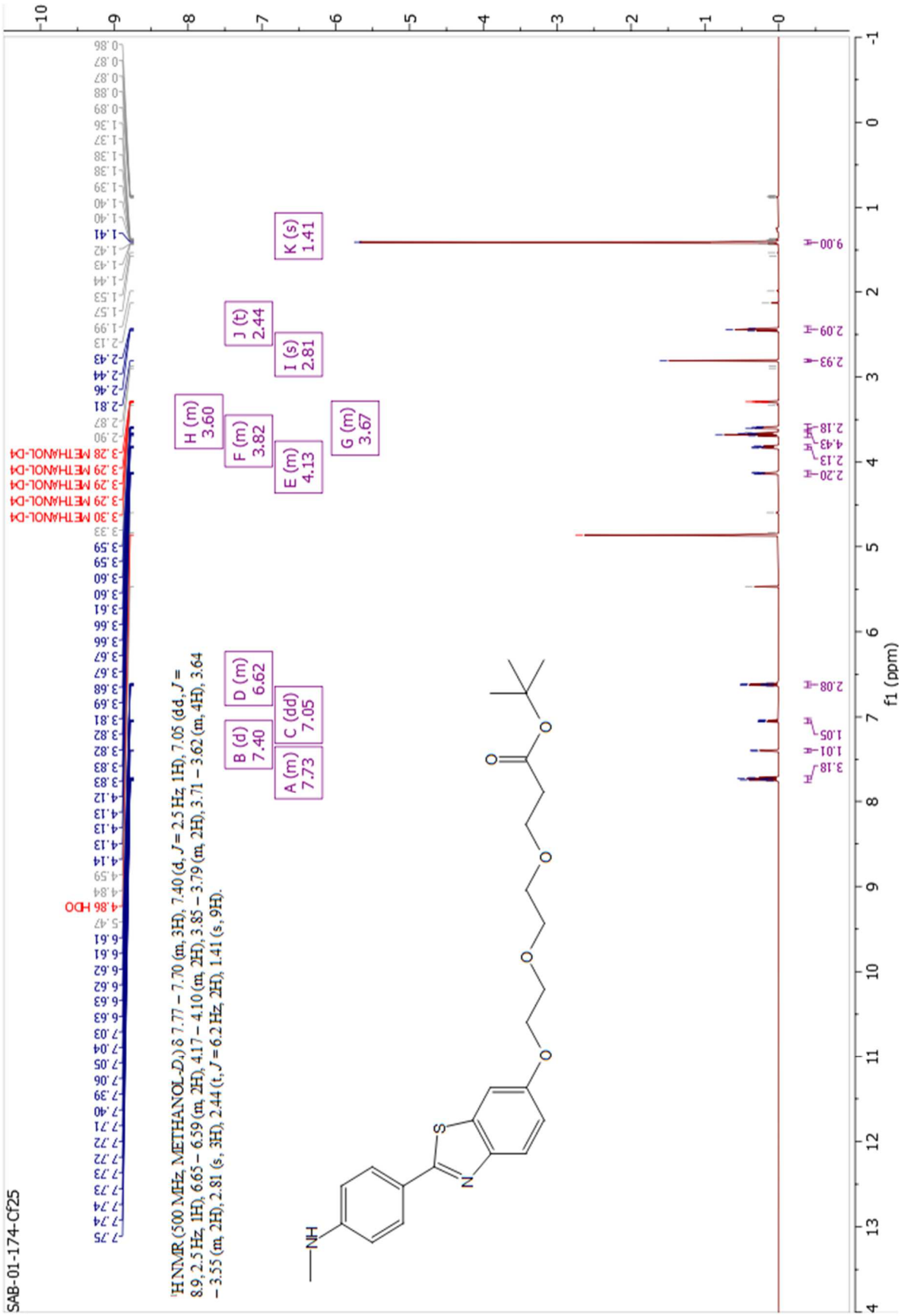

Spectrum 9 Compound 15 ^{1}H NMR

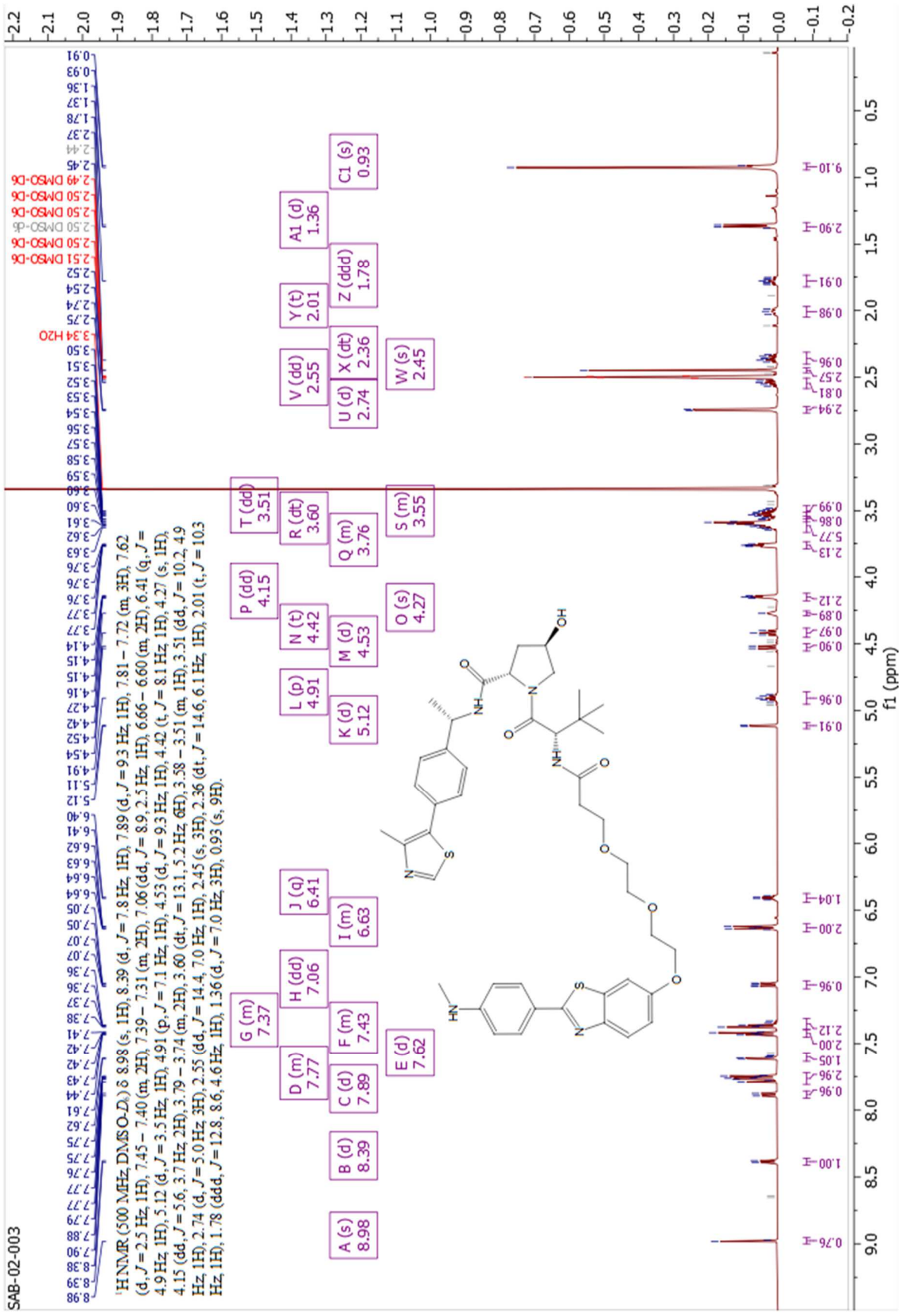

Spectrum 10 Compound 17 ^{1}H NMR

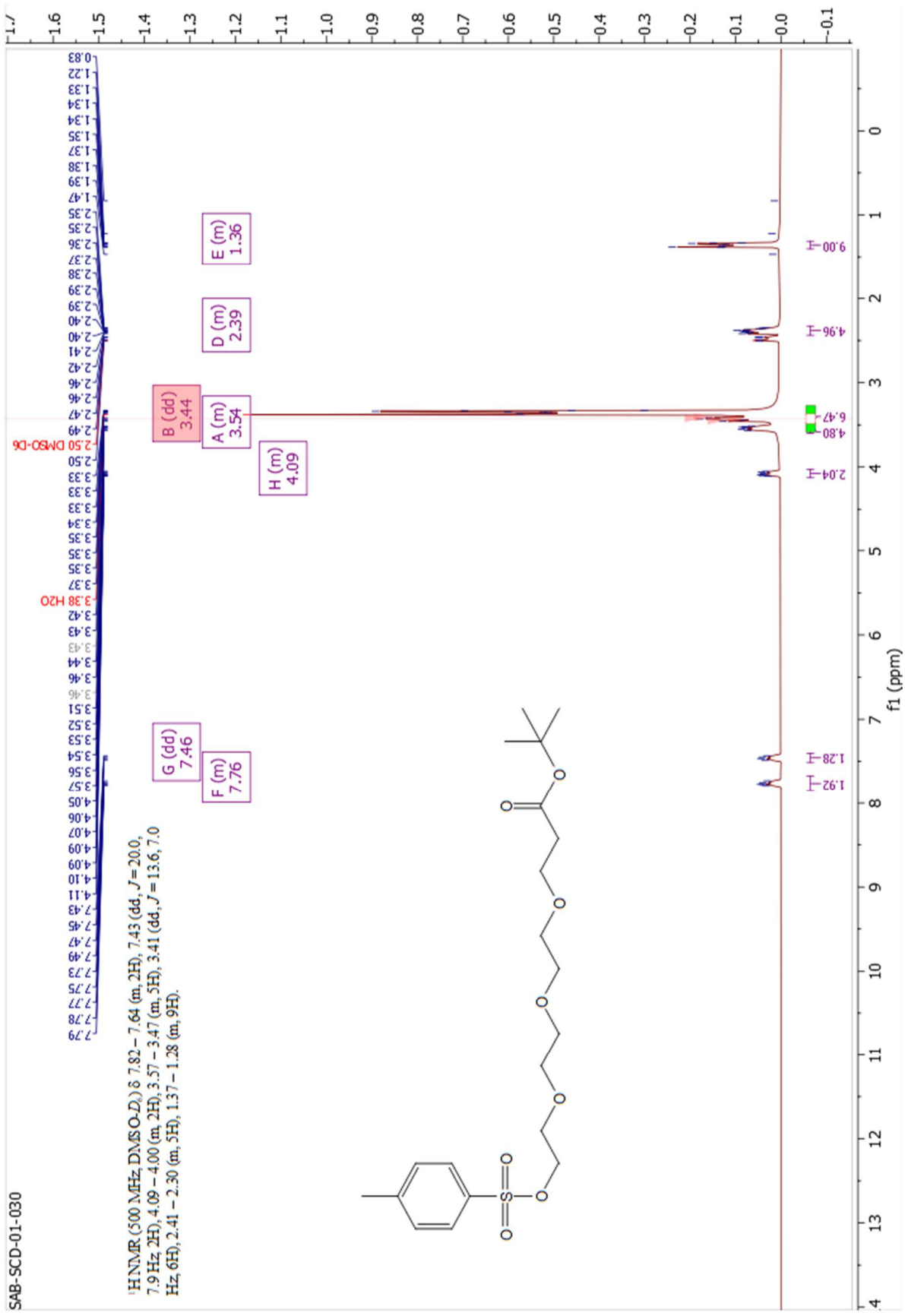

Spectrum 11 Compound 18 ^{1}H NMR

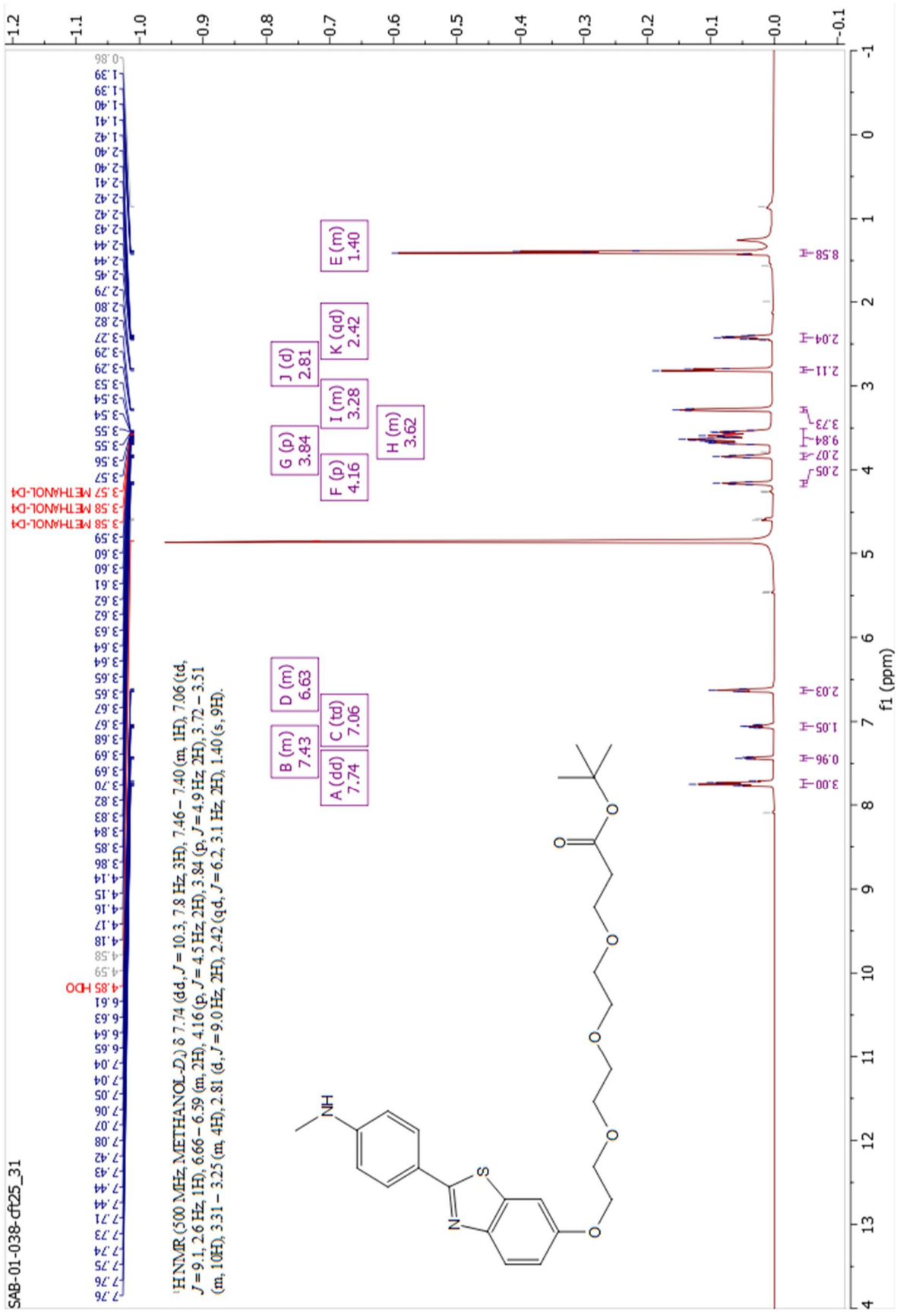

Spectrum 12 Compound 20 ^{1}H NMR

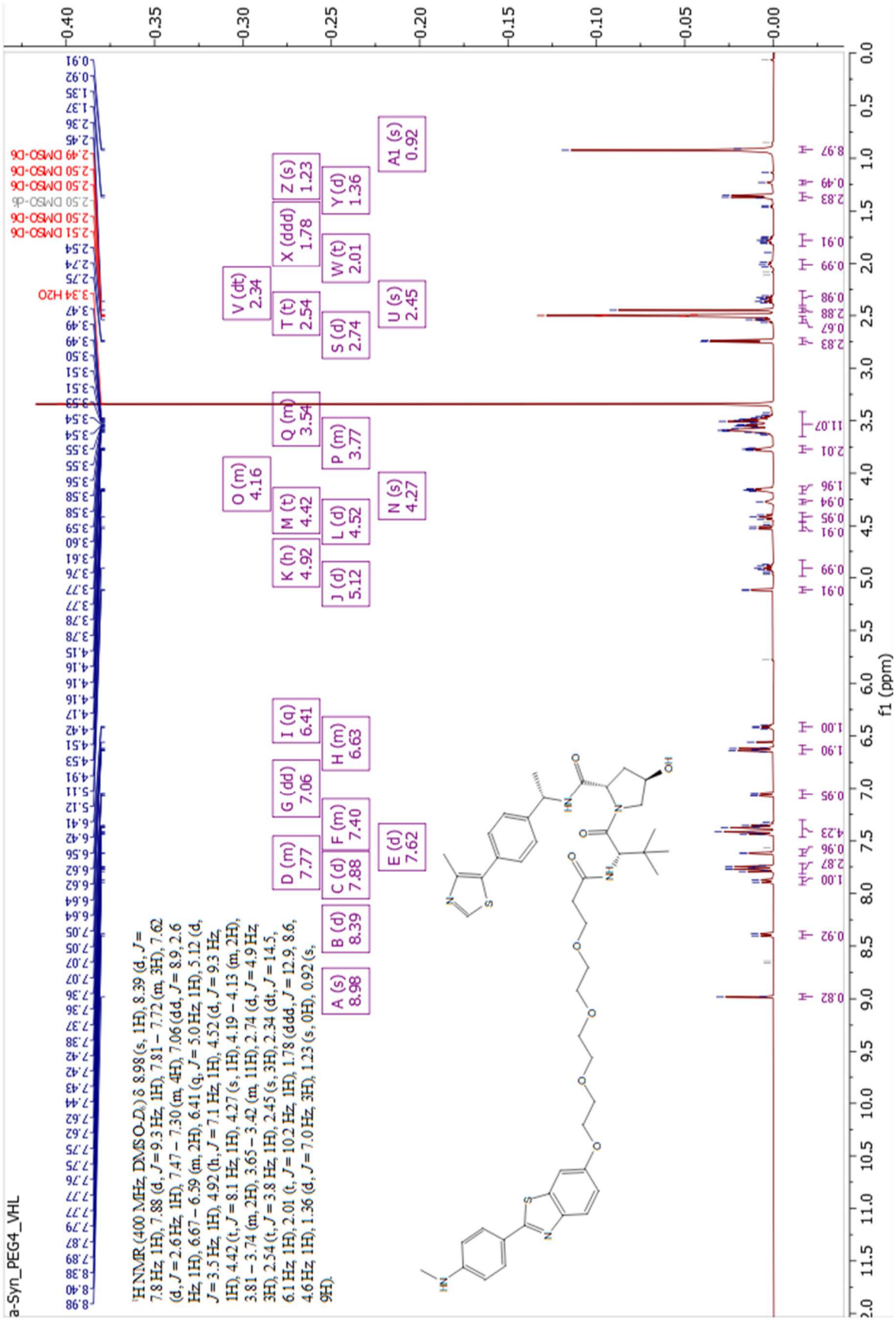

^{1}H NMR (400 MHz, DMSO-D_6) δ 8.98 (s, 1H), 8.39 (d, J = 7.8 Hz, 1H), 7.88 (d, J = 9.3 Hz, 1H), 7.81 – 7.72 (m, 3H), 7.62 (d, J = 2.6 Hz, 1H), 7.47 – 7.30 (m, 4H), 7.06 (dd, J = 8.9, 2.6 Hz, 1H), 6.67 – 6.59 (m, 2H), 6.41 (q, J = 5.0 Hz, 1H), 5.12 (d, J = 3.5 Hz, 1H), 4.92 (h, J = 7.1 Hz, 1H), 4.52 (d, J = 9.3 Hz, 1H), 4.42 (t, J = 8.1 Hz, 1H), 4.27 (s, 1H), 4.19 – 4.13 (m, 2H), 3.81 – 3.74 (m, 2H), 3.65 – 3.42 (m, 11H), 2.74 (d, J = 4.9 Hz, 3H), 2.54 (t, J = 3.8 Hz, 1H), 2.45 (s, 3H), 2.34 (dt, J = 14.5, 6.1 Hz, 1H), 2.01 (t, J = 10.2 Hz, 1H), 1.78 (ddd, J = 12.9, 8.6, 4.6 Hz, 1H), 1.36 (d, J = 7.0 Hz, 3H), 1.23 (s, 0H), 0.92 (s, 9H).

Spectrum 13 Compound 22 ^{1}H NMR

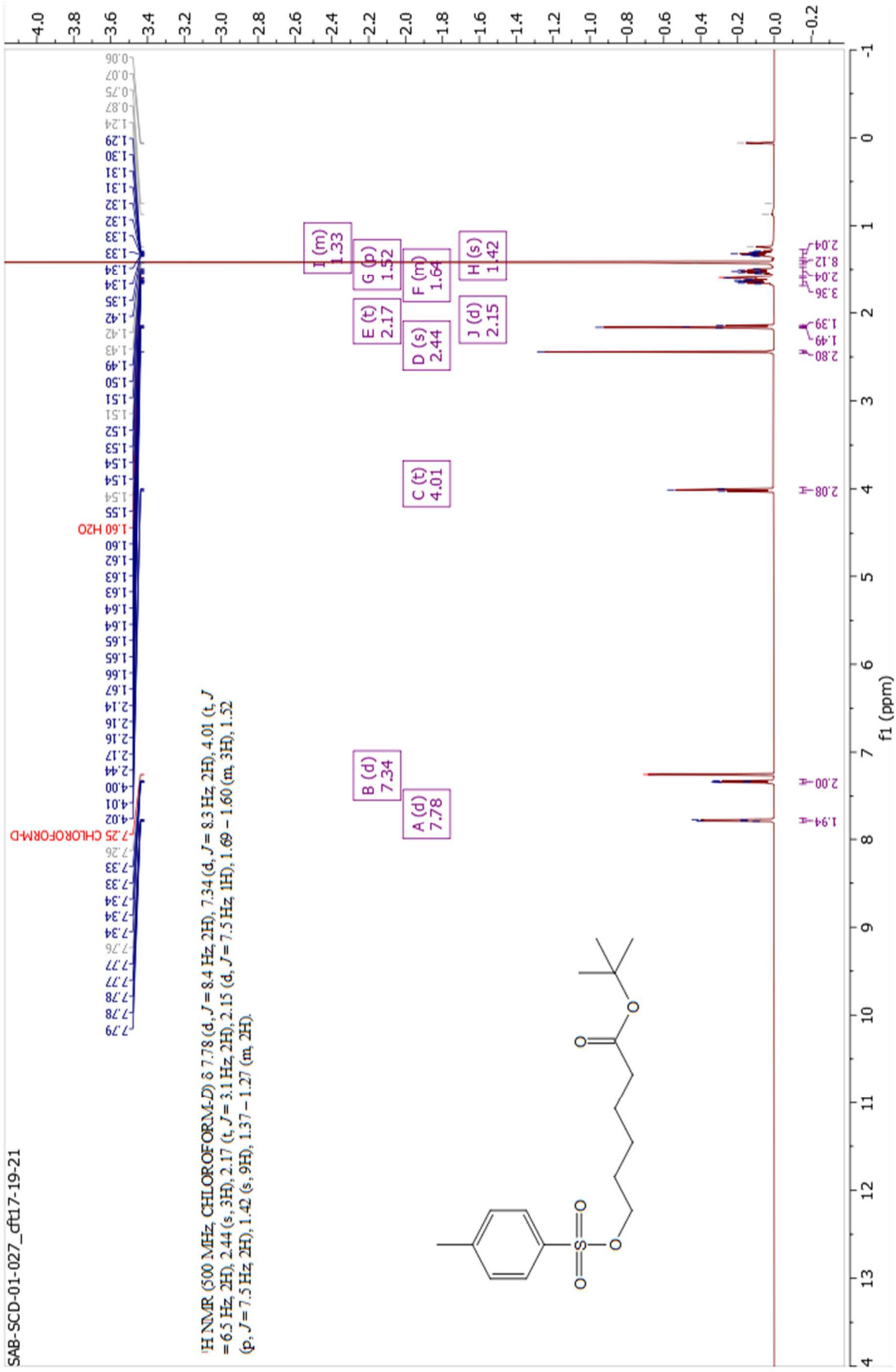

Spectrum 14 Compound 23 ^{1}H NMR

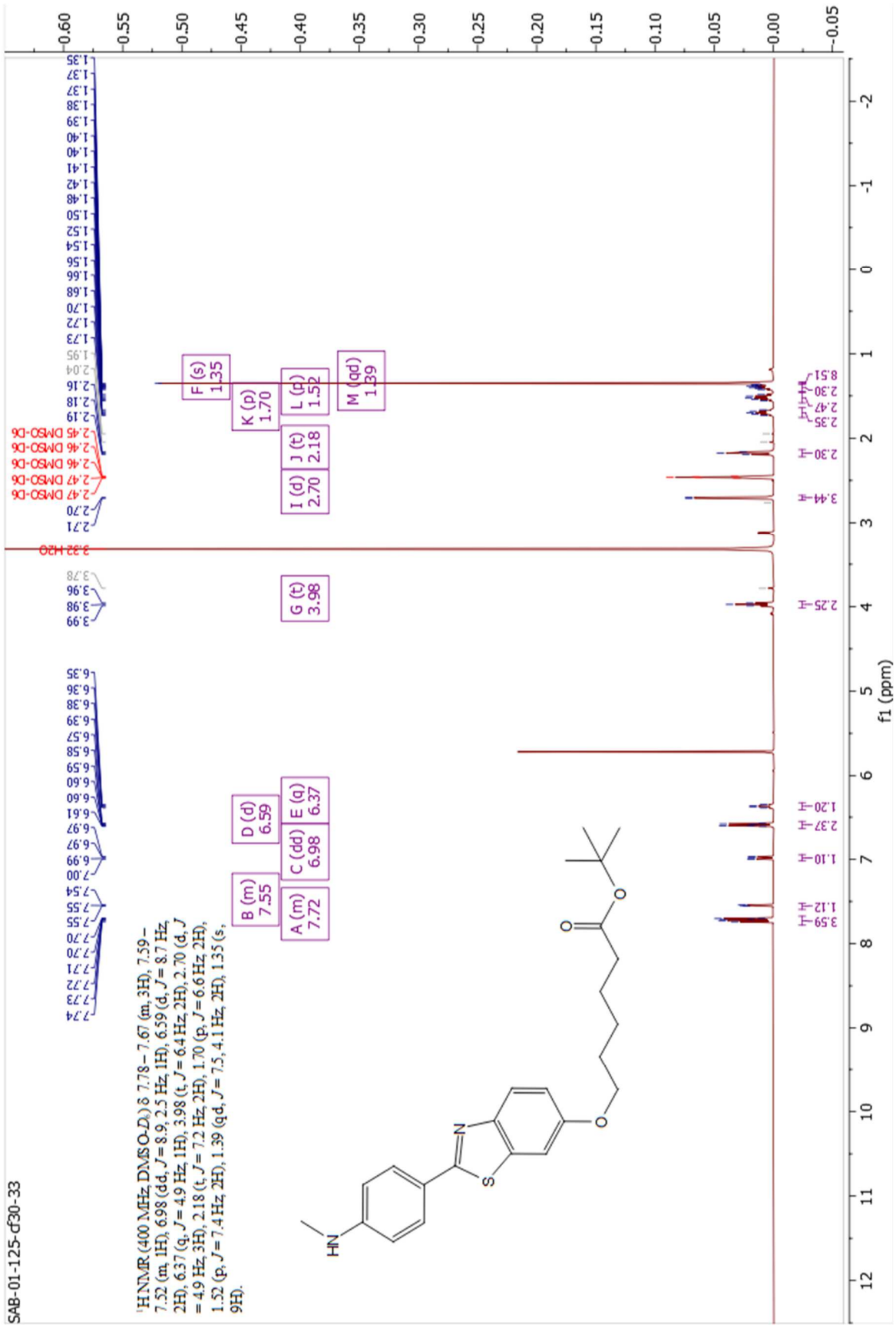

Spectrum 15 Compound 25 ^{1}H NMR

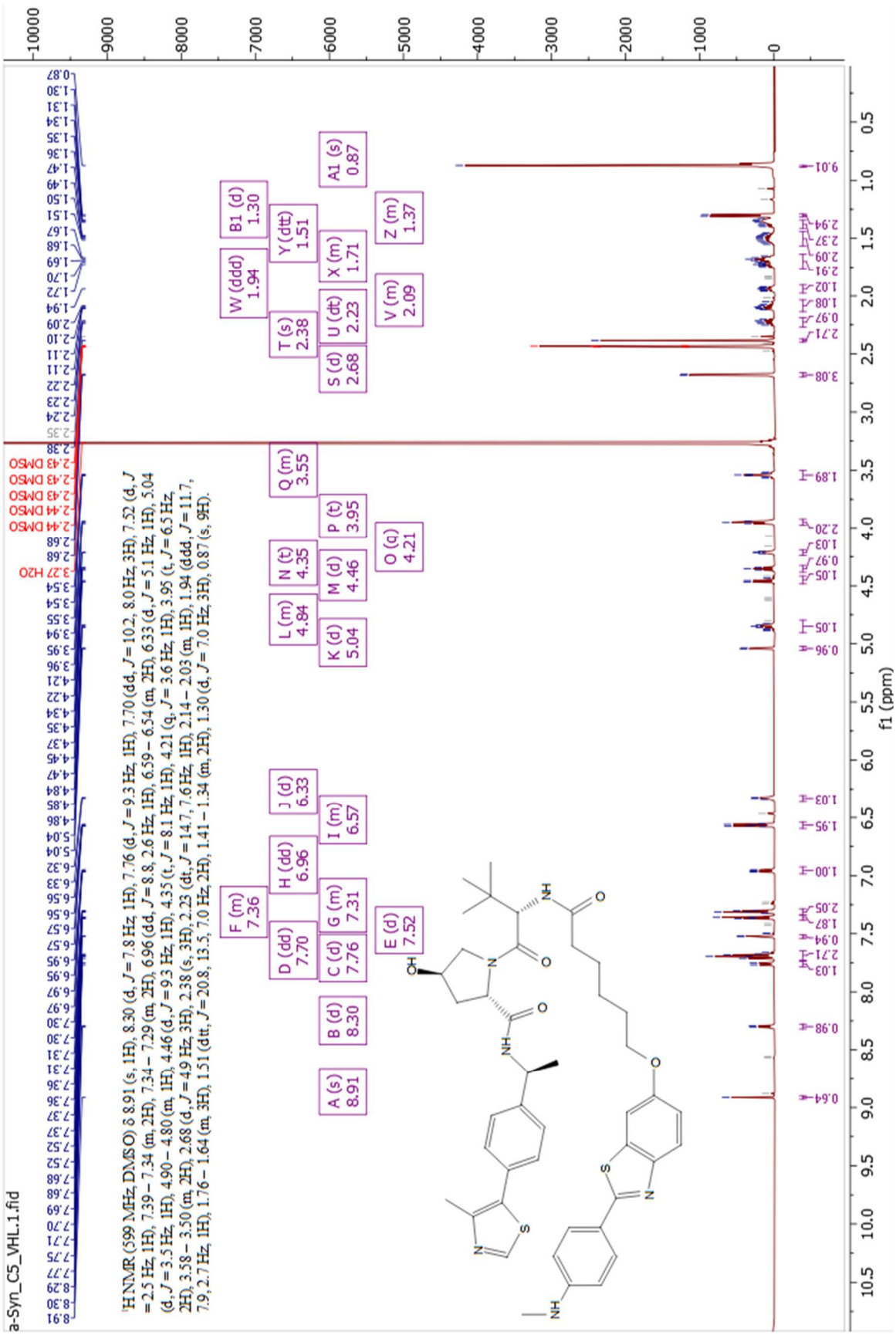

Spectrum 16 Compound 27 ^{1}H NMR

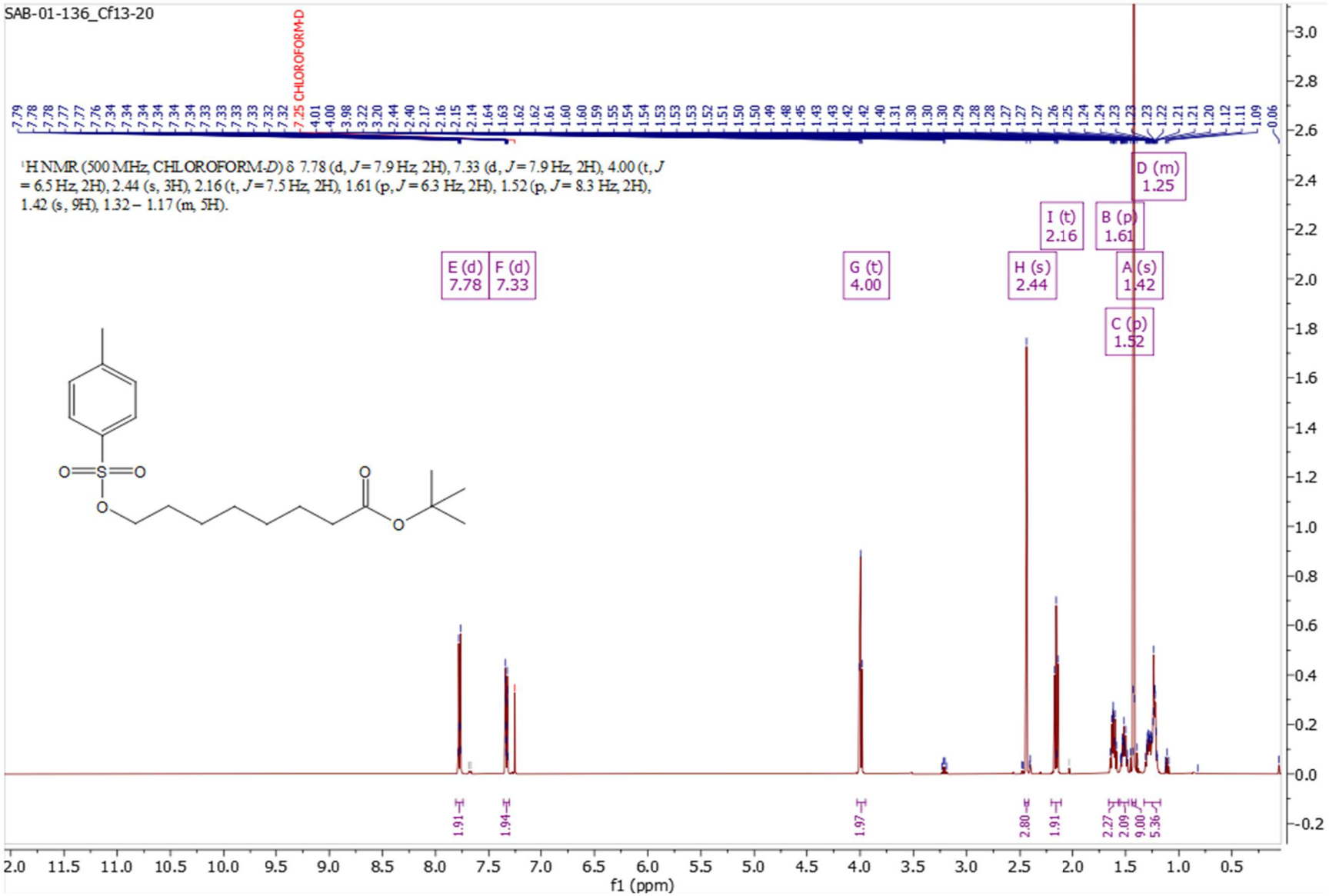

Spectrum 17 Compound 28 ^{1}H NMR

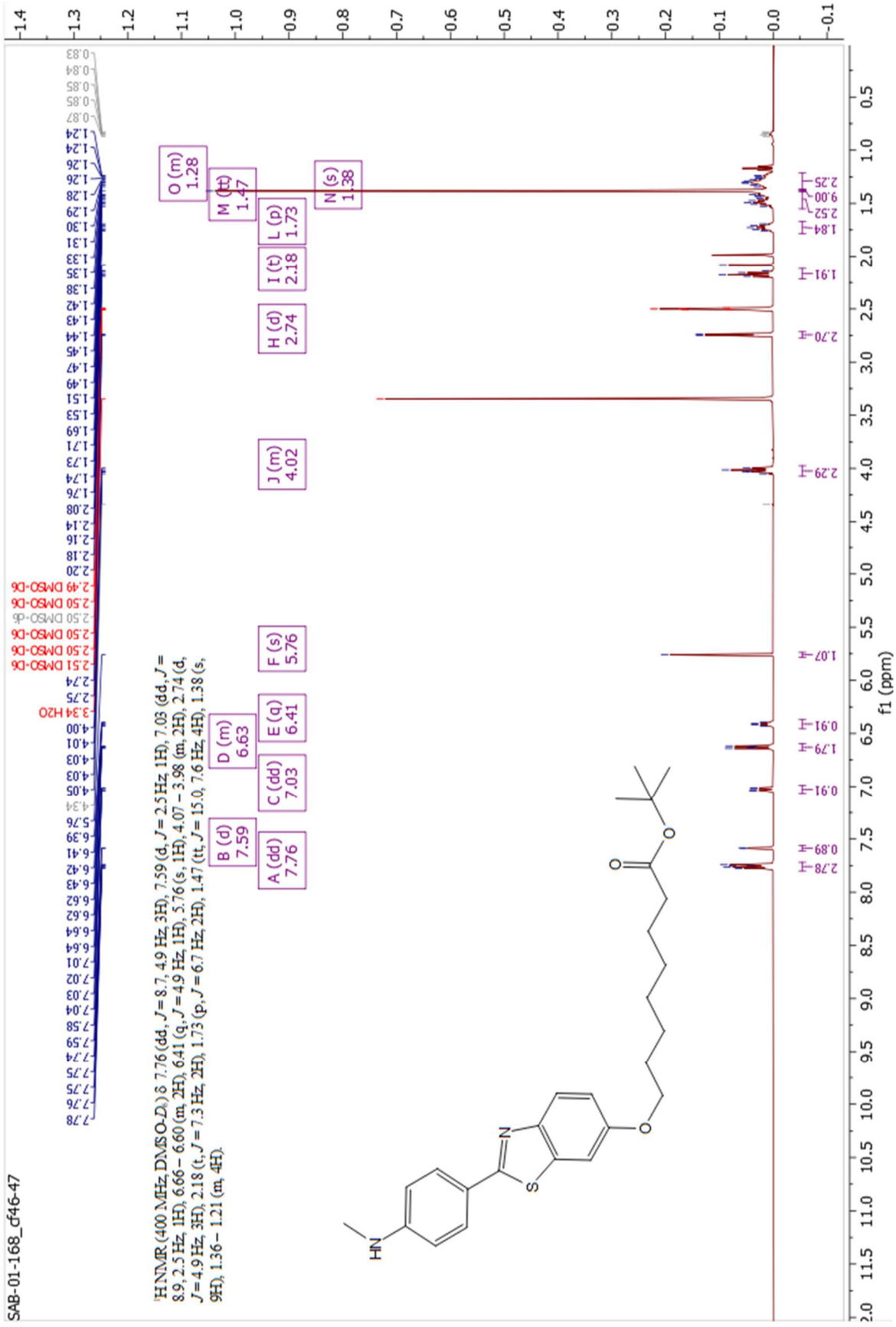

Spectrum 18 Compound 30 ^{1}H NMR

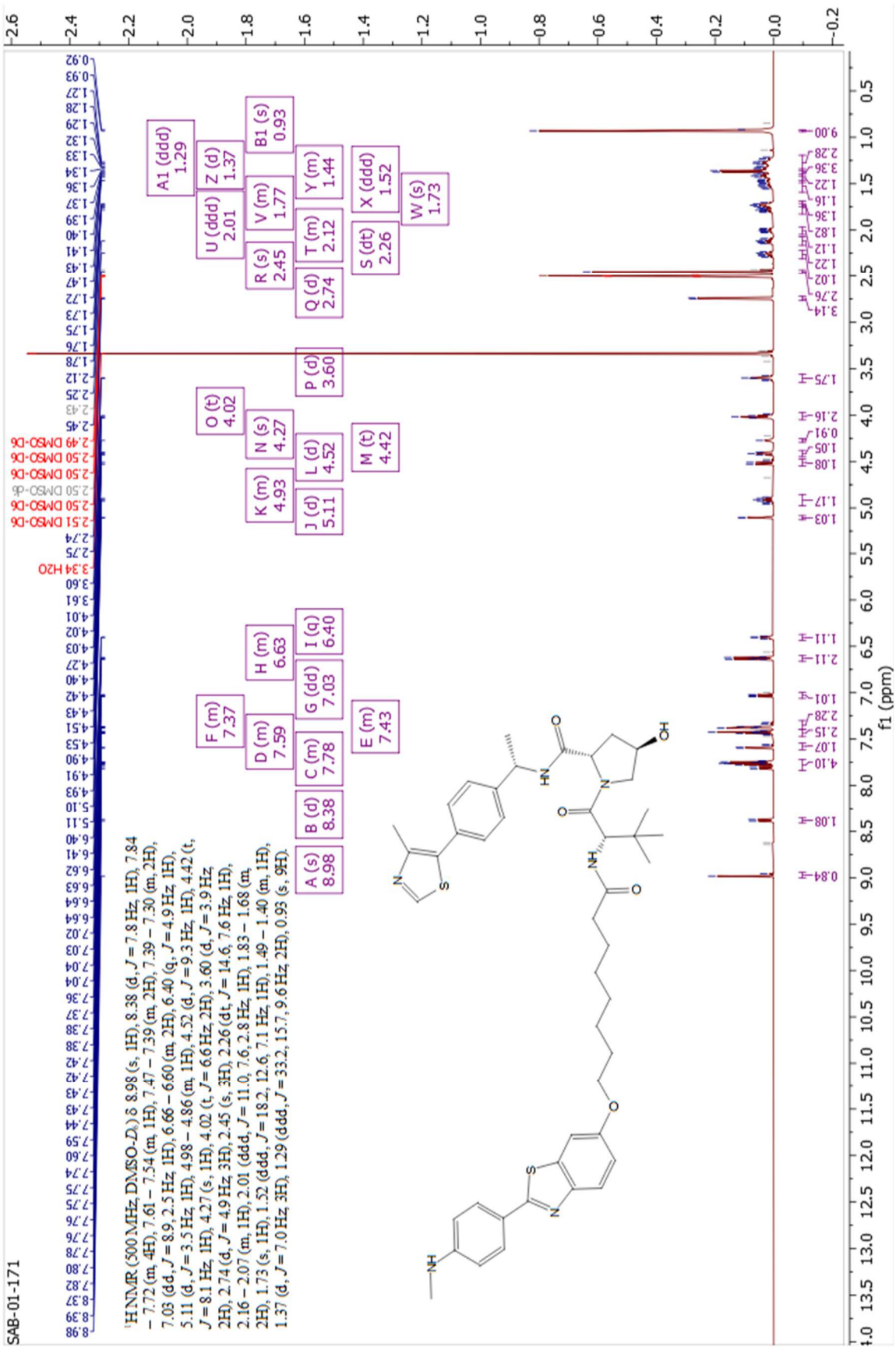

Spectrum 19 Compound 32 ^{1}H NMR

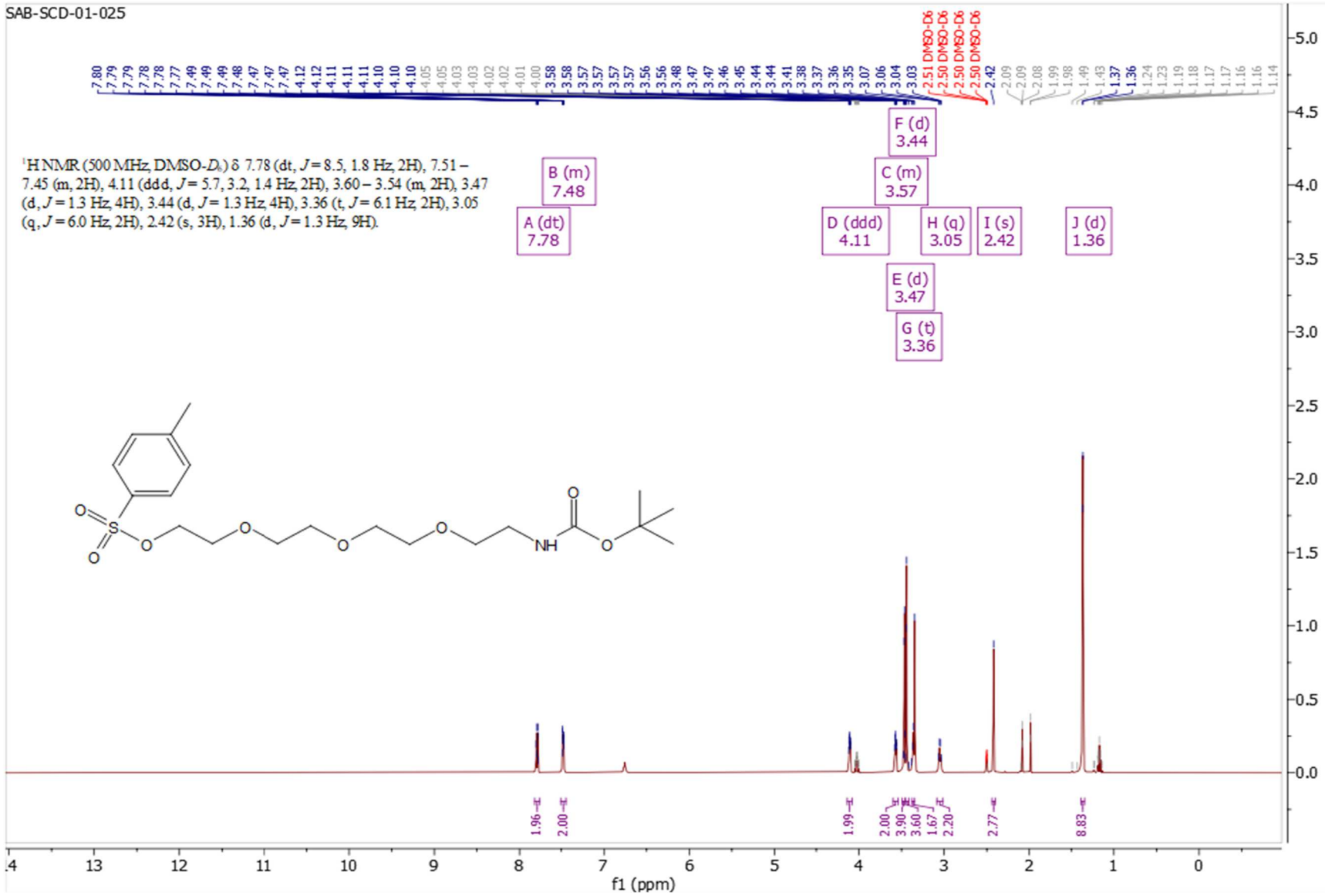

Spectrum 20 Compound 33 ^{1}H NMR

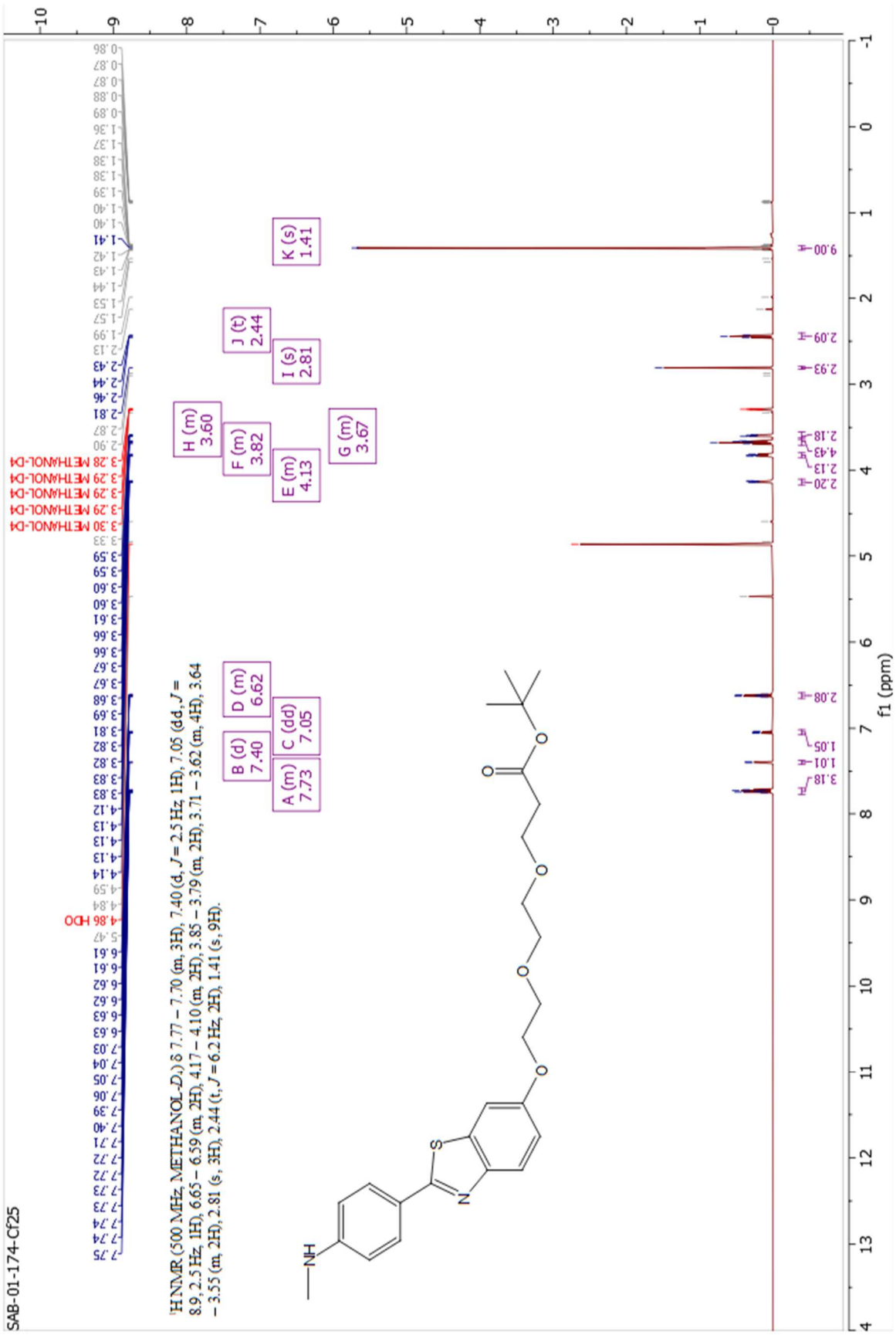

Spectrum 21 Compound 35 ^{1}H NMR

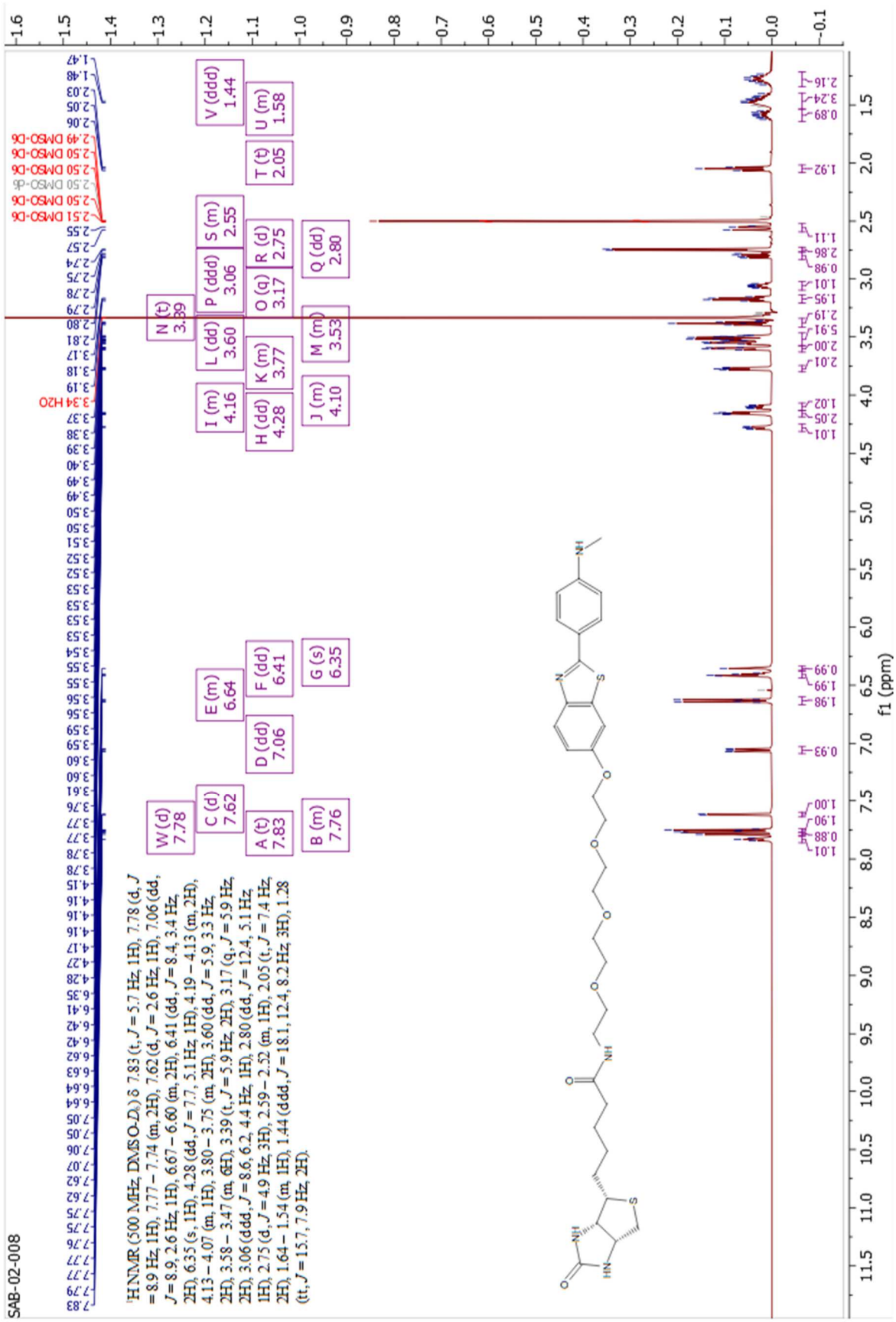

Spectrum 22 Compound 36 ^{1}H NMR

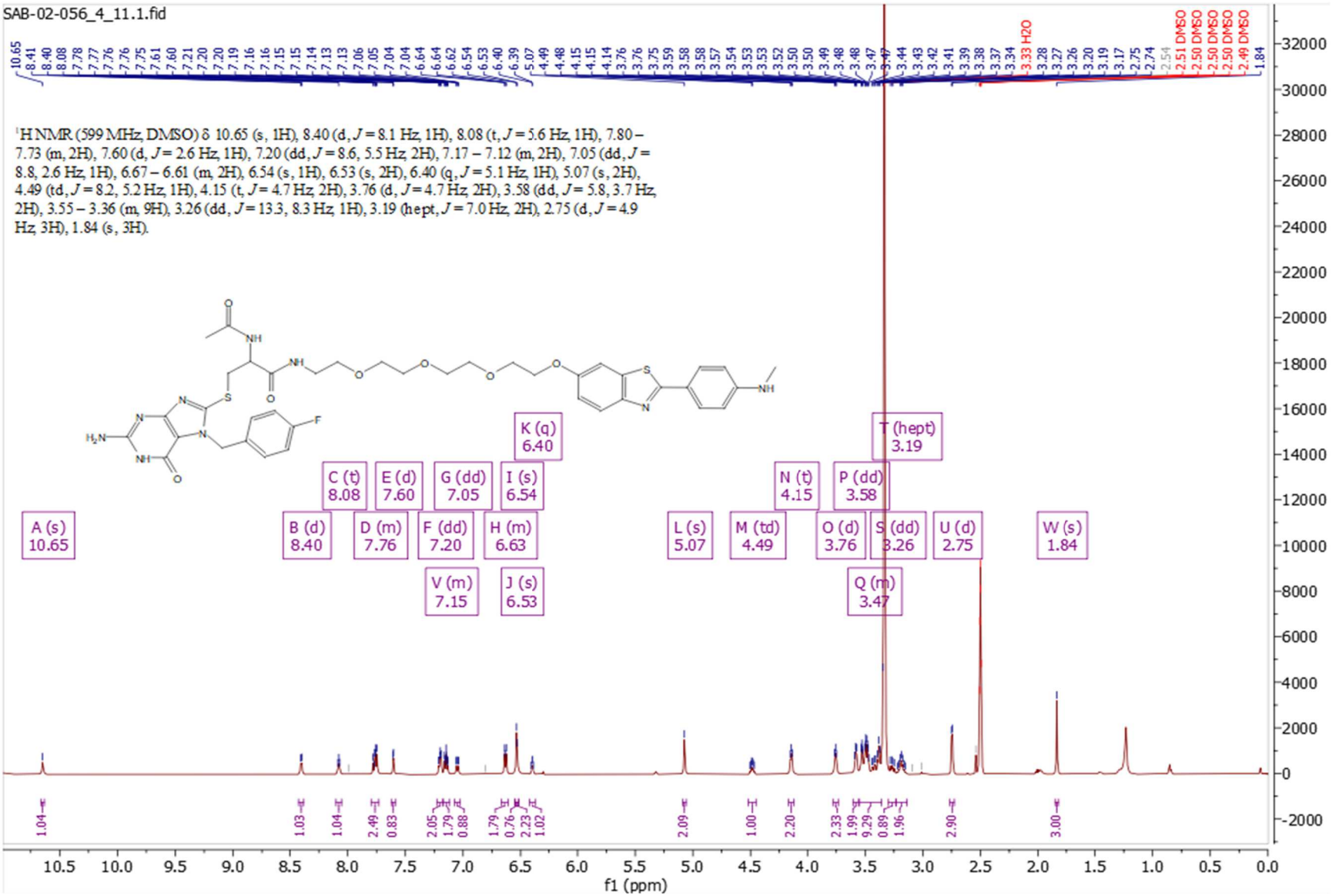

Spectrum 23 Compound 38 ^{1}H NMR

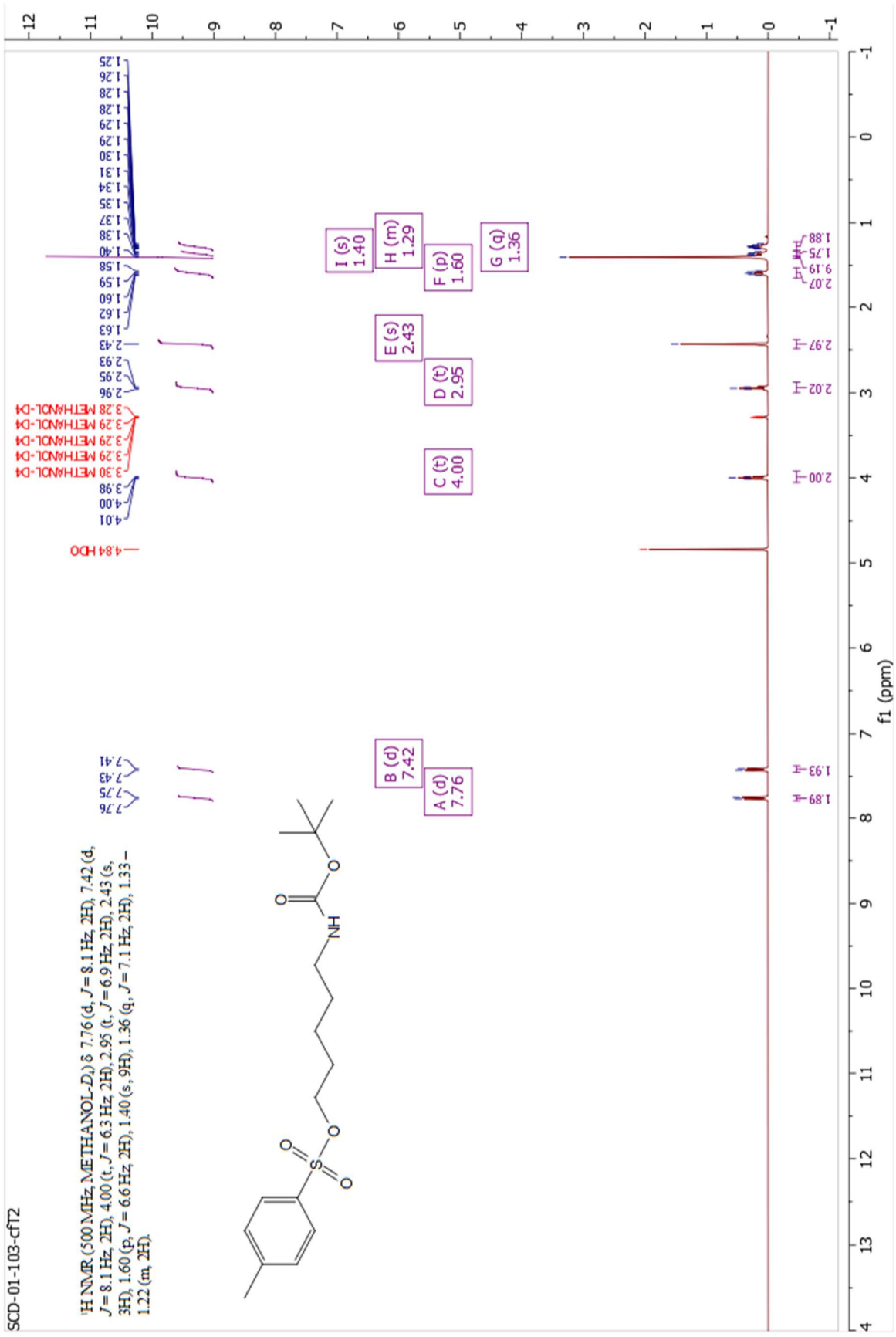

Spectrum 24 Compound 39 ^{1}H NMR

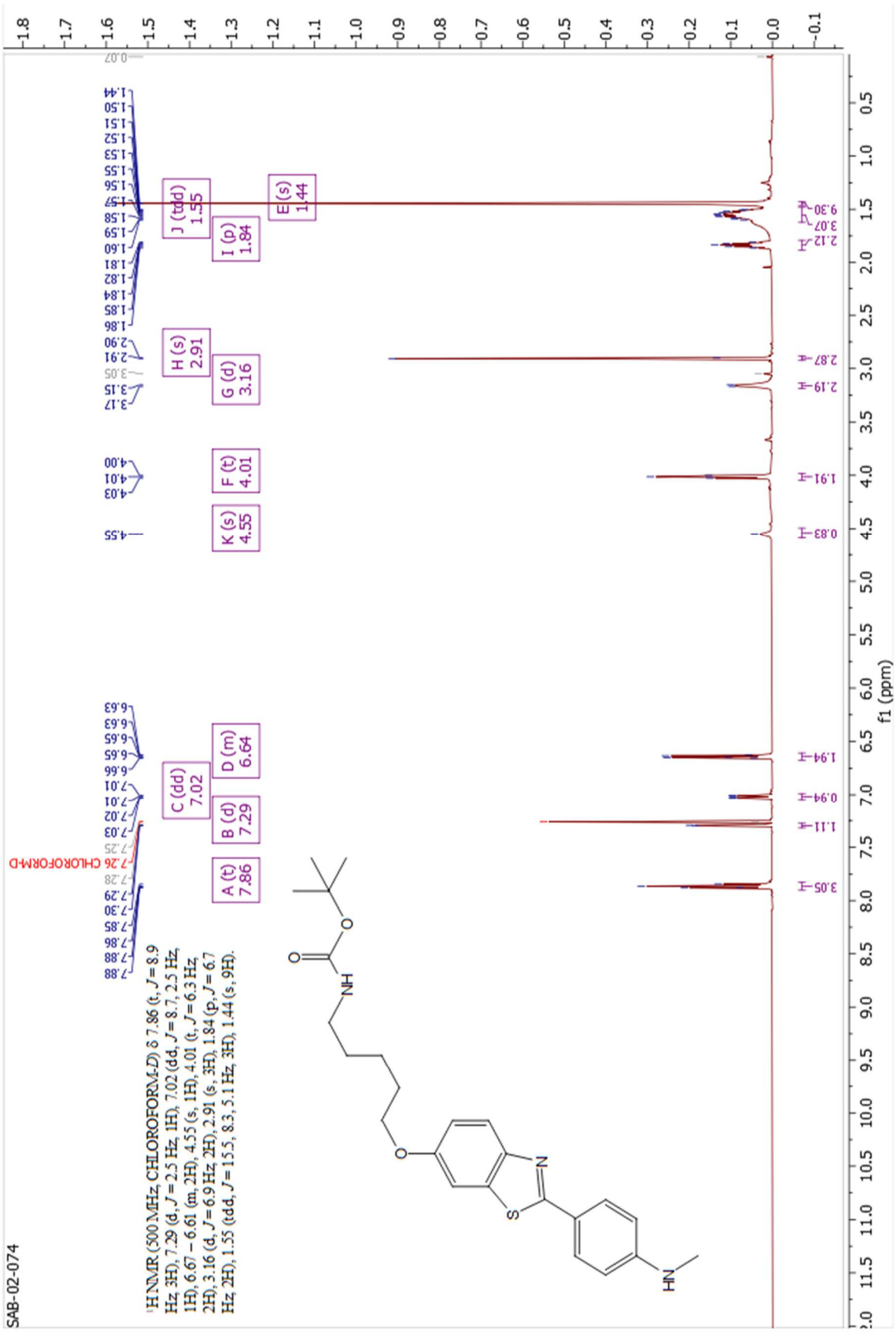

Spectrum 25 Compound 41 ^{1}H NMR

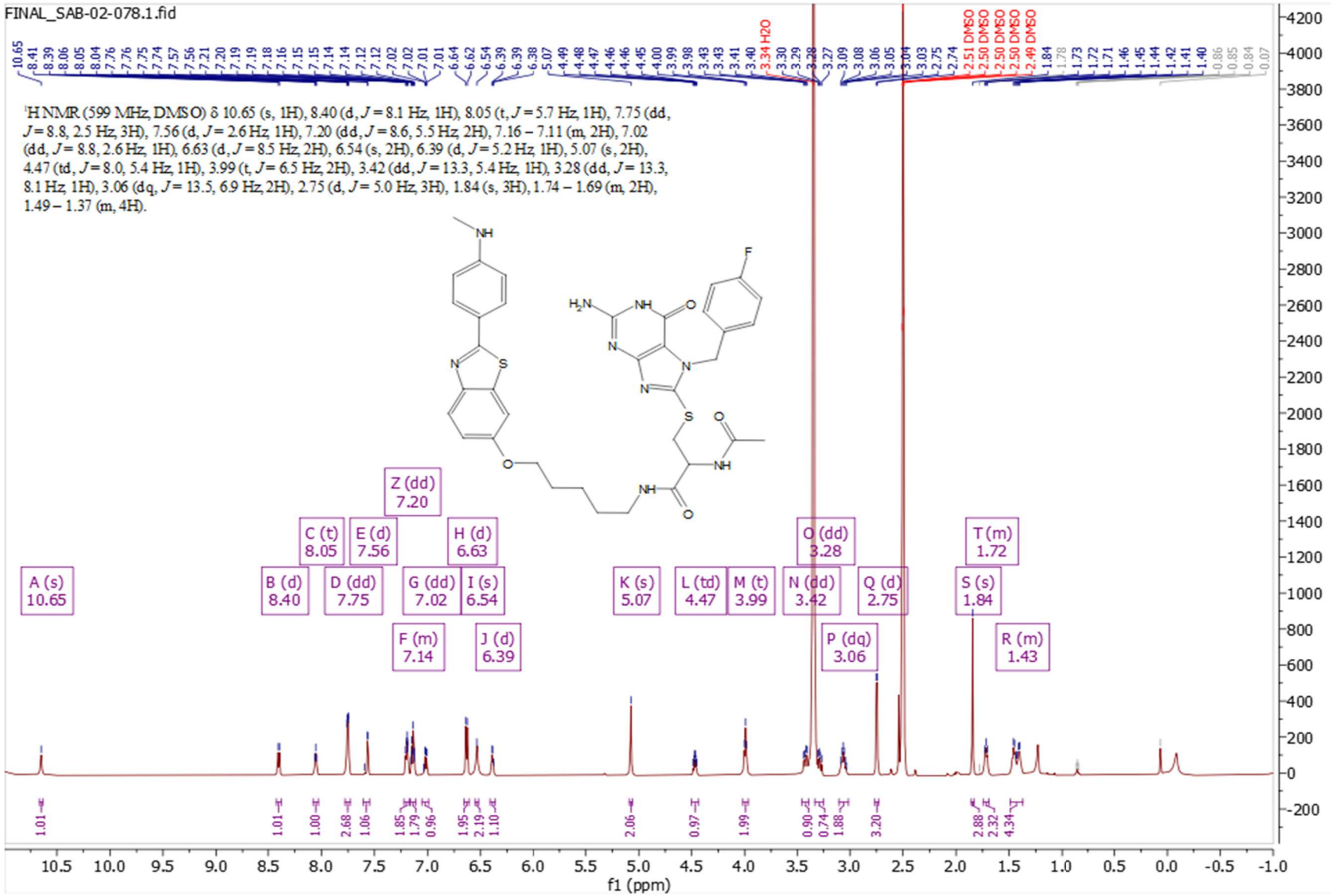

Spectrum 26 Compound 43 ^{1}H NMR

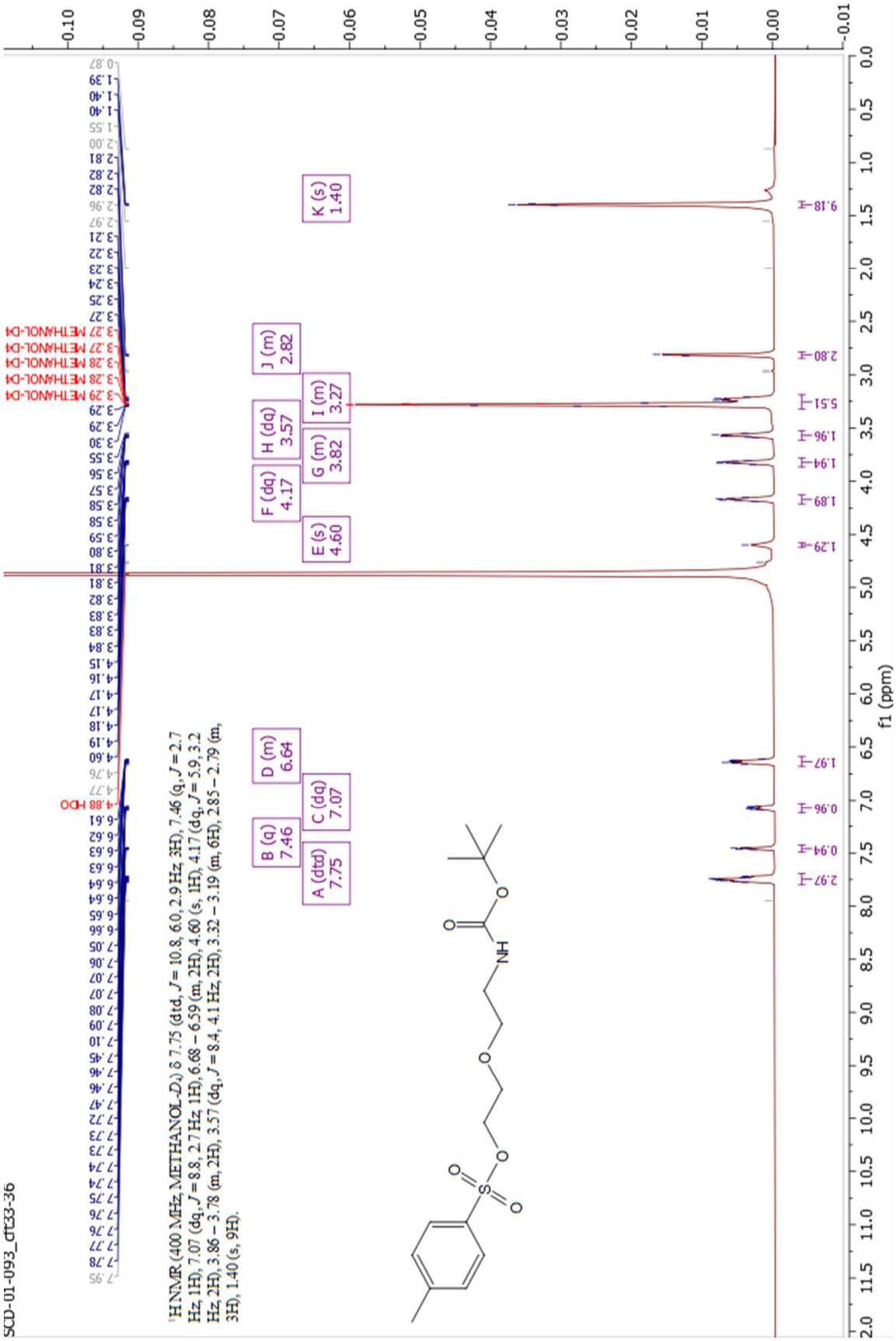

Spectrum 27 Compound 44 ^{1}H NMR

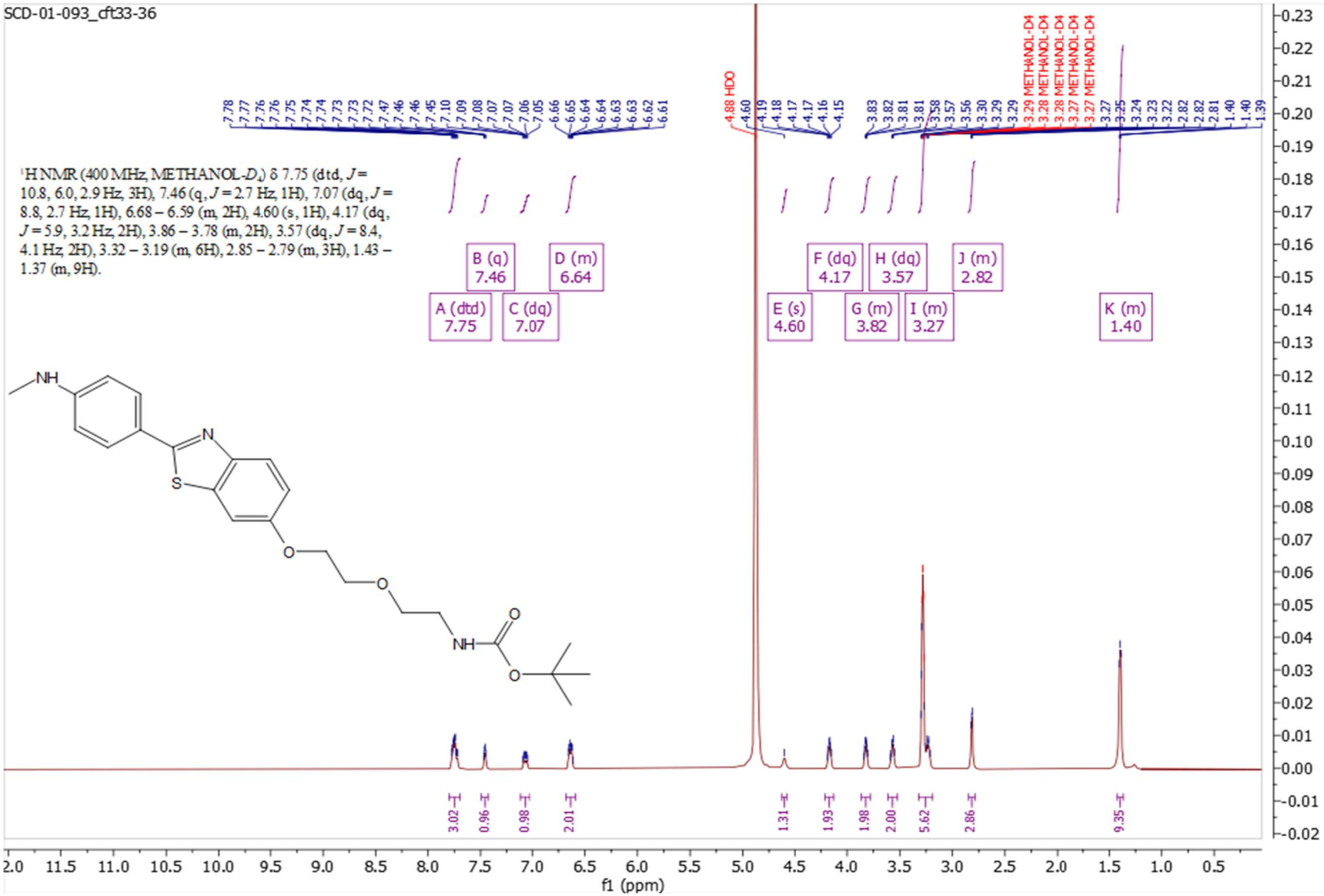

Spectrum 28 Compound 46 ^{1}H NMR

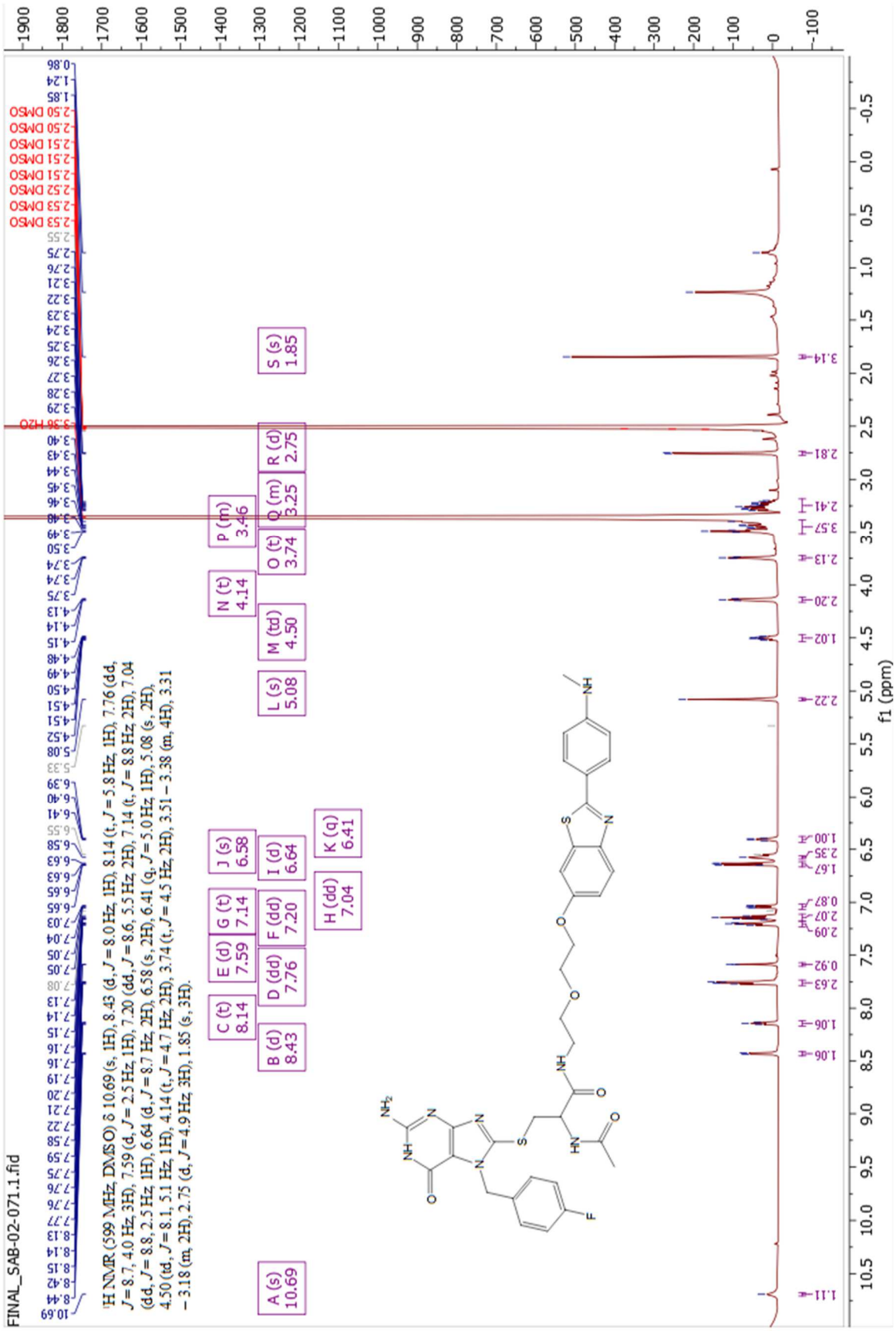

Spectrum 29 Compound 48 ^{1}H NMR

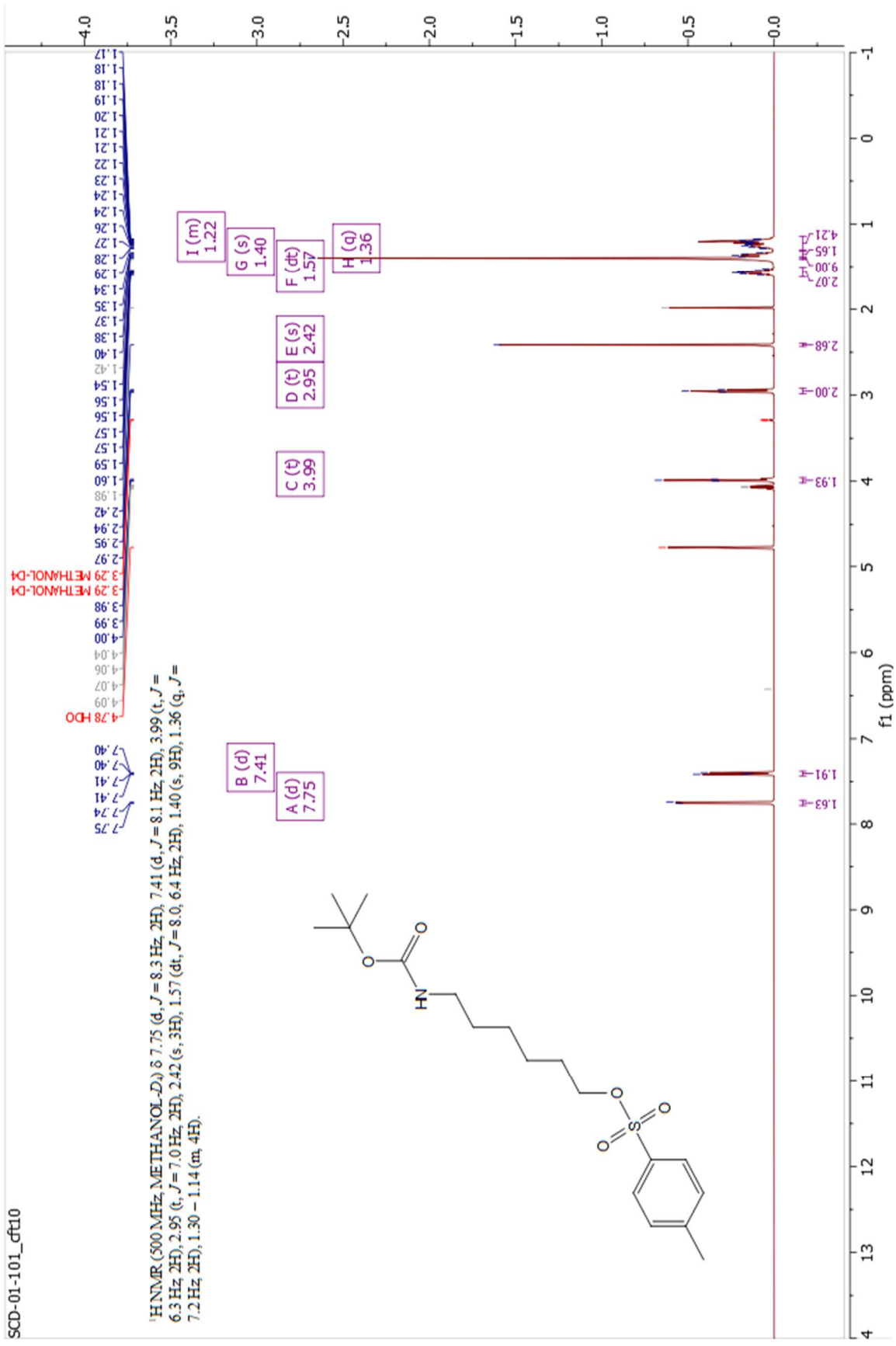

Spectrum 30 Compound 49 ^{1}H NMR

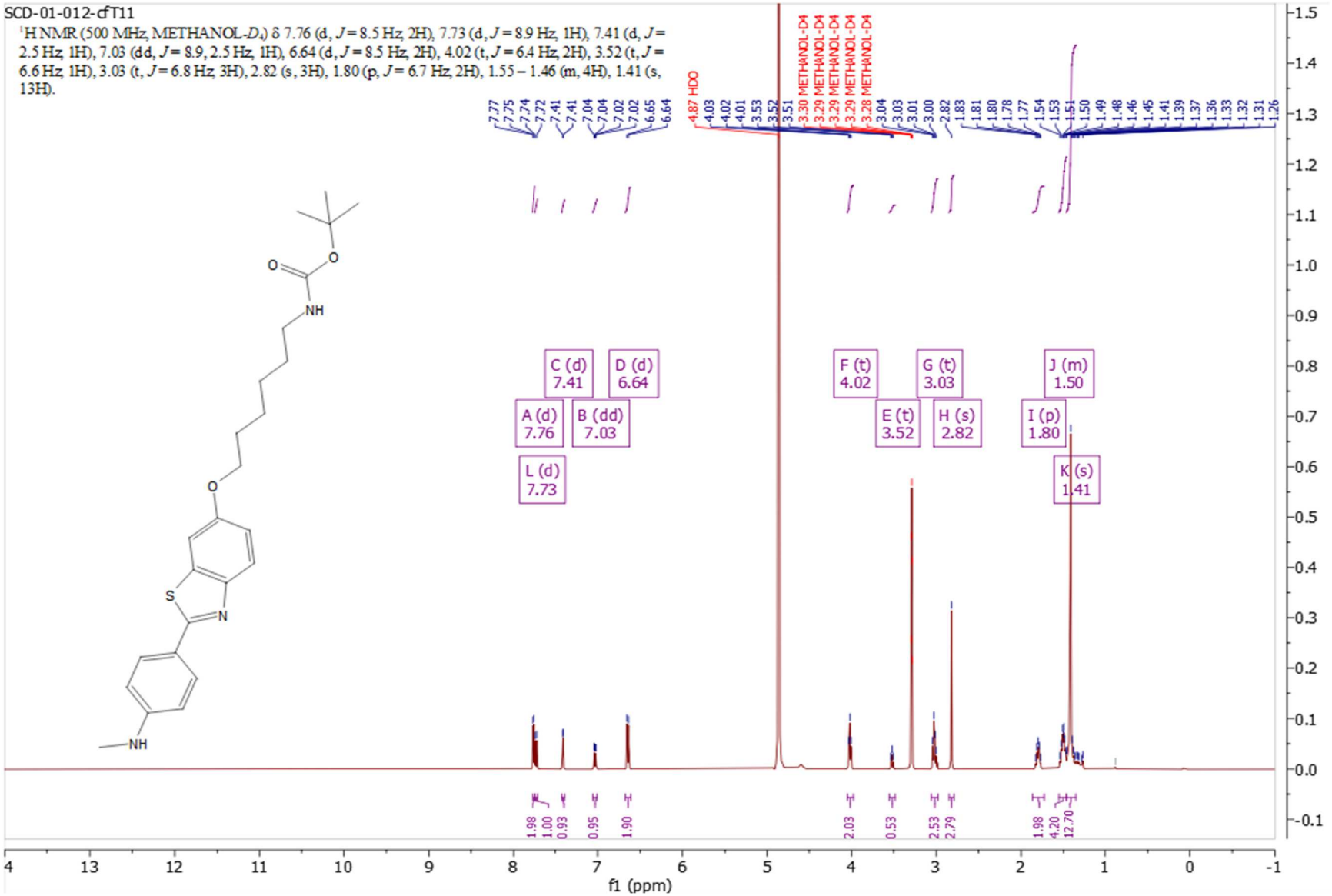

Spectrum 31 Compound 51 ^{1}H NMR

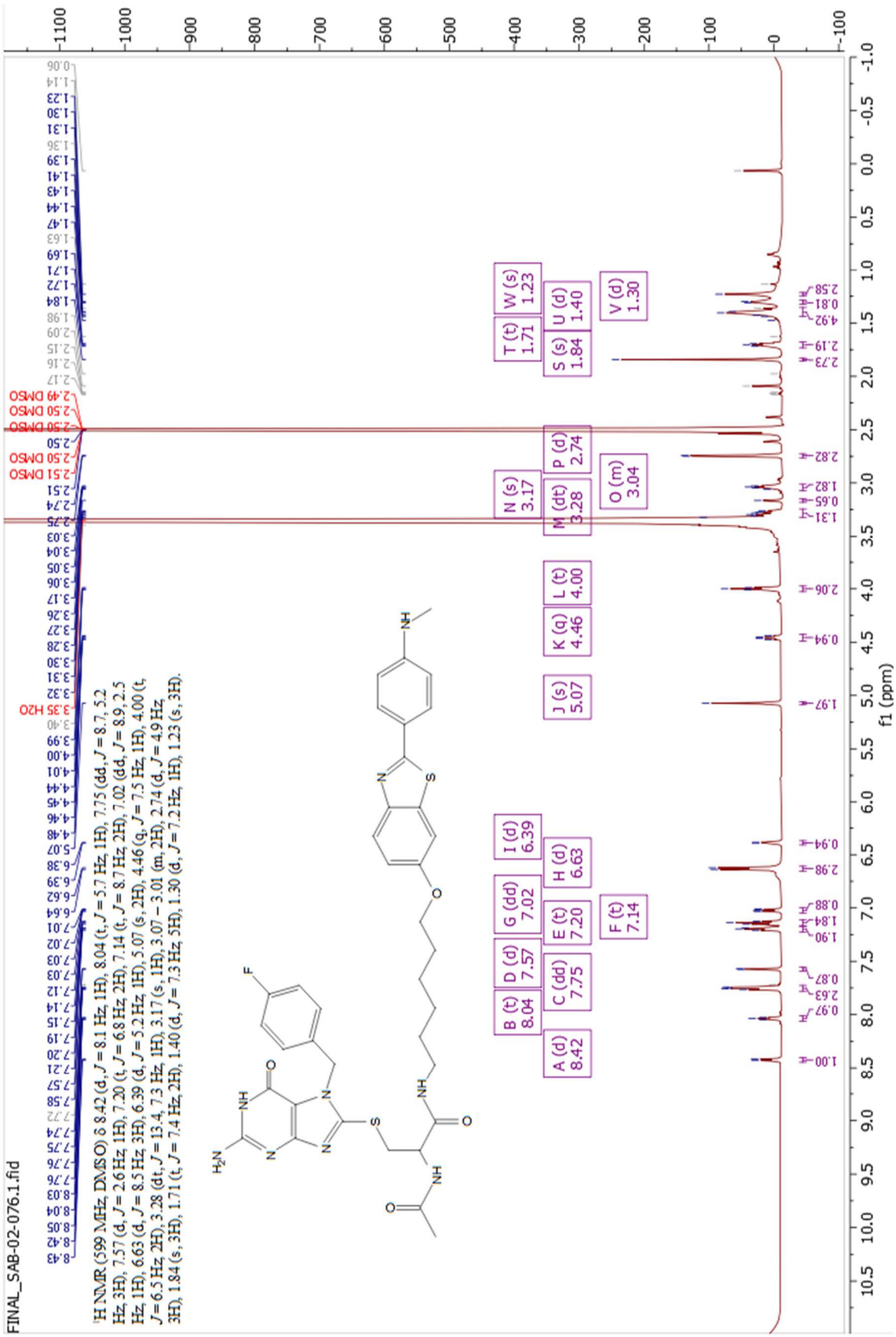

Spectrum 32 Compound 66 ^{1}H NMR

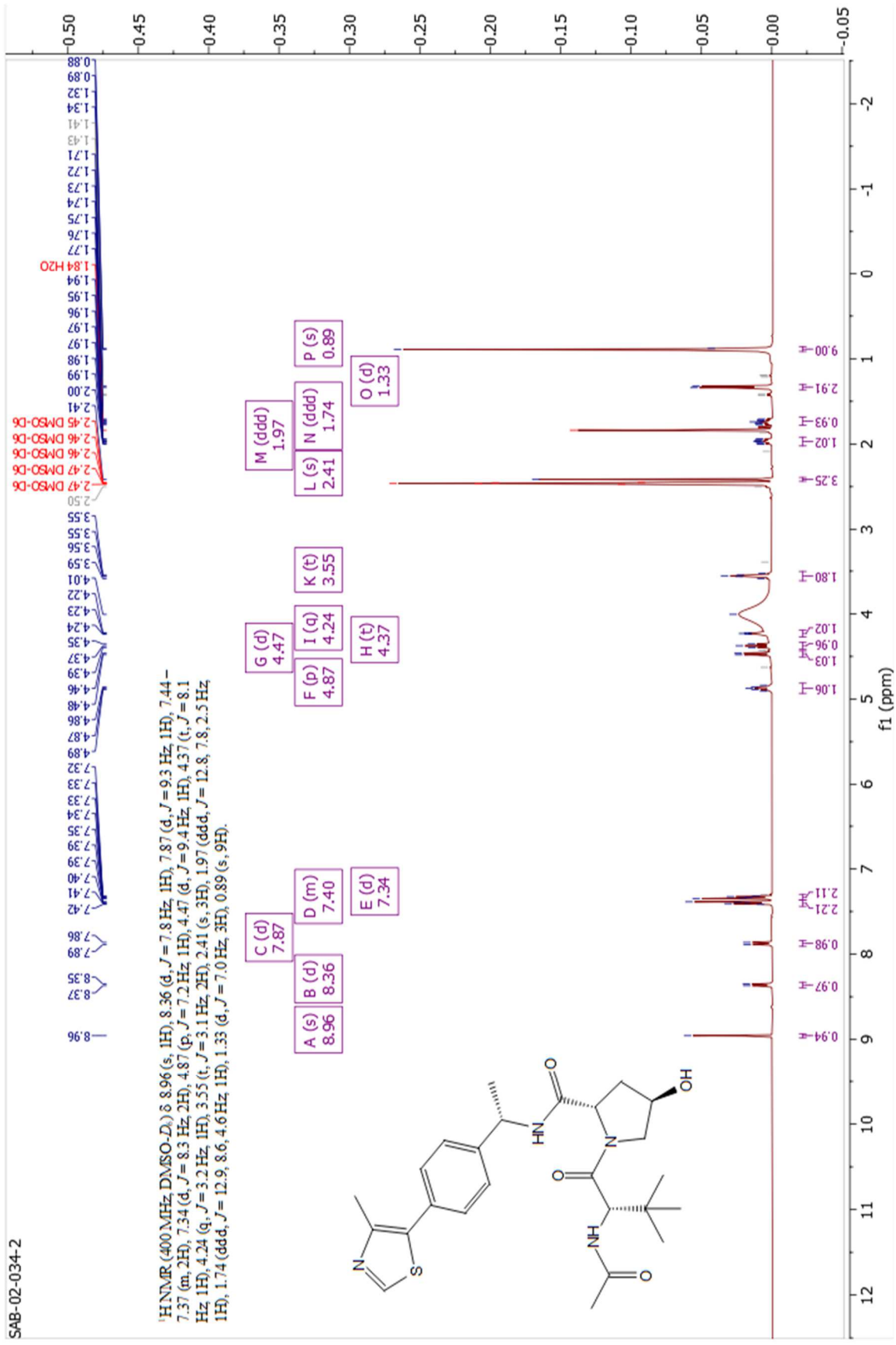

^{1}H NMR (400 MHz, DMSO-D_6) δ 8.96 (s, 1H), 8.36 (d, J = 7.8 Hz, 1H), 7.87 (d, J = 9.3 Hz, 1H), 7.44 – 7.37 (m, 2H), 7.34 (d, J = 8.3 Hz, 2H), 4.87 (p, J = 7.2 Hz, 1H), 4.47 (d, J = 9.4 Hz, 1H), 4.37 (t, J = 8.1 Hz, 1H), 4.24 (q, J = 3.2 Hz, 1H), 3.55 (t, J = 3.1 Hz, 2H), 2.41 (s, 3H), 1.97 (ddd, J = 12.8, 7.8, 2.5 Hz, 1H), 1.74 (ddd, J = 12.9, 8.6, 4.6 Hz, 1H), 1.33 (d, J = 7.0 Hz, 3H), 0.89 (s, 9H).

Chapter 3

Spectrum 33 Compound 53 ^{1}H NMR

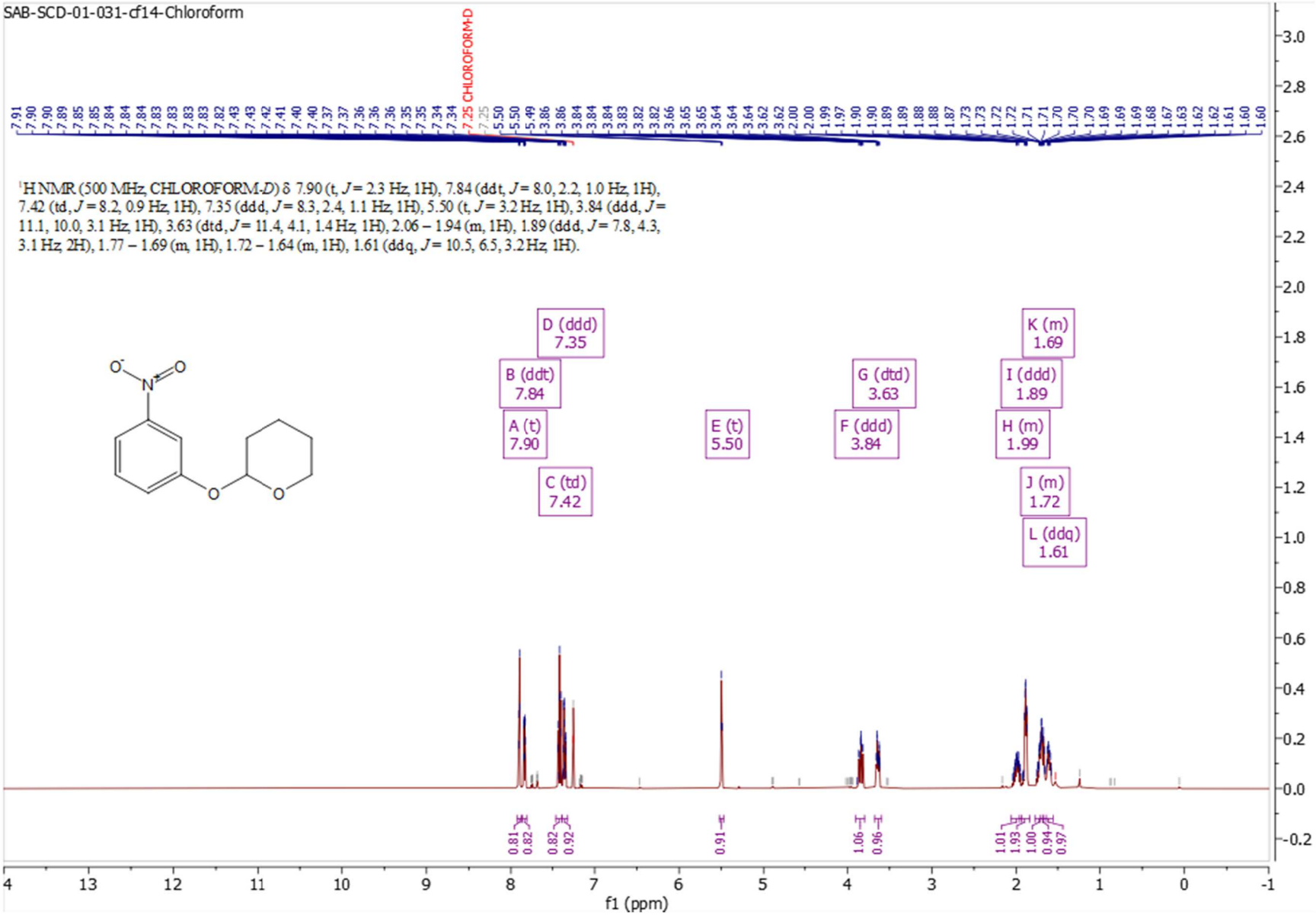

Spectrum 34 Compound 55 ^{1}H NMR

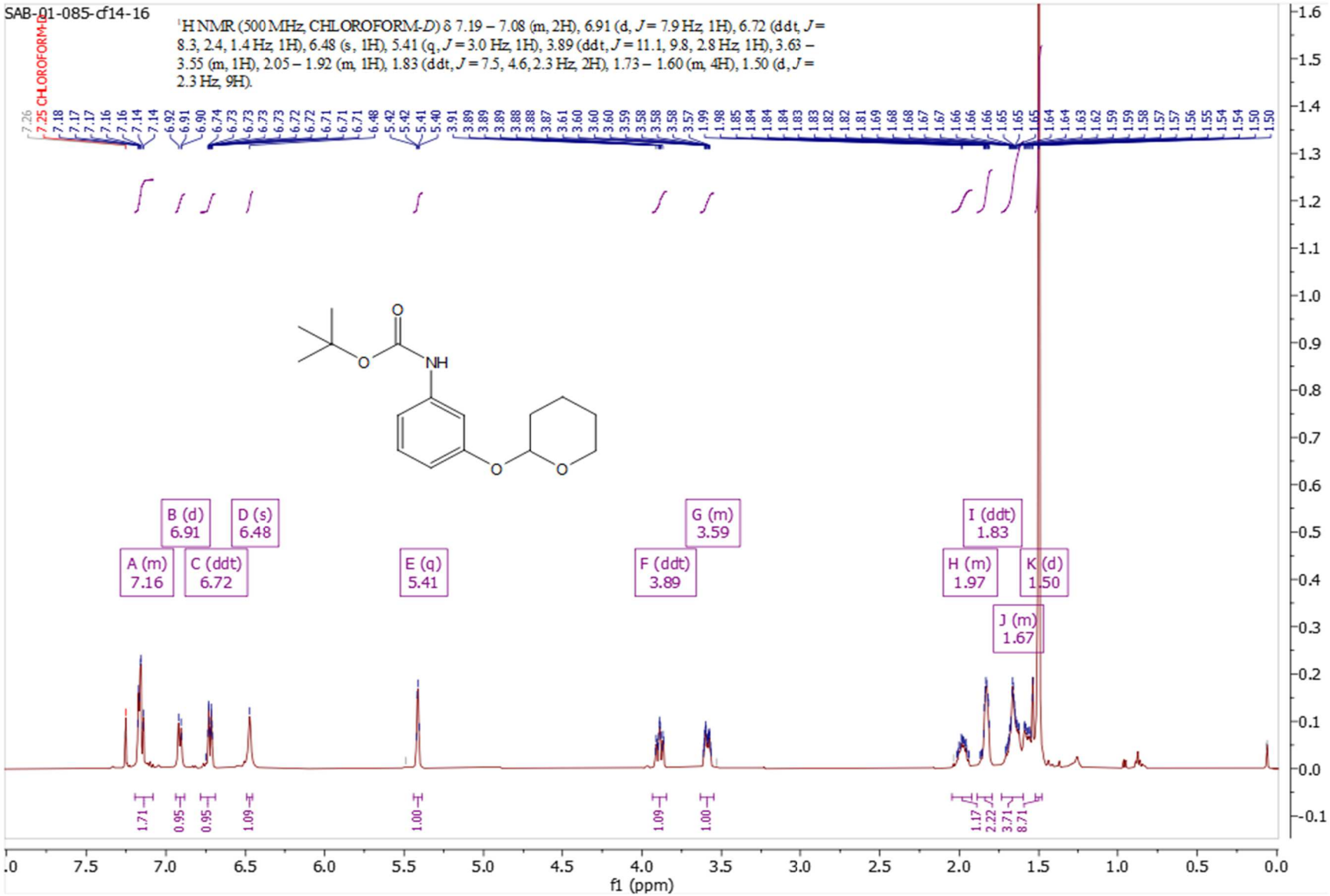

Spectrum 35 Compound 56 ^{1}H NMR

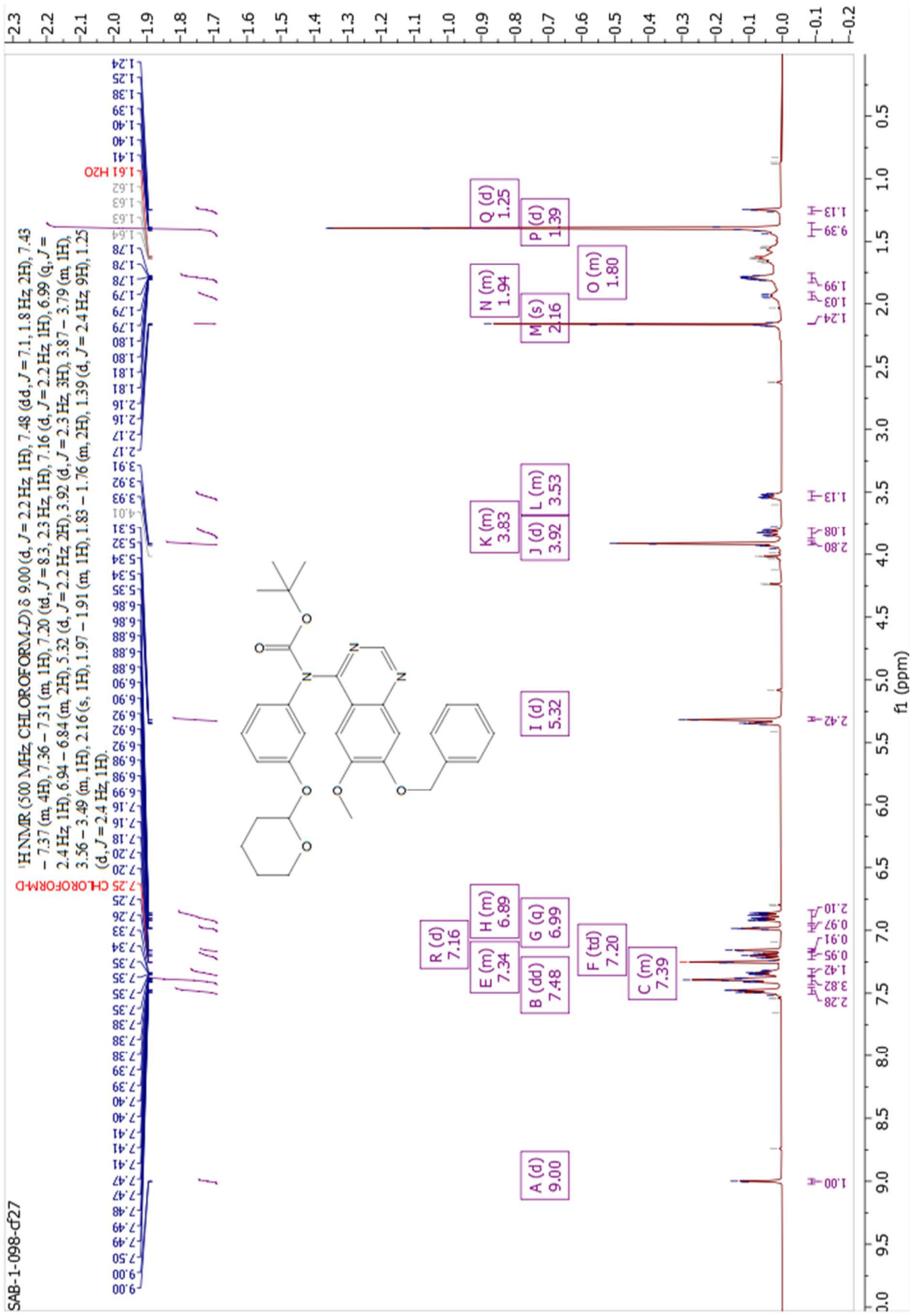

Spectrum 36 Compound 57 ^{1}H NMR

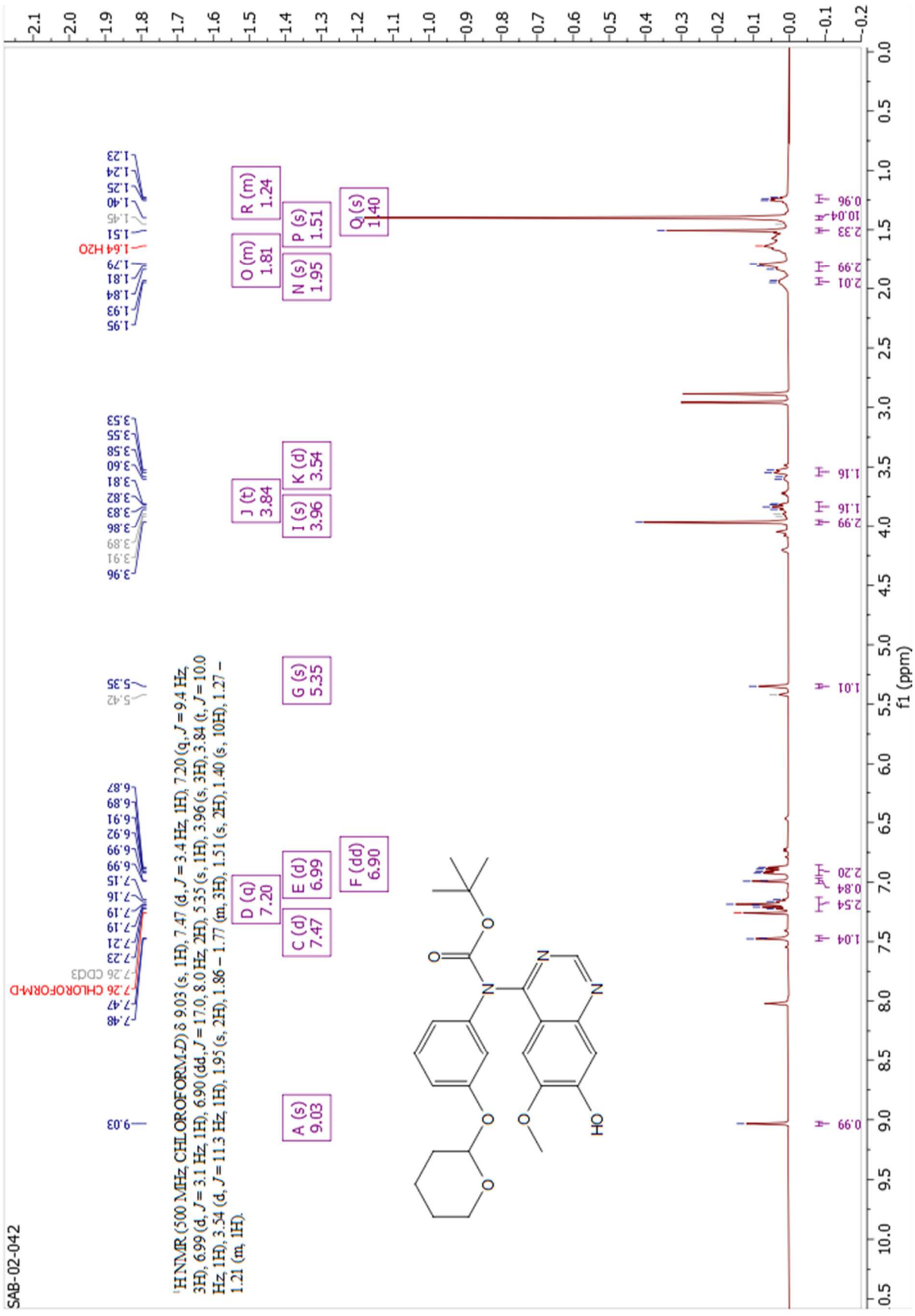

Spectrum 37 Compound 58 ^{1}H NMR

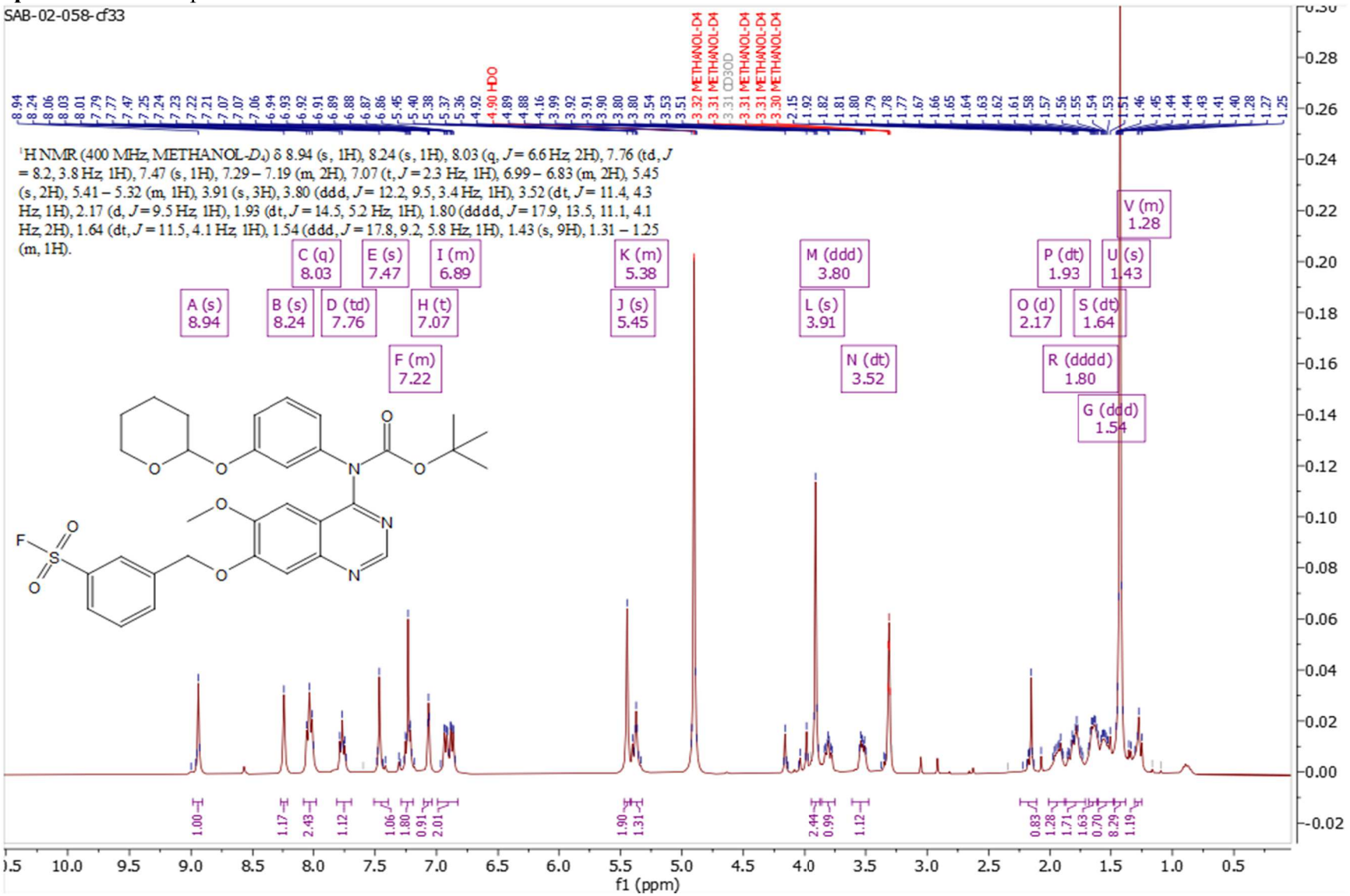

Spectrum 38 Compound 58 ^{19}F NMR

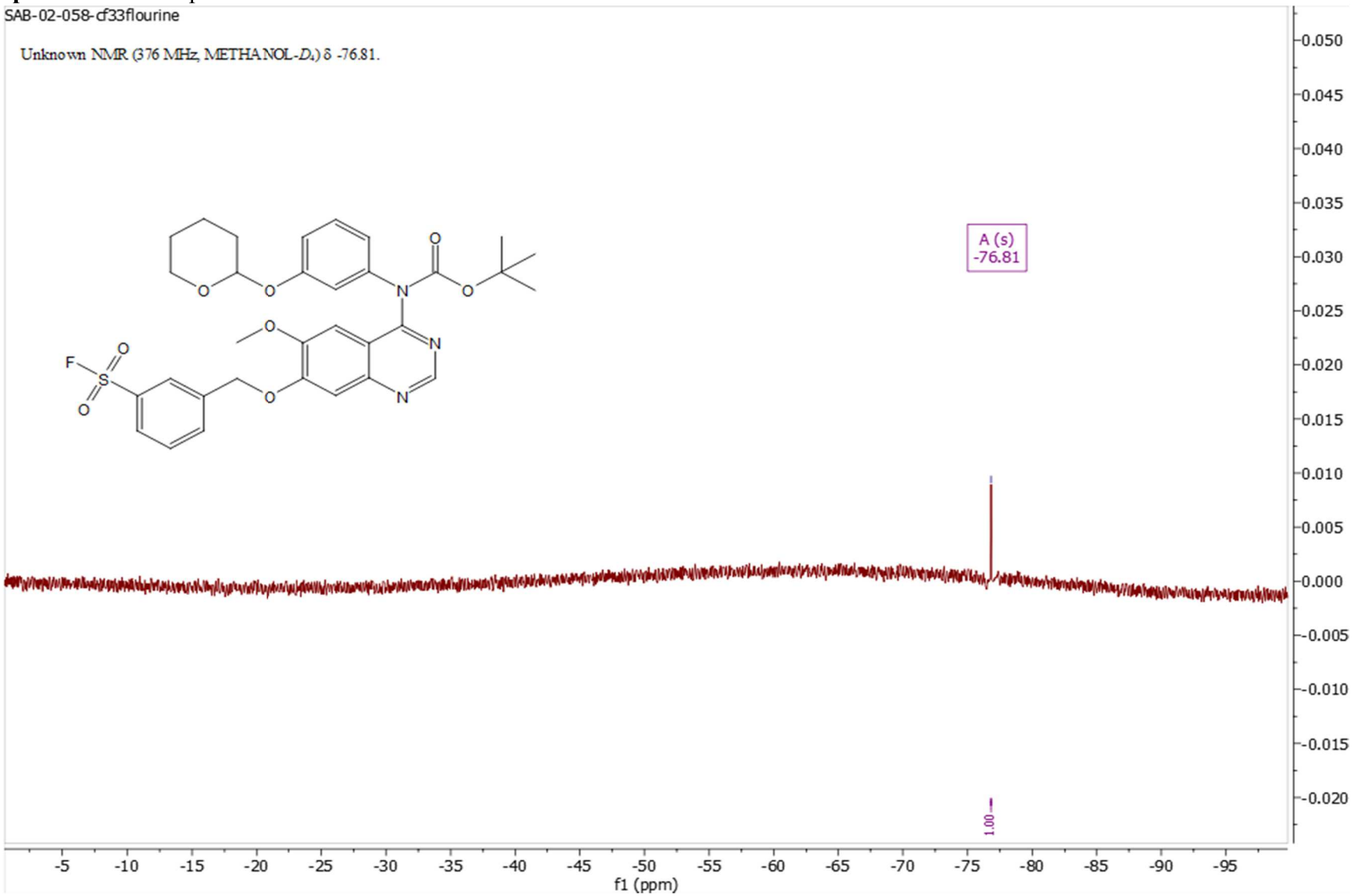

Spectrum 39 Compound 59 ^{1}H NMR

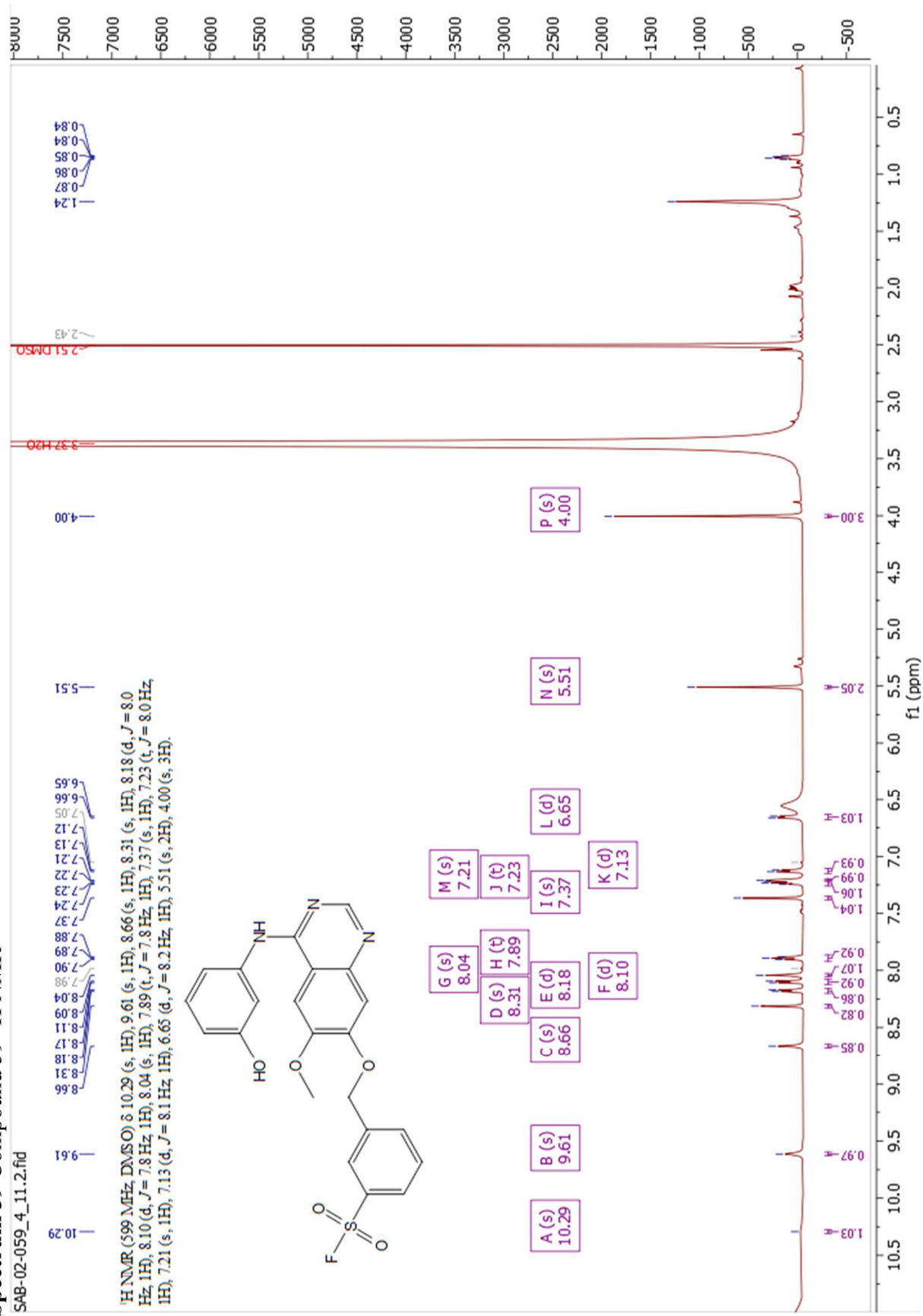

Spectrum 40 Compound 59 ^{19}F NMR

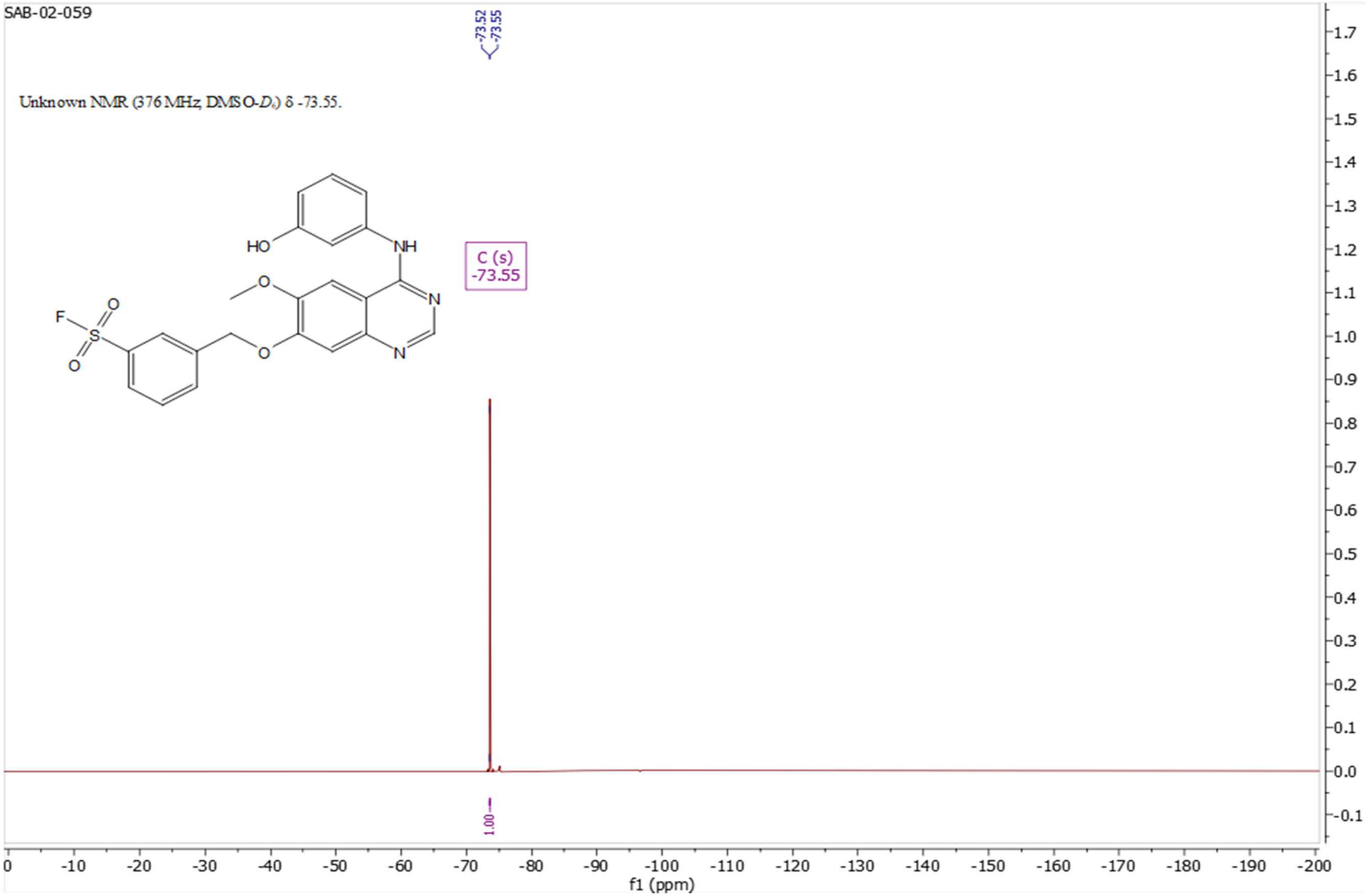

Spectrum 41 Compound 60 ^{1}H NMR

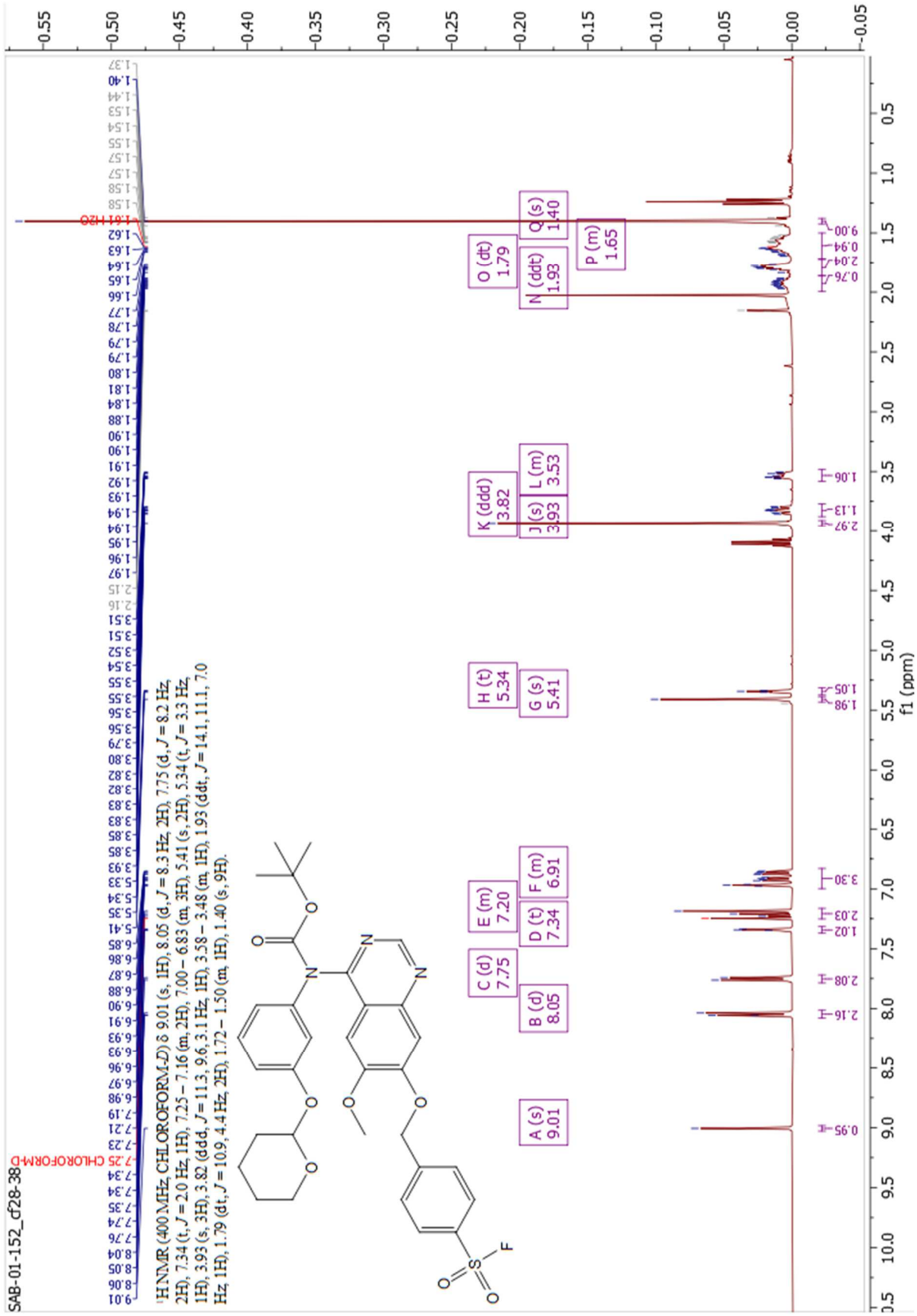

Spectrum 42 Compound 61 ^{1}H NMR

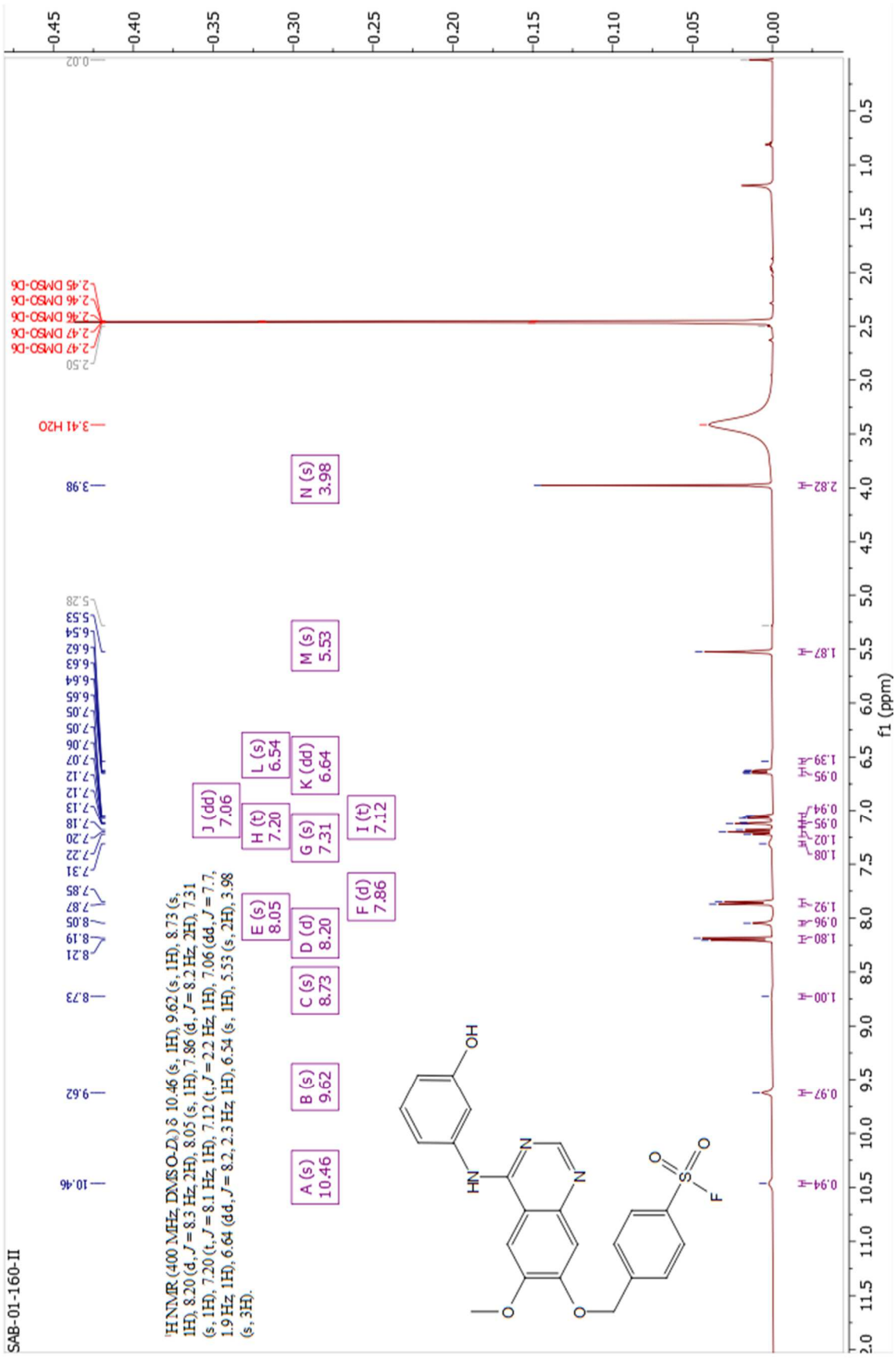

Spectrum 43 Compound 61 ^{19}F NMR

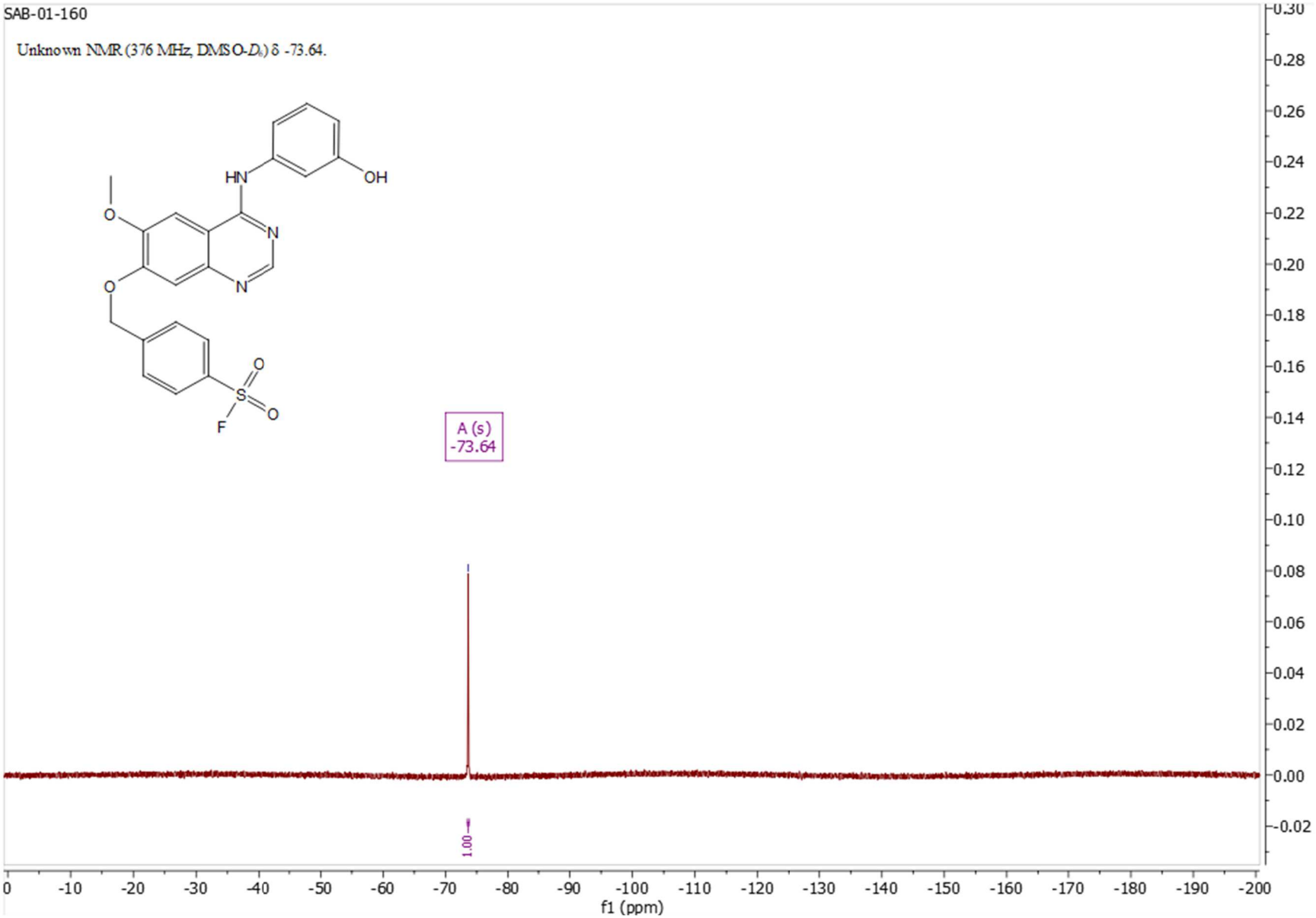

Spectrum 44 Compound 62 ^{1}H NMR

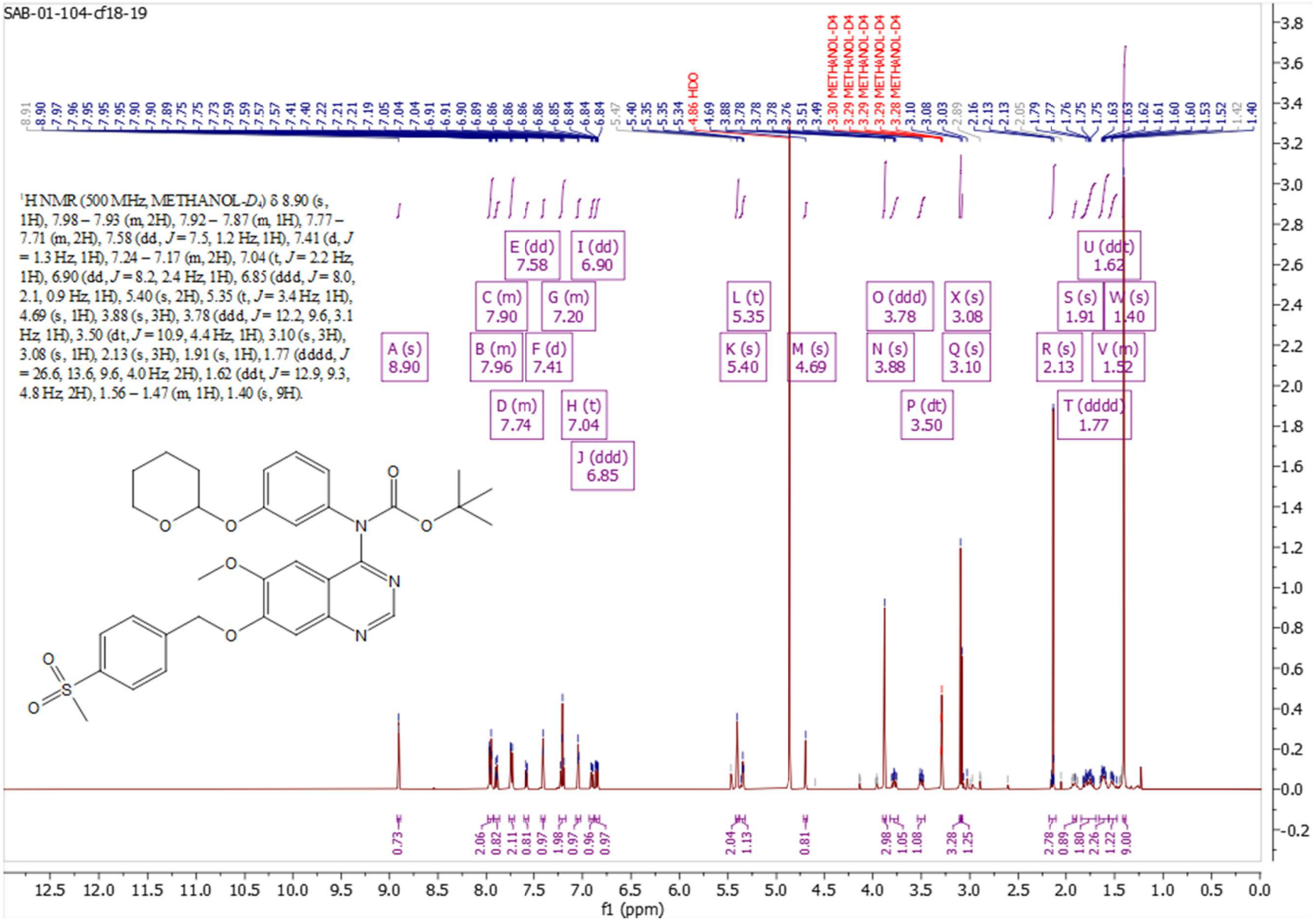

Spectrum 45 Compound 63 ^{1}H NMR

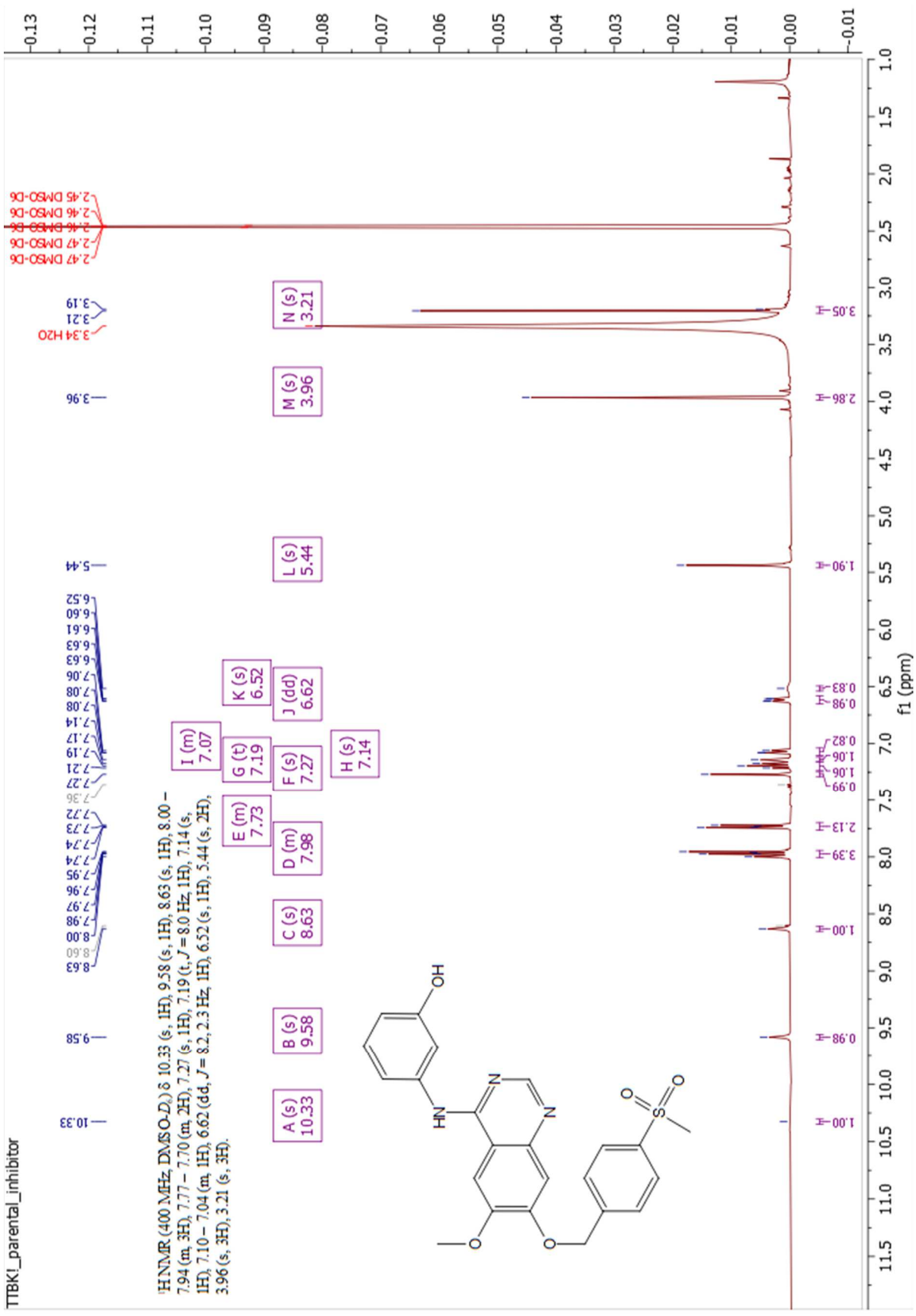

Spectrum 46 Compound 65 ^{1}H NMR

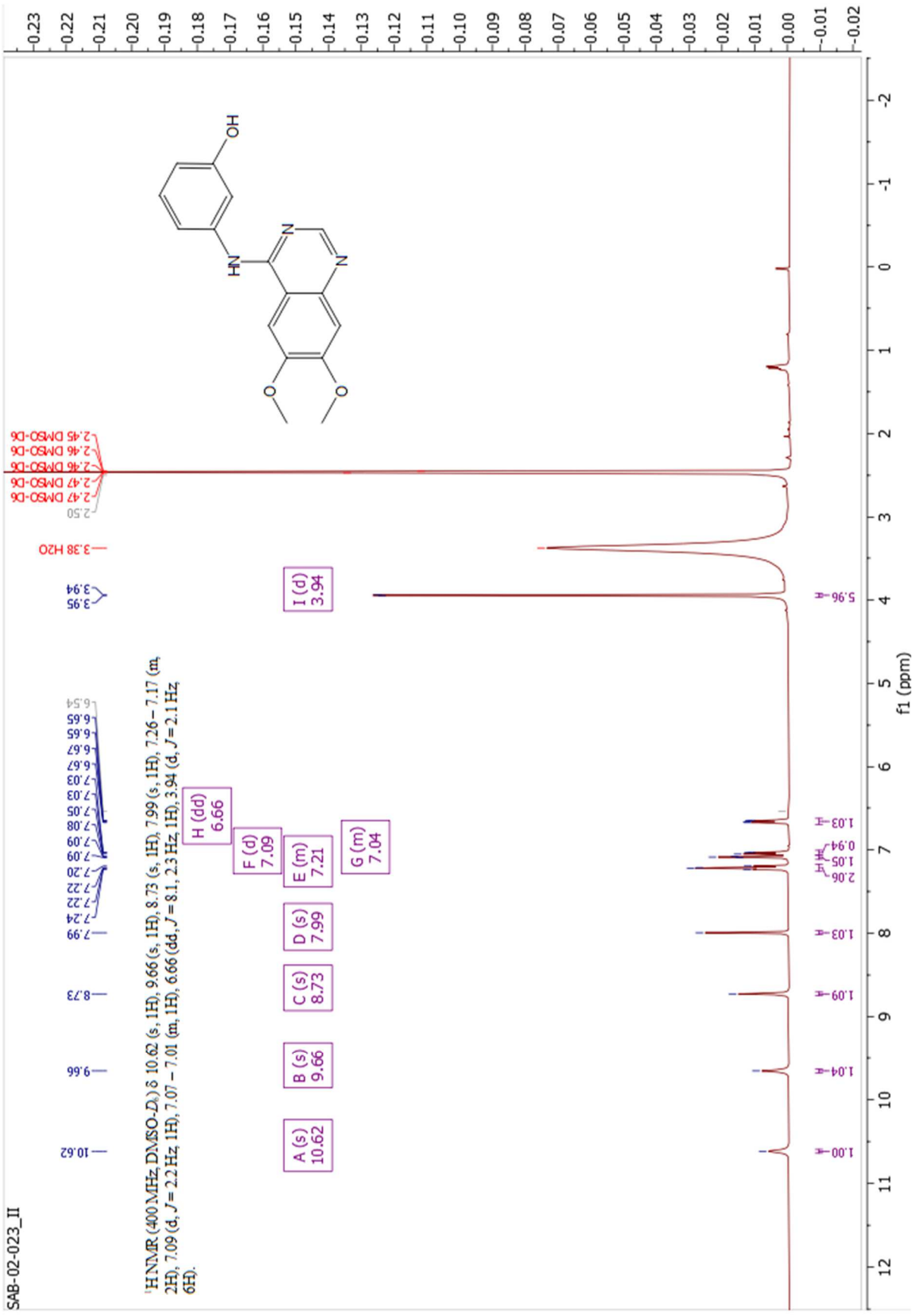

Final Compound Mass Spectra
Chapter 2

Spectrum 48 Compound 10 Photodiode Array

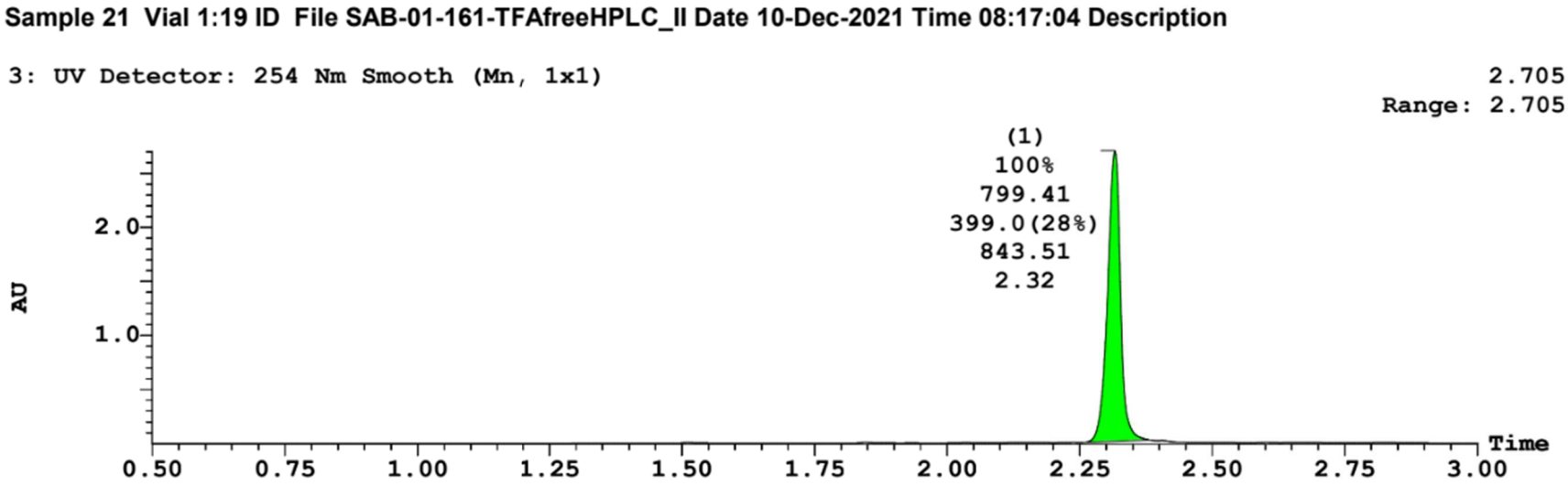

Spectrum 48 Compound 15 Photodiode Array

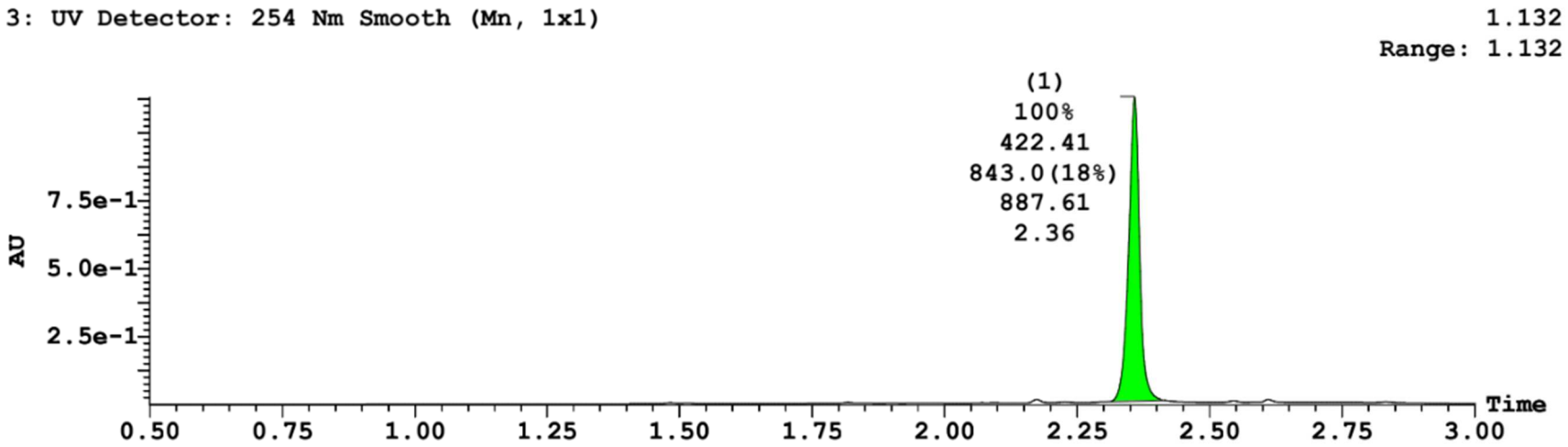

Spectrum 50 Compound 20 Photodiode Array

Sample 5 Vial 1:8 ID File SAB-01-111 Date 27-Sep-2021 Time 12:09:47 Description

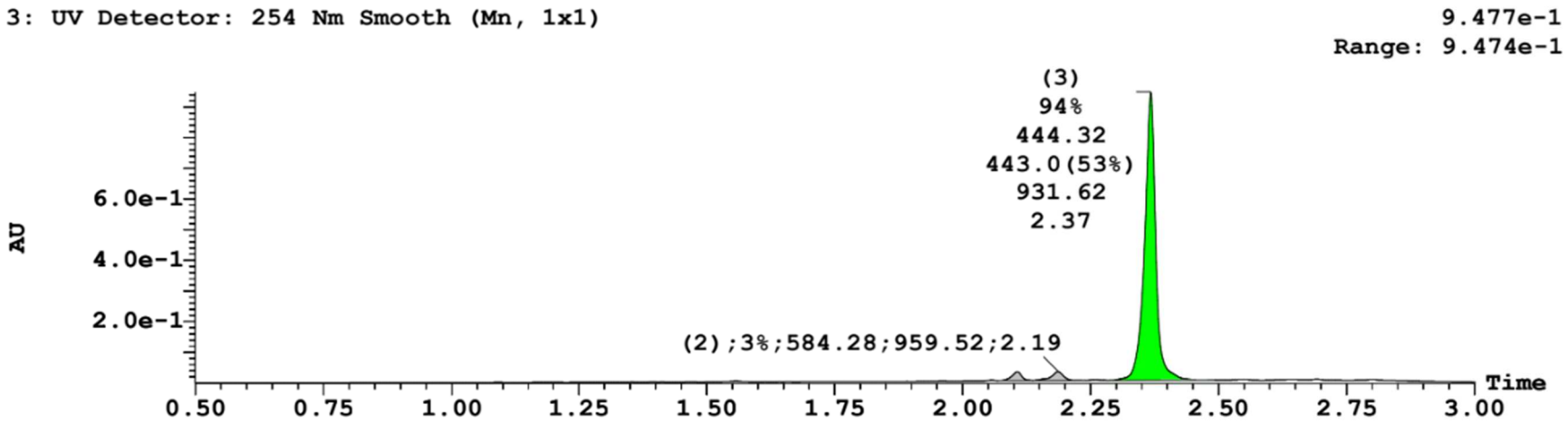

Spectrum 50 Compound 25 Photodiode Array

Sample 20 Vial 1:18 ID File SAB-01-162-TFAfreeHPLC Date 06-Dec-2021 Time 12:22:08 Description

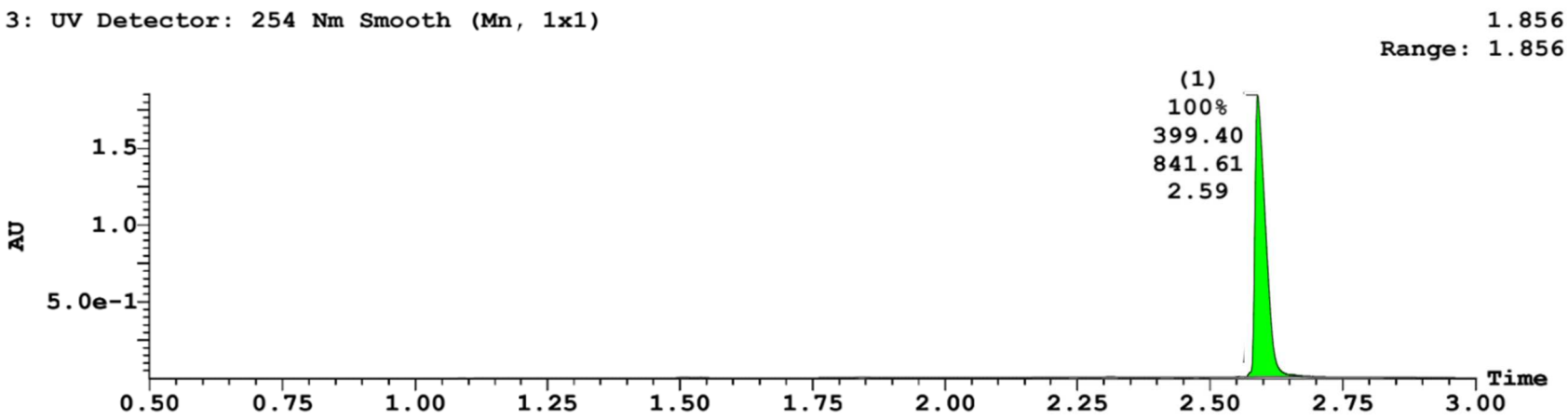

Spectrum 52 Compound 30 Photodiode Array

Sample 22 Vial 1:20 ID File SAB-01-170_purity Date 20-Dec-2021 Time 13:07:34 Description

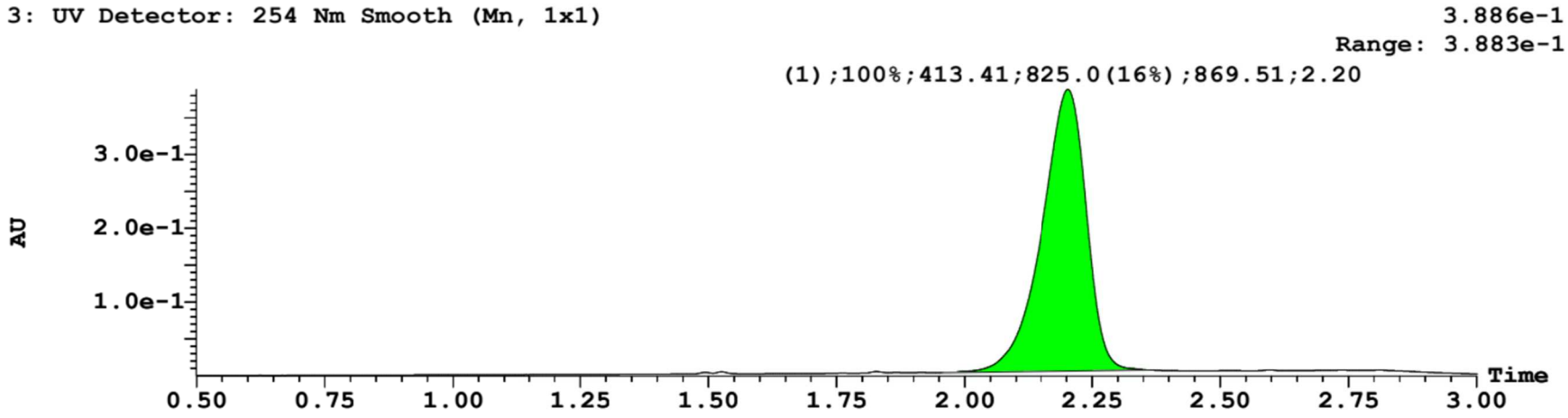

Spectrum 52 Compound 35 Photodiode Array

Sample 25 Vial 1:23 ID File SAB-02-008_V2purity Date 17-Jan-2022 Time 15:17:27 Description

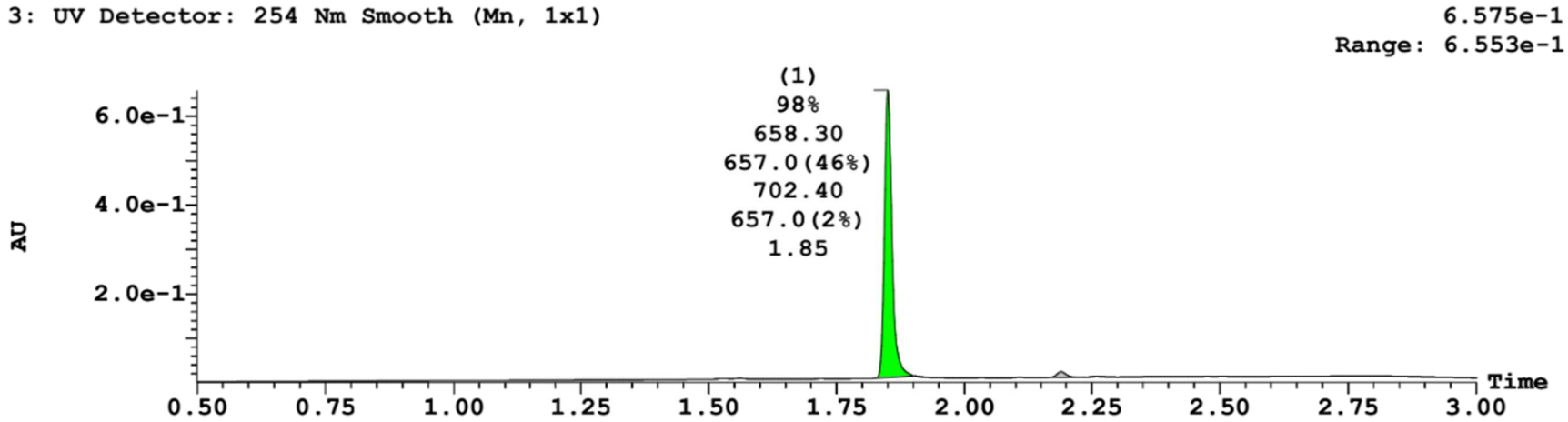

Spectrum 54 Compound 36 Photodiode Array

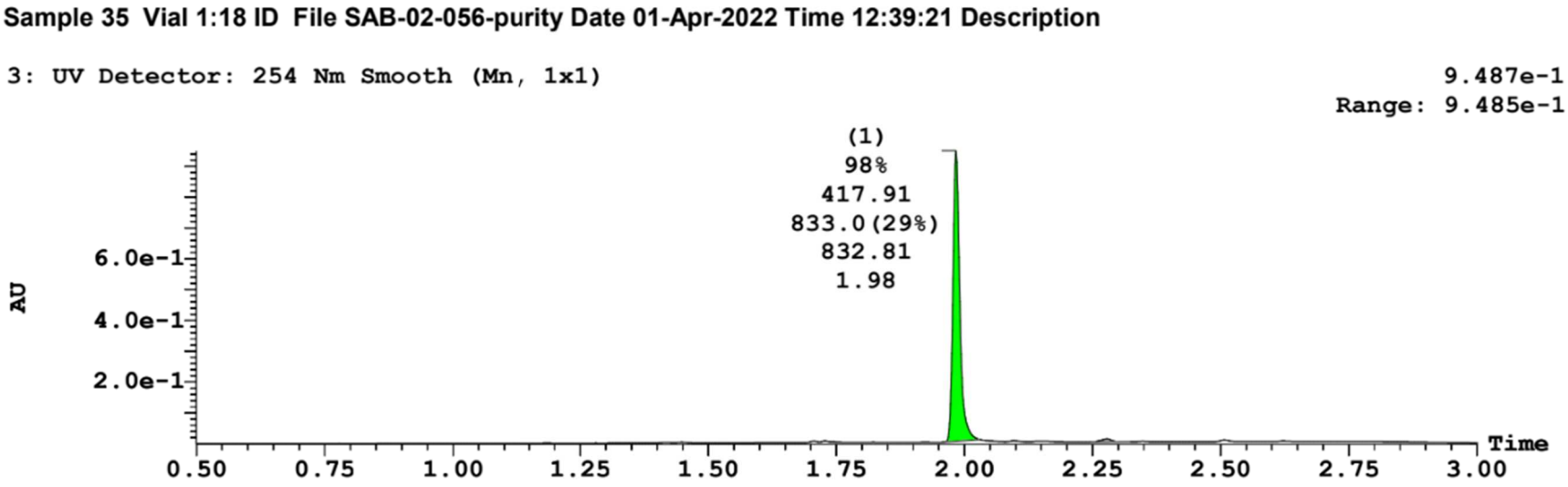

Spectrum 54 Compound 41 Photodiode Array

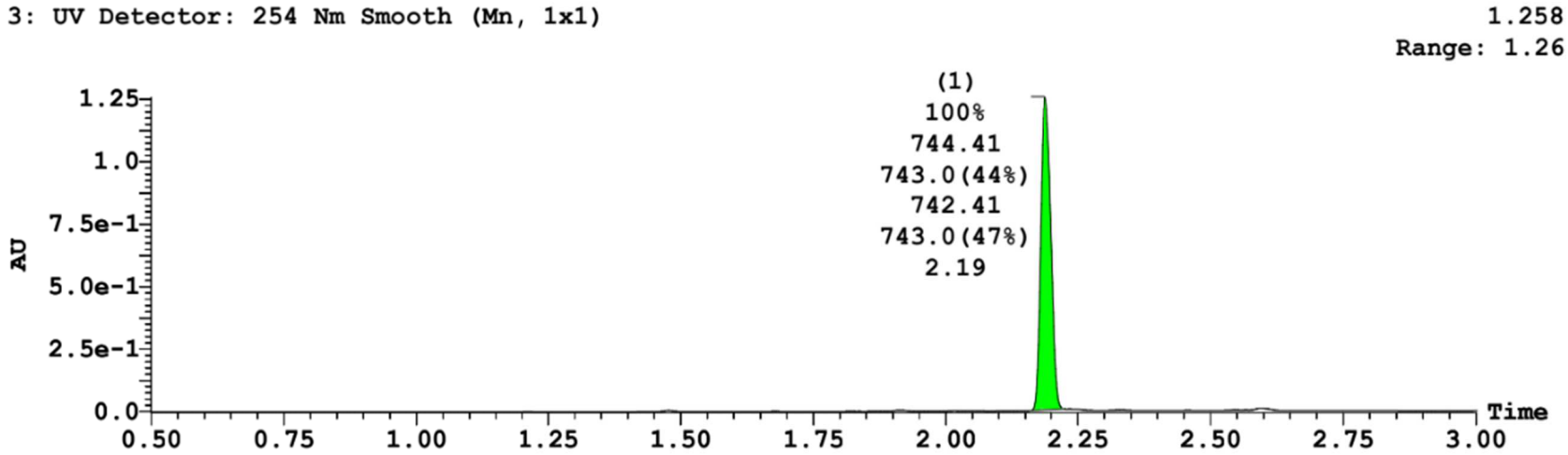

Spectrum 56 Compound 46 Photodiode Array

Sample 3 Vial 1:22 ID File SAB-02-071-purity Date 04-May-2022 Time 09:21:37 Description

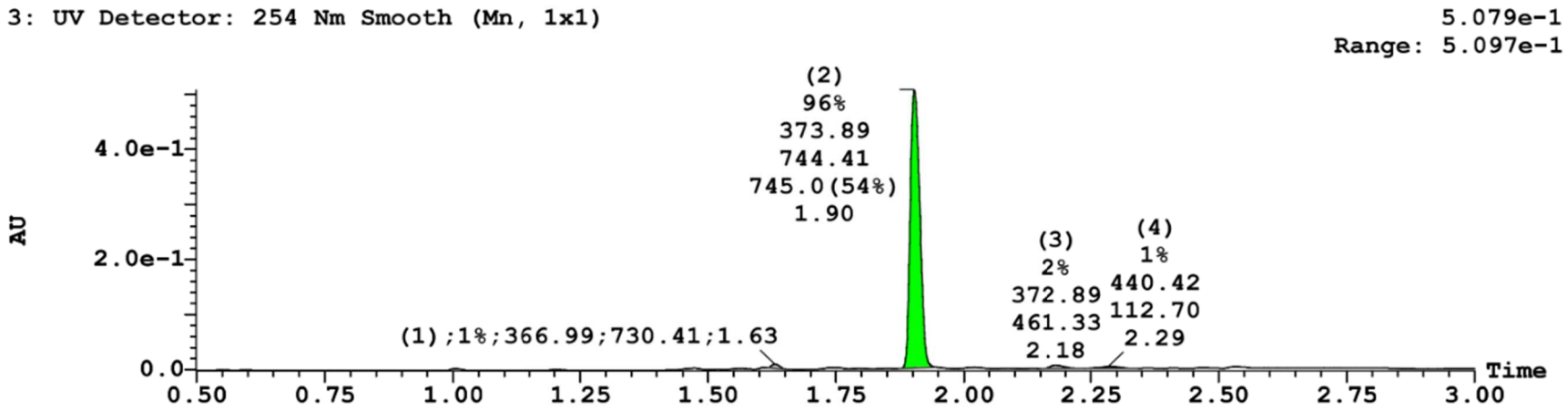

Spectrum 56 Compound 51 Photodiode Array

Sample 2 Vial 1:21 ID File SAB-02-076-purity Date 04-May-2022 Time 08:50:38 Description

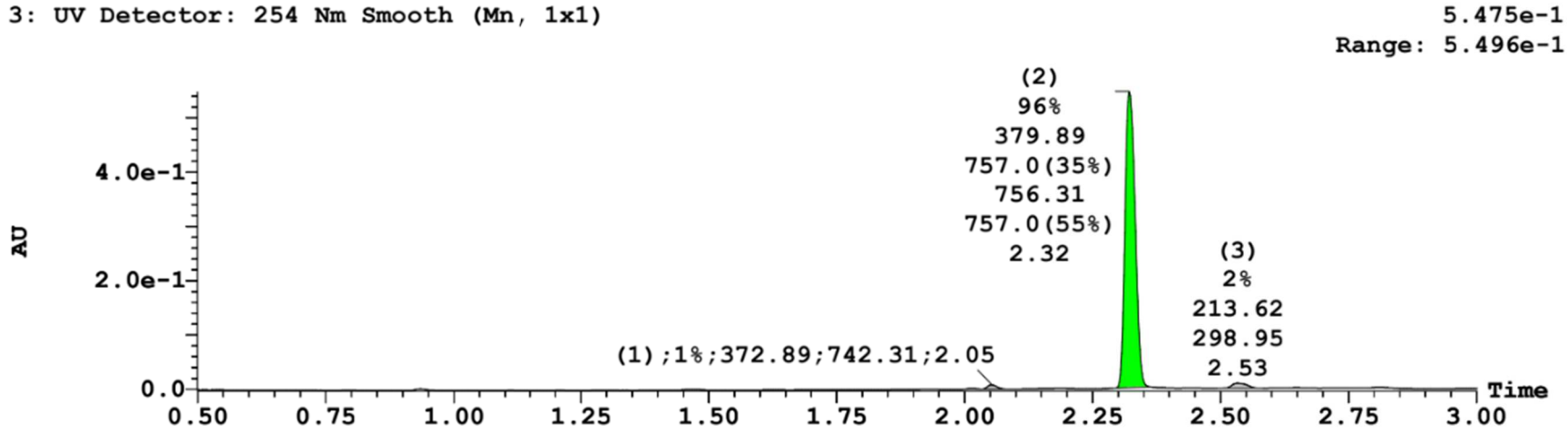

Spectrum 58 Compound 66 Photodiode Array

Sample 31 Vial 1:30 ID File SAB-02-034-purity Date 23-Feb-2022 Time 21:59:02 Description

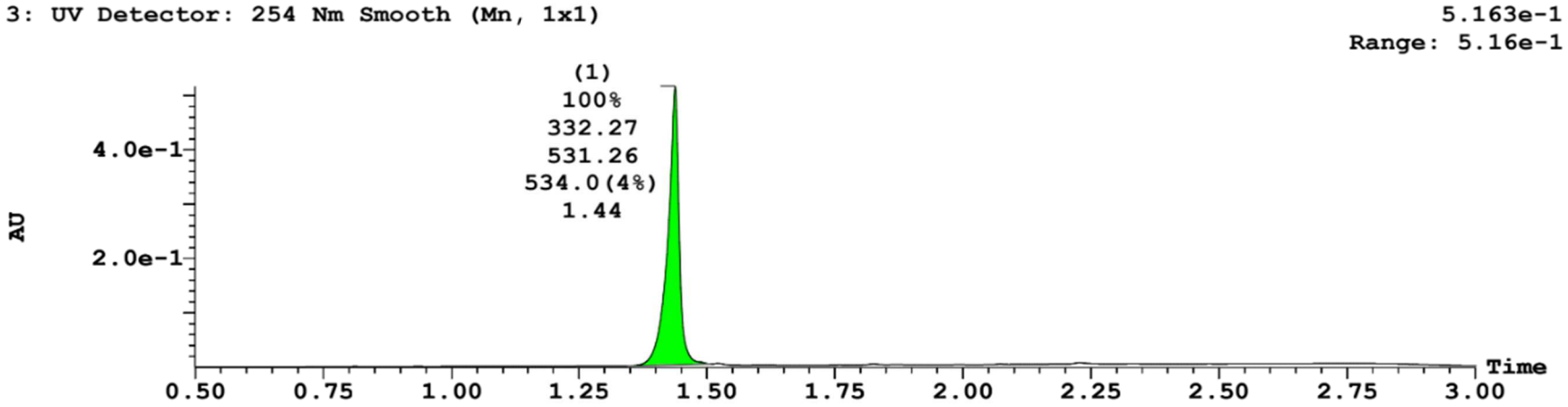

Spectrum 58 Compound 5 Photodiode Array

Sample 32 Vial 1:31 ID File SAB-02-029-purity Date 23-Feb-2022 Time 21:54:12 Description

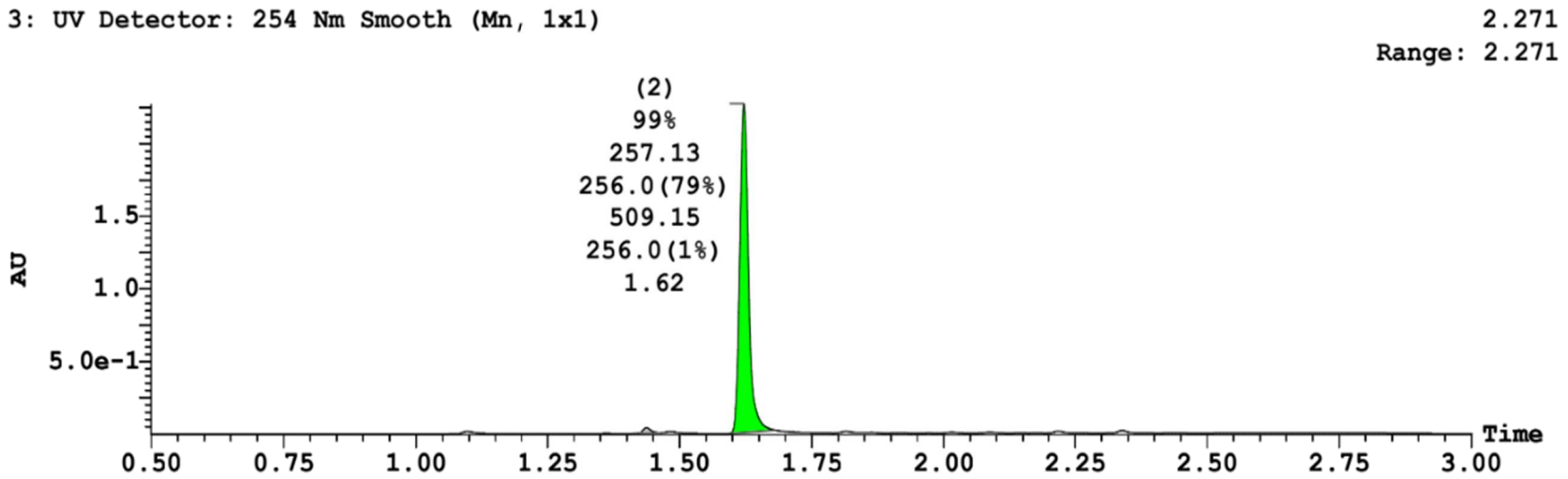

Chapter 3

Spectrum 60 Compound 59 Photodiode Array

Sample 33 Vial 1:31 ID File SAB-02-059 Date 31-Mar-2022 Time 19:17:09 Description

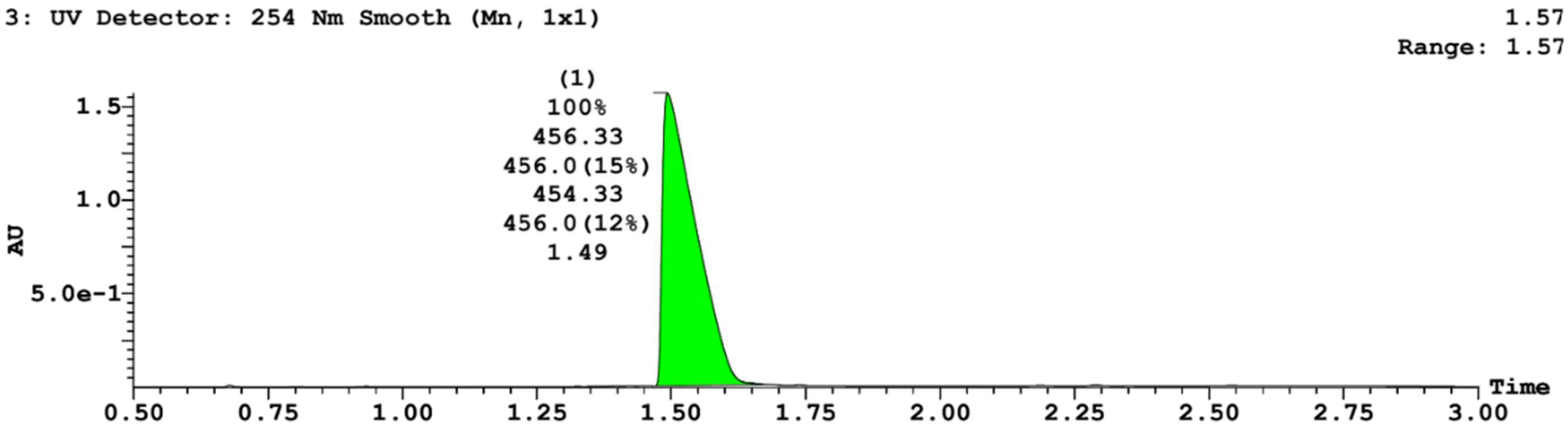

Spectrum 60 Compound 61 Photodiode Array

Sample 29 Vial 1:27 ID File SAB-01-160-purity Date 18-Feb-2022 Time 12:00:54 Description

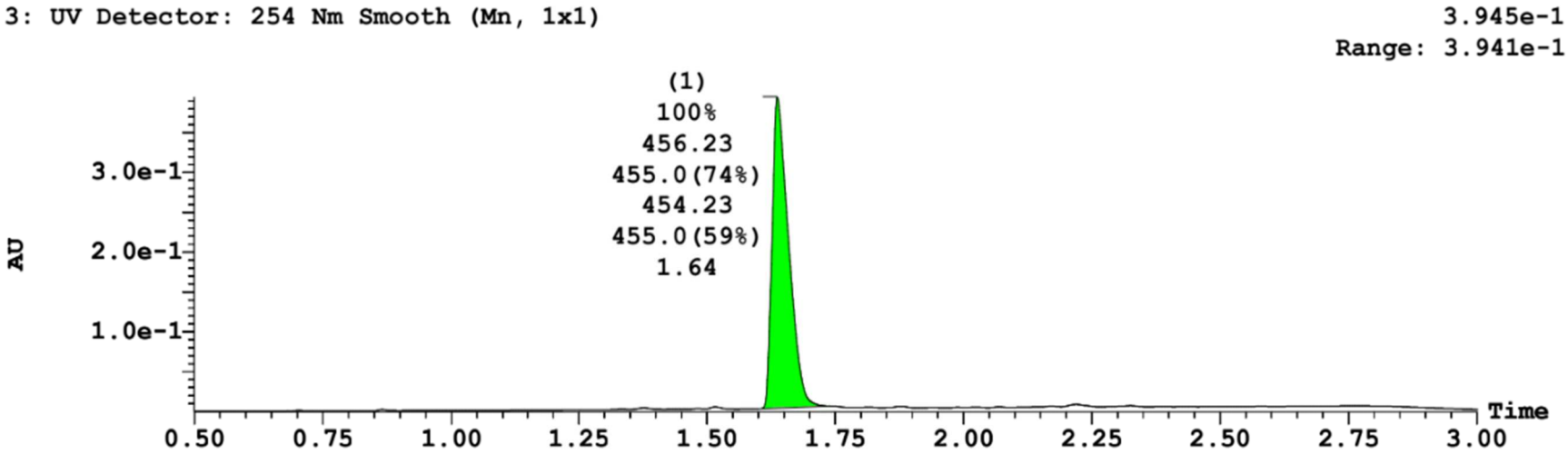

Spectrum 62 Compound 63 Photodiode Array

Sample 27 Vial 1:25 ID File SAB-01-120_III Date 21-Jan-2022 Time 12:10:31 Description

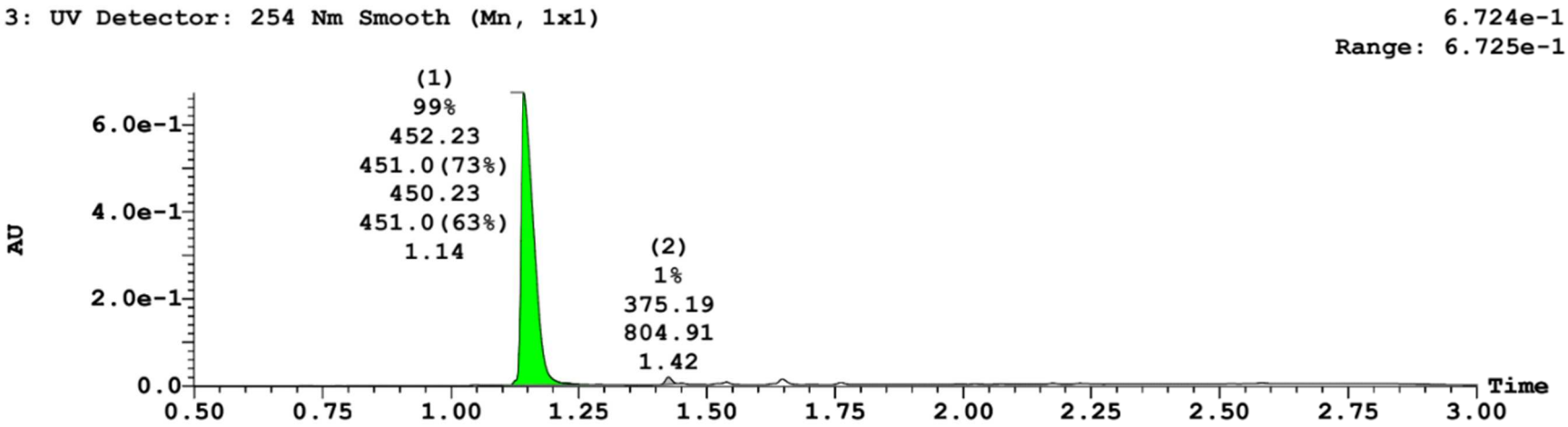

Spectrum 62 Compound 65 Photodiode Array

Sample 28 Vial 1:26 ID File SAB-01-123-purity Date 04-Feb-2022 Time 10:13:08 Description

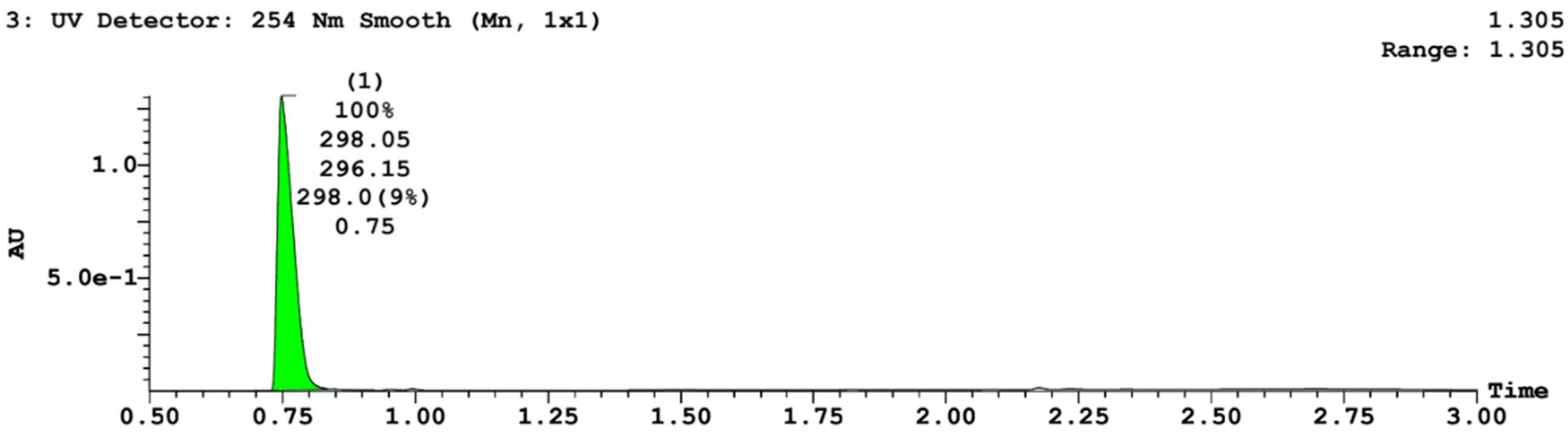

REFERENCES

(1) Ramsay, R. R.; Tipton, K. F. Assessment of Enzyme Inhibition: A Review with Examples from the Development of Monoamine Oxidase and Cholinesterase Inhibitory Drugs. *Mol. A J. Synth. Chem. Nat. Prod. Chem.* **2017**, *22* (7). https://doi.org/10.3390/MOLECULES22071192.

(2) Cristina Mendonça Nogueira, T.; Vinicius Nora de Souza, M. New FDA Oncology Small Molecule Drugs Approvals in 2020: Mechanism of Action and Clinical Applications. *Bioorg. Med. Chem.* **2021**, *46*, 116340. https://doi.org/10.1016/J.BMC.2021.116340.

(3) Fabbro, D. 25 Years of Small Molecular Weight Kinase Inhibitors: Potentials and Limitations. *Mol. Pharmacol.* **2015**, *87* (5), 766–775. https://doi.org/10.1124/MOL.114.095489.

(4) *Targeted protein degraders are redefining how small molecules look and act*.

(5) Sun, X.; Gao, H.; Yang, Y.; He, M.; Wu, Y.; Song, Y.; Tong, Y.; Rao, Y. PROTACs: Great Opportunities for Academia and Industry. *Signal Transduct. Target. Ther. 2019 41* **2019**, *4* (1), 1–33. https://doi.org/10.1038/s41392-019-0101-6.

(6) Schapira, M.; Calabrese, M. F.; Bullock, A. N.; Crews, C. M. Targeted Protein Degradation: Expanding the Toolbox. *Nat. Rev. Drug Discov. 2019 1812* **2019**, *18* (12), 949–963. https://doi.org/10.1038/s41573-019-0047-y.

(7) Li, H.; Dong, J.; Cai, M.; Xu, Z.; Cheng, X. D.; Qin, J. J. Protein Degradation Technology: A Strategic Paradigm Shift in Drug Discovery. *J. Hematol. Oncol. 2021 141* **2021**, *14* (1), 1–23. https://doi.org/10.1186/S13045-021-01146-7.

(8) Lilienbaum, A. Relationship between the Proteasomal System and Autophagy. *Int. J. Biochem. Mol. Biol.* **2013**, *4* (1), 1.

(9) Ciechanover, A. The Ubiquitin–Proteasome Pathway: On Protein Death and Cell Life. *EMBO J.* **1998**, *17* (24), 7151–7160. https://doi.org/10.1093/EMBOJ/17.24.7151.

(10) Takahashi, D.; Moriyama, J.; Nakamura, T.; Miki, E.; Takahashi, E.; Sato, A.; Akaike, T.; Itto-Nakama, K.; Arimoto, H. *AUTACs: Cargo-Specific Degraders Using Selective Autophagy | Elsevier Enhanced Reader*. Molecular Cell. https://reader.elsevier.com/reader/sd/pii/S109727651930694X?token=A793B13EFB8919D10F0FE719BF9D0BA02011891DF945C552A32BCF62E39B07D7783DEC11C5770A54605558EBBBB9D586&originRegion=us-east-1&originCreation=20211020034125 (accessed 2021-10-19).

(11) Naro, Y.; Darrah, K.; Deiters, A. Optical Control of Small Molecule-Induced Protein Degradation. *J. Am. Chem. Soc.* **2020**, *142* (5), 2193–2197. https://doi.org/10.1021/JACS.9B12718.

(12) Steinebach, C.; Lindner, S.; Udeshi, N. D.; Mani, D. C.; Kehm, H.; Köpff, S.; Carr, S. A.; Gütschow, M.; Krönke, J. Homo-PROTACs for the Chemical Knockdown of Cereblon. *ACS Chem. Biol.* **2018**, *13* (9), 2771–2782. https://doi.org/10.1021/ACSCHEMBIO.8B00693/SUPPL_FILE/CB8B00693_SI_001.PDF.

(13) Lebraud, H.; Heightman, T. D. Protein Degradation: A Validated Therapeutic Strategy

with Exciting Prospects. *Essays Biochem.* **2017**, *61* (5), 517–527. https://doi.org/10.1042/EBC20170030.

(14) Schreiber, S. L. The Rise of Molecular Glues. *Cell* **2021**, *184* (1), 3–9. https://doi.org/10.1016/J.CELL.2020.12.020.

(15) Handschumacher, R. E.; Harding, M. W.; Rice, J.; Drugge, R. J.; Speicher, D. W. Cyclophilin: A Specific Cytosolic Binding Protein for Cyclosporin A. *Science (80-.).* **1984**, *226* (4674), 544–547. https://doi.org/10.1126/SCIENCE.6238408.

(16) Liu, J.; Farmer, J. D.; Lane, W. S.; Friedman, J.; Weissman, I.; Schreiber, S. L. Calcineurin Is a Common Target of Cyclophilin-Cyclosporin A and FKBP-FK506 Complexes. *Cell* **1991**, *66* (4), 807–815. https://doi.org/10.1016/0092-8674(91)90124-H.

(17) Sakamoto, K. M.; Kim, K. B.; Kumagai, A.; Mercurio, F.; Crews, C. M.; Deshaies, R. J. Protacs: Chimeric Molecules That Target Proteins to the Skp1-Cullin-F Box Complex for Ubiquitination and Degradation. *Proc. Natl. Acad. Sci. U. S. A.* **2001**, *98* (15), 8554–8559. https://doi.org/10.1073/PNAS.141230798.

(18) Sakamoto, K. M.; Kim, K. B.; Verma, R.; Ransick, A.; Stein, B.; Crews, C. M.; Deshaies, R. J. Development of Protacs to Target Cancer-Promoting Proteins for Ubiquitination and Degradation *. *Mol. Cell. Proteomics* **2003**, *2* (12), 1350–1358. https://doi.org/10.1074/MCP.T300009-MCP200.

(19) Schneekloth, J. S.; Fonseca, F. N.; Koldobskiy, M.; Mandal, A.; Deshaies, R.; Sakamoto, K.; Crews, C. M. Chemical Genetic Control of Protein Levels: Selective in Vivo Targeted Degradation. *J. Am. Chem. Soc.* **2004**, *126* (12), 3748–3754. https://doi.org/10.1021/JA039025Z/SUPPL_FILE/JA039025ZSI20040128_034802.PDF.

(20) Lee, H.; Puppala, D.; Choi, E. Y.; Swanson, H.; Kim, K. B. Targeted Degradation of the Aryl Hydrocarbon Receptor by the PROTAC Approach: A Useful Chemical Genetic Tool. *ChemBioChem* **2007**, *8* (17), 2058–2062. https://doi.org/10.1002/CBIC.200700438.

(21) Schneekloth, A. R.; Pucheault, M.; Tae, H. S.; Crews, C. M. Targeted Intracellular Protein Degradation Induced by a Small Molecule: En Route to Chemical Proteomics. *Bioorg. Med. Chem. Lett.* **2008**, *18*, 5904–5908. https://doi.org/10.1016/j.bmcl.2008.07.114.

(22) Krönke, J.; Udeshi, N. D.; Narla, A.; Grauman, P.; Hurst, S. N.; McConkey, M.; Svinkina, T.; Heckl, D.; Comer, E.; Li, X.; Ciarlo, C.; Hartman, E.; Munshi, N.; Schenone, M.; Schreiber, S. L.; Carr, S. A.; Ebert, B. L. Lenalidomide Causes Selective Degradation of IKZF1 and IKZF3 in Multiple Myeloma Cells. *Science (80-.).* **2014**, *343* (6168), 301–305. https://doi.org/10.1126/SCIENCE.1244851/SUPPL_FILE/KRONKE-SM-REV.PDF.

(23) Fischer, E. S.; Böhm, K.; Lydeard, J. R.; Yang, H.; Stadler, M. B.; Cavadini, S.; Nagel, J.; Serluca, F.; Acker, V.; Lingaraju, G. M.; Tichkule, R. B.; Schebesta, M.; Forrester, W. C.; Schirle, M.; Hassiepen, U.; Ottl, J.; Hild, M.; Beckwith, R. E. J.; Harper, J. W.; Jenkins, J. L.; Thomä, N. H. Structure of the DDB1–CRBN E3 Ubiquitin Ligase in Complex with Thalidomide. *Nat. 2014 5127512* **2014**, *512* (7512), 49–53. https://doi.org/10.1038/nature13527.

(24) Bondeson, D. P.; Mares, A.; Smith, I. E. D.; Ko, E.; Campos, S.; Miah, A. H.; Mulholland, K. E.; Routly, N.; Buckley, D. L.; Gustafson, J. L.; Zinn, N.; Grandi, P.; Shimamura, S.; Bergamini, G.; Faelth-Savitski, M.; Bantscheff, M.; Cox, C.; Gordon, D. A.; Willard, R. R.; Flanagan, J. J.; Casillas, L. N.; Votta, B. J.; Den Besten, W.; Famm, K.; Kruidenier, L.; Carter, P. S.; Harling, J. D.; Churcher, I.; Crews, C. M. Catalytic in Vivo Protein Knockdown by Small-Molecule PROTACs. *Nat. Chem. Biol. 2015 118*

2015, *11* (8), 611–617. https://doi.org/10.1038/nchembio.1858.

(25) Yang, W.; Hamilton, J. L.; Kopil, C.; Beck, J. C.; Tanner, C. M.; Albin, R. L.; Ray Dorsey, E.; Dahodwala, N.; Cintina, I.; Hogan, P.; Thompson, T. Current and Projected Future Economic Burden of Parkinson's Disease in the U.S. *npj Park. Dis. 2020 61* **2020**, *6* (1), 1–9. https://doi.org/10.1038/s41531-020-0117-1.

(26) Pang, S. Y. Y.; Ho, P. W. L.; Liu, H. F.; Leung, C. T.; Li, L.; Chang, E. E. S.; Ramsden, D. B.; Ho, S. L. The Interplay of Aging, Genetics and Environmental Factors in the Pathogenesis of Parkinson's Disease. *Transl. Neurodegener.* **2019**, *8* (1). https://doi.org/10.1186/S40035-019-0165-9.

(27) Lücking, C. B.; Brice, A. Alpha-Synuclein and Parkinson's Disease. *Cell. Mol. Life Sci. C. 2000 5713* **2000**, *57* (13), 1894–1908. https://doi.org/10.1007/PL00000671.

(28) Zhang, G.; Xia, Y.; Wan, F.; Ma, K.; Guo, X.; Kou, L.; Yin, S.; Han, C.; Liu, L.; Huang, J.; Xiong, N.; Wang, T. New Perspectives on Roles of Alpha-Synuclein in Parkinson's Disease. *Front. Aging Neurosci.* **2018**, *0*, 370. https://doi.org/10.3389/FNAGI.2018.00370.

(29) Höhn, A.; Tramutola, A.; Cascella, R. Proteostasis Failure in Neurodegenerative Diseases: Focus on Oxidative Stress. *Oxid. Med. Cell. Longev.* **2020**, *2020*. https://doi.org/10.1155/2020/5497046.

(30) Zharikov, A. D.; Cannon, J. R.; Tapias, V.; Bai, Q.; Horowitz, M. P.; Shah, V.; El Ayadi, A.; Hastings, T. G.; Greenamyre, J. T.; Burton, E. A. ShRNA Targeting α-Synuclein Prevents Neurodegeneration in a Parkinson's Disease Model. *J. Clin. Invest.* **2015**, *125* (7), 2721–2735. https://doi.org/10.1172/JCI64502.

(31) Gorbatyuk, O. S.; Li, S.; Nash, K.; Gorbatyuk, M.; Lewin, A. S.; Sullivan, L. F.; Mandel, R. J.; Chen, W.; Meyers, C.; Manfredsson, F. P.; Muzyczka, N. In Vivo RNAi-Mediated α-Synuclein Silencing Induces Nigrostriatal Degeneration. *Mol. Ther.* **2010**, *18* (8), 1450–1457. https://doi.org/10.1038/MT.2010.115.

(32) Lewis, J.; Melrose, H.; Bumcrot, D.; Hope, A.; Zehr, C.; Lincoln, S.; Braithwaite, A.; He, Z.; Ogholikhan, S.; Hinkle, K.; Kent, C.; Toudjarska, I.; Charisse, K.; Braich, R.; Pandey, R. K.; Heckman, M.; Maraganore, D. M.; Crook, J.; Farrer, M. J. In Vivo Silencing of Alpha-Synuclein Using Naked SiRNA. *Mol. Neurodegener.* **2008**, *3* (1), 1–10. https://doi.org/10.1186/1750-1326-3-19/TABLES/1.

(33) Silva, M. C.; Ferguson, F. M.; Cai, Q.; Donovan, K. A.; Nandi, G.; Patnaik, D.; Zhang, T.; Huang, H. T.; Lucente, D. E.; Dickerson, B. C.; Mitchison, T. J.; Fischer, E. S.; Gray, N. S.; Haggarty, S. J. Targeted Degradation of Aberrant Tau in Frontotemporal Dementia Patient-Derived Neuronal Cell Models. *Elife* **2019**, *8*. https://doi.org/10.7554/ELIFE.45457.

(34) Wang, W.; Zhou, Q.; Jiang, T.; Li, S.; Ye, J.; Zheng, J.; Wang, X.; Liu, Y.; Deng, M.; Ke, D.; Wang, Q.; Wang, Y.; Wang, J. Z. A Novel Small-Molecule PROTAC Selectively Promotes Tau Clearance to Improve Cognitive Functions in Alzheimer-like Models. *Theranostics* **2021**, *11* (11), 5279–5295. https://doi.org/10.7150/THNO.55680.

(35) Ebrahimi-Fakhari, D.; Cantuti-Castelvetri, I.; Fan, Z.; Rockenstein, E.; Masliah, E.; Hyman, B. T.; McLean, P. J.; Unni, V. K. Distinct Roles In Vivo for the Ubiquitin–Proteasome System and the Autophagy–Lysosomal Pathway in the Degradation of α-Synuclein. *J. Neurosci.* **2011**, *31* (41), 14508. https://doi.org/10.1523/JNEUROSCI.1560-11.2011.

(36) Nozal, V.; Martinez, A. Tau Tubulin Kinase 1 (TTBK1), a New Player in the Fight against Neurodegenerative Diseases. *Eur. J. Med. Chem.* **2019**, *161*, 39–47. https://doi.org/10.1016/J.EJMECH.2018.10.030.

(37) Takahashi, M.; Tomizawa, K.; Sato, K.; Ohtake, A.; Omori, A. A Novel Tau-Tubulin Kinase from Bovine Brain. *FEBS Lett.* **1995**, *372* (1), 59–64. https://doi.org/10.1016/0014-5793(95)00955-9.

(38) Chaki, M.; Airik, R.; Ghosh, A. K.; Giles, R. H.; Chen, R.; Slaats, G. G.; Wang, H.; Hurd, T. W.; Zhou, W.; Cluckey, A.; Gee, H. Y.; Ramaswami, G.; Hong, C. J.; Hamilton, B. A.; Červenka, I.; Ganji, R. S.; Bryja, V.; Arts, H. H.; Van Reeuwijk, J.; Oud, M. M.; Letteboer, S. J. F.; Roepman, R.; Husson, H.; Ibraghimov-Beskrovnaya, O.; Yasunaga, T.; Walz, G.; Eley, L.; Sayer, J. A.; Schermer, B.; Liebau, M. C.; Benzing, T.; Le Corre, S.; Drummond, I.; Janssen, S.; Allen, S. J.; Natarajan, S.; O'Toole, J. F.; Attanasio, M.; Saunier, S.; Antignac, C.; Koenekoop, R. K.; Ren, H.; Lopez, I.; Nayir, A.; Stoetzel, C.; Dollfus, H.; Massoudi, R.; Gleeson, J. G.; Andreoli, S. P.; Doherty, D. G.; Lindstrad, A.; Golzio, C.; Katsanis, N.; Pape, L.; Abboud, E. B.; Al-Rajhi, A. A.; Lewis, R. A.; Omran, H.; Lee, E. Y. H. P.; Wang, S.; Sekiguchi, J. M.; Saunders, R.; Johnson, C. A.; Garner, E.; Vanselow, K.; Andersen, J. S.; Shlomai, J.; Nurnberg, G.; Nurnberg, P.; Levy, S.; Smogorzewska, A.; Otto, E. A.; Hildebrandt, F. Exome Capture Reveals ZNF423 and CEP164 Mutations, Linking Renal Ciliopathies to DNA Damage Response Signaling. *Cell* **2012**, *150* (3), 533–548. https://doi.org/10.1016/J.CELL.2012.06.028.

(39) Jackson, P. K. TTBK2 Kinase: Linking Primary Cilia and Cerebellar Ataxias. *Cell* **2012**, *151* (4), 697–699. https://doi.org/10.1016/J.CELL.2012.10.027.

(40) Watanabe, T.; Kakeno, M.; Matsui, T.; Sugiyama, I.; Arimura, N.; Matsuzawa, K.; Shirahige, A.; Ishidate, F.; Nishioka, T.; Taya, S.; Hoshino, M.; Kaibuchi, K. TTBK2 with EB1/3 Regulates Microtubule Dynamics in Migrating Cells through KIF2A Phosphorylation. *J. Cell Biol.* **2015**, *210* (5), 737–751. https://doi.org/10.1083/JCB.201412075/VIDEO-9.

(41) Tomizawa, K.; Omori, A.; Ohtake, A.; Sato, K.; Takahashi, M. Tau-Tubulin Kinase Phosphorylates Tau at Ser-208 and Ser-210, Sites Found in Paired Helical Filament-Tau. *FEBS Lett.* **2001**, *492* (3), 221–227. https://doi.org/10.1016/S0014-5793(01)02256-6.

(42) Bouskila, M.; Esoof, N.; Gay, L.; Fang, E. H.; Deak, M.; Begley, M. J.; Cantley, L. C.; Prescott, A.; Storey, K. G.; Alessi, D. R. TTBK2 Kinase Substrate Specificity and the Impact of Spinocerebellar-Ataxia-Causing Mutations on Expression, Activity, Localization and Development. *Biochem. J.* **2011**, *437* (1), 157–167. https://doi.org/10.1042/BJ20110276.

(43) Liachko, N. F.; McMillan, P. J.; Strovas, T. J.; Loomis, E.; Greenup, L.; Murrell, J. R.; Ghetti, B.; Raskind, M. A.; Montine, T. J.; Bird, T. D.; Leverenz, J. B.; Kraemer, B. C. The Tau Tubulin Kinases TTBK1/2 Promote Accumulation of Pathological TDP-43. *PLOS Genet.* **2014**, *10* (12), e1004803. https://doi.org/10.1371/JOURNAL.PGEN.1004803.

(44) Sato, S.; Xu, J.; Okuyama, S.; Martinez, L. B.; Walsh, S. M.; Jacobsen, M. T.; Swan, R. J.; Schlautman, J. D.; Ciborowski, P.; Ikezu, T. Spatial Learning Impairment, Enhanced CDK5/P35 Activity, and Downregulation of NMDA Receptor Expression in Transgenic Mice Expressing Tau-Tubulin Kinase 1. *J. Neurosci.* **2008**, *28* (53), 14511–14521. https://doi.org/10.1523/JNEUROSCI.3417-08.2008.

(45) Bort, G.; Sylla-Iyarreta Veitía, M.; Ferroud, C. Straightforward Synthesis of PET Tracer Precursors Used for the Early Diagnosis of Alzheimers Disease through Suzuki–Miyaura Cross-Coupling Reactions. *Tetrahedron* **2013**, *69* (35), 7345–7353. https://doi.org/10.1016/J.TET.2013.06.085.

(46) Wang, M.; Lu, J.; Wang, M.; Yang, C. Y.; Wang, S. Discovery of SHP2-D26 as a First, Potent, and Effective PROTAC Degrader of SHP2 Protein. *J. Med. Chem.* **2020**, *63* (14), 7510–7528. https://doi.org/10.1021/ACS.JMEDCHEM.0C00471/SUPPL_FILE/JM0C00471_SI_004.PDB.